

QUANTITATIVE ASSESSMENT OF PULMONARY FUNCTION

A thesis submitted to

THE UNIVERSITY OF ASTON IN BIRMINGHAM

for the degree of

DOCTOR OF PHILOSOPHY

by

LAMORNA ANNE SPRY, M.Phil, B.Sc (HONS)

June, 1979

QUANTITATIVE ASSESSMENT OF PULMONARY FUNCTION

Lamorna Anne Spry

A thesis submitted to the University of Aston in Birmingham
for the Degree of Doctor of Philosophy.

June, 1979

SUMMARY

In a search for more quantitative assessment of pulmonary function, the research concentrated on two major areas of investigation:

Gross impairment of pulmonary gas exchange processes can often be attributed to regional deformation of normal ventilation-specific ventilation distributions. Hence, the first topic of investigation considers the recovery of such distributions in normal and diseased states, by a new method with which these distributions can be confidently recovered from inert gas elimination studies. The method is tested using theoretical nitrogen washout data and subsequently used to analyse experimental data from ten normal and two abnormal subjects. The recovered quasi-continuous distributions of ventilation to specific ventilation suggest that whereas young normal lungs behave as two principle respiratory zones of volume ratio 6.04, this ratio increases rapidly with age, and large deviations from the observed 'normal' pattern occur in diseased states.

The second area of research considers the existence of pulmonary arteriovenous blood shunts which direct blood away from the ventilated regions of the lung, causing severe hypoxia. By means of a mathematical model of non-steady state inert gas exchange, a new method is described for rapid and accurate detection of shunt. The effects of regional inequalities of ventilation and perfusion, together with tracer solubility, are studied. The method is shown to merely require the continuous sampling of injectate and arterial blood tracer concentrations and the accuracy is independent of end-capillary gas concentrations and tracer solubility.

PULMONARY
DISTRIBUTIONS
SIMULATION
SHUNT

C O N T E N T S

Summary	
Declaration	
Acknowledgements	
List of Figures	

PART I: RECOVERY OF THE DISTRIBUTION OF VENTILATION
 AND SPECIFIC VENTILATION IN THE HUMAN LUNG

CHAPTER 1	INTRODUCTION	1
i	Background of research	1
ii	An overview of the thesis	6
iii	Conclusions	7
CHAPTER 2	REVIEW OF METHODS TO RECOVER DETAILED LUNG DISTRIBUTIONS	9
i	Recovering continuous distributions	9
ii	Recovering quasi-continuous distributions	11
CHAPTER 3	A NEW TECHNIQUE FOR OBTAINING UNIQUE DISTRIBUTIONS	18
i	The lung model	18
ii	Reducing the number of unknowns	21
iii	Determining a suitable parametric function by compartment fitting	22
iv	Recovering quasi-continuous distributions by parametrization fitting	28

CHAPTER 4	RECOVERY OF THEORETICAL DISTRIBUTIONS	31
i	Delta type functions	31
ii	Bimodal distribution	36
iii	Recovery of further distributions	39
iv	Discussion	40
CHAPTER 5	RECOVERY OF FRACTIONAL VENTILATION TO SPECIFIC VENTILATION FROM EXPERIMENTAL N ₂ WASHOUT CURVES	43
i	Introduction	43
ii	Experimental Method	45
iii	Compartmental fitting: 7 compartment lung model	46
iv	Conclusions from the compartmental fitting	50
v	Parametrization fitting: 100 compartment lung model	52
vi	Conclusions from the parametrization fits	56
CHAPTER 6	CONCLUSIONS	58
i	Recovery of theoretical distributions	58
ii	Recovery of distributions from experimental N ₂ washout curves	60

PART II: DETECTING AND QUANTIFYING PULMONARY
 ARTERIOVENOUS BLOOD SHUNTS

CHAPTER 7	BACKGROUND	64
CHAPTER 8	THE MATHEMATICAL MODEL	72
i	Non steady state inert gas exchange	72
ii	Homogeneous lung with true shunt	75
iii	Heterogeneous lung with no true shunt	75
iv	Heterogeneous lung with true shunt	77
CHAPTER 9	RESULTS OF SIMULATION	78
i	Homogeneous lung with no true shunt	78
ii	Heterogeneous lung with no true shunt	79
iii	Homogeneous lung with true shunt	79
iv	Heterogeneous lung with true shunt	81
CHAPTER 10	PRACTICAL APPLICATIONS OF THEORY	81
i	Recovering true shunt with a bolus of tracer gas	82
ii	Experimental measurement of non-steady state retention	83
iii	Conclusions	86
FUTURE WORK		88
APPENDIX 1	LIST OF SYMBOLS	94
APPENDIX 2	COMPUTER MINIMIZATION ROUTINE, "MINUIT"	98

DECLARATION

No part of the work described in this thesis has been submitted in support of an application for another degree or qualification of this or any other University or other institute of learning.

No part of the work described in this thesis has been done in collaboration with any other person.

Lanorra Anne Spry

ACKNOWLEDGEMENTS

I would like to express my gratitude to Dr. D. A. Scrimshire for his guidance and supervision, and to Professor R. H. Thornley for enabling the work to be carried out in the Production Engineering Department. The Physics and Mathematical Physics Departments of Birmingham University are thanked for the use of their computer facilities and the Anaesthetics Department of the Queen Elizabeth Hospital, Birmingham, are thanked for the use of experimental apparatus.

I am also very grateful for the financial support given by the Science Research Council.

Finally, sincere thanks are expressed to my husband and parents for their support and encouragement throughout the project.

List of Figures

1. (A) Non-steady state inert gas retention as a function of time evaluated from a lung model with distributions of \dot{V} and \dot{Q} as in figure 2A.
(B) Comparison of non-steady state inert gas retention as a function of time for two different lung models (a) a homogeneous lung and (b) a lung with a distribution as in figure 2A.
N.B. The curves are almost indistinguishable in the early stages of uptake.
2. (A) Distribution of fractional perfusion as a function of ventilation-perfusion ratio in a lung model, from which curve 1 (A) was produced.
(B) Distribution recovered using parametrization techniques and data from figure 1(A).
3. Compartmental fit to nitrogen washout data produced by a *delta type* function.
4. Effect of noise on the recovery of a *delta type* function using parametrization techniques (100 lung compartments).
5. Effect of the number of lung model compartments (N_{compt}) on the recovery of a *delta type* function using parametrization techniques (2% noise)

6. Effect of the number of breaths of the N_2 washout curve (N_{data}) on the recovery of a *delta type* function using parametrization techniques. (100 lung compartments)
7. Effect of maldetermining the inefficiency parameter E on the recovery of a *delta type* function using parametrization techniques (100 lung compartments).
8. Original *bimodal* 'hand drawn' distribution of fractional ventilation as a function of specific ventilation (20 compartments)
9. Compartmental fit to N_2 washout data generated from the distribution in figure 8. Demonstrates the effect of 2% noise on the data.
10. Effect of noise on the recovery of a *bimodal* function using parametrization techniques (100 compartments)
11. Effect of number of lung model compartments (N_{compt}) on the recovery of a *delta type* function using parametrization techniques (2% noise)
11. (A) Parametrization fit with only seven lung model compartments demonstrating the recoverability of bimodal features (2% noise)
12. Effect of the number of breaths of the N_2 washout curve (N_{data}) on the recovery of a *bimodal* function, using parametrization techniques (100 lung compartments)

13. Effect of maldetermining the inefficiency parameter E on the recovery of a *bimodal* function using parametrization techniques (100 lung compartments)
14. A 10 compartment parametrization to a *geometric progression* type distribution using a *padé* approximate, together with a direct compartmental fit (no noise)
N.B. The parametrization fit is indistinguishable from the true distribution
15. Compartmental fit to a straight line distribution
16. Compartmental fit to an original eight compartment delta type function
17. Parametrization fit (10 compartments) to a broad log normal type distribution
18. Parametrization fit to a broad bimodal distribution
19. Experimental set-up for obtaining multi-breath nitrogen washout curves
20. Nitrogen washout curves obtained for all twelve subjects, (curves for subjects 11 and 12 were obtained from reference 39)
21. Compartmental fit to nitrogen washout data from young normals (subjects 1 - 7: Group I)
22. Compartmental fit to nitrogen washout data from subject 8 of Group II (older normal)

23. Compartmental fit to nitrogen washout data from subjects 9 and 10 of Group II (older normals)
24. Compartmental fit to nitrogen washout data from subjects 11 and 12: Group III (diagnosed abnormal)
25. Parametrization fits (100 lung compartments) to nitrogen washout data from all twelve subjects
26. Graph to show increase of volume ratio (V_{L1}/V_{L2}) with age. (N.B. Both subjects 11 and 12 do not correspond to the trend observed for normals)
27. Graph to show increase of R with age
28. Effect of pulmonary abnormalities on the evaluation of true shunt by methods A and B and the average of methods A and B
29. Modelling a true intra-pulmonary blood shunt
30. Compartmental lung model with *no* true blood shunt
31. Compartmental lung model *with* a true blood shunt
32. Retention as a function of time during non-steady state tracer gas uptake (no true shunt). Homogeneous lung, gas solubility 0.5
33. Retention as a function of time in the non-steady state in a lung model with \dot{Q} and \dot{V} inequalities but no true blood shunt

34. Retention as a function of time in the non-steady state in a lung model *with* a 10% true blood shunt (Homogeneous lung model)
35. Non-steady state retention as a function of time in a lung model with 10% true shunt and Q and V inequalities (Heterogeneous lung model)
36. Effect of solubility on the recovery of the true shunt
37. Effect of the size of the true shunt (heterogeneous lung models)
38. Graph to show the recoverability of true shunt when P_{VG} is not constant.

PART I

RECOVERY OF THE DISTRIBUTION OF VENTILATION
AND SPECIFIC VENTILATION IN THE HUMAN LUNG

Part I: Recovery of the distribution of ventilation and
specific ventilation in the human lung

CHAPTER 1

INTRODUCTION

1.1 Background of Research

Uneven ventilation of the human lung was postulated as early as 1888 (1), but it was Krogh (2) and later Haldane and Priestley (3), who recognised the influence of uneven ventilation and perfusion on gas exchange, and established a new area of pulmonary research. Since the effect of uneven ventilation and perfusion on gas exchange was realised, pulmonary physiologists have attempted to find methods of evaluating those distributions in the hope of associating certain observed patterns of \dot{V}_A and \dot{Q} inequality with specific diseases. Not only could this be of invaluable diagnostic use, but could also be used to assess the effect of certain therapies on lung function, thus enabling predictions to be made as to the potential benefit of different therapeutic interventions.

The fundamental concept of the lung as a heterogenous gas exchanger has been validated by numerous experiments (4-9), but the ability of either bronchspirometric techniques, or more recent, external radioactive gas counting methods

(4, 5, 10 → 13), to resolve detailed information on regional \dot{V}_A and \dot{Q} inequalities has remained limited.

However, another approach to resolving the problem of quantitative analysis was made possible by the pioneering work of Rahn (14) and Riley and Cournand (15, 16) in which they conceived the lung as consisting of three compartments representing "venous admixture", "physiological dead space" and an "ideal point". From such a model they demonstrated how oxygen and carbon dioxide partial pressures in the alveolar air and in the arterial blood differ and depend upon the magnitude of the \dot{V}_A/\dot{Q} variations existing in the lung. Their work brought a new insight into pulmonary physiology and was a major contribution to the problem of quantifying \dot{V}_A/\dot{Q} inequalities.

Of the numerous investigators continuing the seminal work of Rahn, those worthy of particular mention are Briscoe (17, 18) and Briscoe and Cournand (19). By relating a two compartment model of the lung to the effectiveness of the lung in oxygenating blood, and by graphical "curve stripping" methods applied to the washin and washout of inert gases, they were able to define the fractional volume and ventilation of two groups of more and less ventilated alveoli. Their results illustrated major differences between emphysematous and normal lungs. In brief, normal lungs were found to behave as if

about half their volume was half as well ventilated as the rest of the lung, whereas, emphysematous lungs behaved as if three-quarters of the lung was only one-fifth to one-tenth as well ventilated as the remaining quarter. Although it was fully accepted (17-20) that the treatment of the lung as two or even three compartments could not be a realistic representation of the true functioning of the lung, the work of Briscoe and Cournand proved to be an invaluable aid to the understanding of pulmonary gas exchange principles.

The lung is known to consist of millions of alveoli¹ which help to make up a multitude of miniature gas exchangers. With this in mind, Farhi and Rahn (21) had been drawn to the conclusion that the distributions of \dot{V}_A and \dot{Q} are more akin to continuous rather than discrete functions. They considered the effects of a hypothetical logarithmic normal distribution of \dot{V}_A/\dot{Q} ratios and showed how it could produce appreciable A-a oxygen and carbon dioxide gradients.

The concept of recovering continuous distributions of \dot{V}_A and \dot{Q} was further explored by Gomez (22-24) and later by Gomez et al (25). By assuming a certain parametric function for the ventilation or blood flow distributions, direct numerical integration techniques were used to obtain distributions in various normal and abnormal lungs.

1.

Hansen and Ampaya (Appl. Physiol. 38, 990-995, 75) estimate that 336 → 454 million alveoli exist in the human lung.

Significant differences were found between normal lungs and those with pulmonary obstructive diseases. However, because of the restrictions of direct numerical integration, the parametrization cannot recover bi or trimodal distributions and does not appear to be able to resolve areas of very low specific ventilation.

As an alternative solution to the recovery of continuous \dot{V}_A/\dot{Q} distributions, Lenfant and Okubo (26, 27) suggested using Laplace transforms and the change in arterial O_2 saturation with increasing F_{IO_2} during a nitrogen washout. The blood flow distribution as a function of the clearance time constant was obtained by means of an iteration procedure, and from the inversion of the Laplace transform by an approximation method. From their results, they were able to suggest that the predominant disturbance, in diseased subjects, is in the relationship between ventilation and lung volume rather than between lung volume and blood flow. However, their methodology was later criticized on the grounds of inaccuracy in respect of the Laplace transform inversion (28).

The problem of discovering the true existing \dot{V}_A/\dot{Q} distributions appeared to be finally solved when Wagner et al (29) described their theory based on the retention of six inert gases. Using the basic steady state equation developed by Farhi (30) and assuming a one hundred compartment lung model, they were able to express the retention of six inert gases in terms of

fractional ventilation and perfusion and solubility. By using the method of least squares to compare theoretical retention to experimentally measured values they were thus able to solve for values of \dot{V}_A and \dot{Q} to each compartment. The technique was relatively simple and allowed consistent reproducibility of theoretical distributions. Jaliwala et al (31) later added non-negativity constraints and fully investigated the effects of noise.

It seemed the problem of recovering continuous distributions had been resolved until Olszowka (32) demonstrated how the distributions obtained by Wagner et al were non-unique. Their systems involved the use of six data points to evaluate one hundred unknown parameters, and under such conditions the system is heavily underdetermined. A number of distributions can be found which equally well fit the six data points. In an attempt to overcome this severe theoretical criticism, Evans and Wagner (33) proposed a 'bounds analysis' and Lewis et al (34) suggested the use of an increased number of data points by means of the nitrogen washout test. But neither Evans and Wagner, nor Lewis et al, have discovered a way of overcoming the basic criticism lodged by Olszowka.

1.ii An Overview of the Thesis

In the forthcoming chapters a new method will be presented which combines parametrizing the distribution with standard computer minimization procedures. The method recovers unique solutions and overcomes many of the criticisms lodged at previous models. Nitrogen washout curves are examined for twelve subjects; ten normal and two diagnosed as having obstructive pulmonary disorders. Comparison is made between standard compartmental fitting techniques (29), using a seven compartment lung model, and the new parametrization method with one hundred lung compartments. The method is shown to give good reproducibility in the presence of random error, and although only distributions similar to the chosen parametrization can be recovered, the minimization procedure is capable of indicating whether the parametrization is a sensible representation. Numerical integration of the distribution is not necessary, due to the addition of a computer minimization routine. Hence the parametrization can be more representative of the true distribution than those demonstrated by Gomez et al. Distributions are presented of fractional ventilation as a function of specific ventilation for all twelve subjects. The theory, described in chapter 3, provides a system with more data points than unknowns, such that Olszowka's criticisms regarding under-determined systems do not apply, and reproduction of a number of theoretical distributions, described in chapter 4, show

a high degree of resolution.

1.iii Conclusions

A number of important conclusions result from analysis of the experimental N₂ washout data obtained from the normal and abnormal subjects. It appears that modelling the lungs as a small number of compartments is very useful as an indication of the presence of an abnormality. Ensuing parametrization analysis, which allows the lung to be considered as a continuum, shows the lung to consist of two main respiratory zones with a volume ratio of 6.04 (\pm 1.79) in normals and which increases with age. Total ventilation to these zones is less uniform amongst normals which corroborates similar statements made by Lenfant and Okubo (27), but inhomogeneities within the zones are found to be well-defined throughout the normal group.

In conclusion, qualitative analysis and semi-quantitative analysis of the lung may be obtained from fitting data to a small number of lung compartments. However, in order to classify diseases for diagnostic and therapeutic purposes, more detailed information is required. Although the parametrization of a distribution does 'force' the recovered distribution to some extent, nevertheless the combination of parametrizing the distribution with computer minimization routines, allows more realistic functions to be produced, and principal features

of the original distributions are preserved. This technique offers a new approach to the recovery of quasi-continuous distributions of ventilation, lung volume and, in future studies, blood flow.

CHAPTER 2

REVIEW OF METHODS TO RECOVER DETAILED LUNG DISTRIBUTIONS

2.i Recovering Continuous Distributions

The effects of uneven ventilation, lung volume and perfusion on gas exchange have long been recognised, although the measurement of such possible inequalities existing in the lungs has posed many problems. Following the conclusions of Farhi and Rahn (21), numerous investigators began to search for ways of recovering continuous distributions of ventilation, lung volume and perfusion. The treatment of the lung as a continuum proved, however, to be a highly complex mathematical problem. One of the most significant contributions to the field came from Lenfant and Okubo (27), in which using a standard lung model, they expressed the increase in oxygen content during a nitrogen washout as an integral function of the blood flow, ventilation and lung volume distributions. From successive transformations of the original gas exchange equations, a final expression was obtained as in equation (1), the symbols being explained in Appendix 1.

$$h(t) = \frac{B}{Q_T} \int_0^{\infty} T q(T) e^{-t/T} dT \quad (1)$$

Using an approximation method, this expression is now in a form to obtain $q(T)$ by means of a Laplace Transform inversion. Lenfant and Okubo were able to demonstrate blood flow distributions in both normals and abnormals. By similar techniques, Okubo and Lenfant (26) were also able to determine volume and ventilation distributions. The approximation method used to obtain the inversion of the Laplace Transform has, however, been criticised because of its inability to resolve any detailed structure of the distributions. Thus, recovered distributions will tend to be broader and smoother than the true distributions, and direct inversion of the Laplace Transform is made impossible by the very large effects of experimental errors. Nevertheless, important overall conclusions were made from the recovered distributions. It was discovered that for the majority of normals, most of the blood flow distribution follows the pattern of lung volume inequalities very closely, whereas the ventilation distribution varies to a large extent even amongst normals, and does not necessarily resemble the lung volume distribution. Moreover, it was concluded that ventilation-lung volume inequalities have a more significant effect on pulmonary gas exchange than ventilation perfusion inequalities.

Previous research by Gomez (22-24) and later by Gomez et al (25) also considered the various distributions in the lung as continuous mathematical functions. Initially, Gomez

used the direct Laplace transform as a means of obtaining solutions to integral equations of gas exchange, but subsequently suggested parametrization of functions such as blood flow, so that the distribution functions could be determined by direct numerical analysis. Using this technique, studies were made of specific ventilation distributions from nitrogen washout curves obtained from normal and emphysematous subjects. Strikingly different distributions were obtained for normal and diseased subjects. In normals the pattern was assymmetric with the function resembling a beta type function. In pulmonary obstructive diseases the principle characteristic was the occurrence of a narrow peak amplitude at very much lower values of the specific tidal ventilation. Although the continuous distributions recovered by Gomez et al do show deviations amongst subject groups, the parametrization functions used to define the distributions of specific ventilation are not general enough to recover detailed structure.

2.ii Recovering Quasi-Continuous Distributions

With the advent of more sophisticated computer minimization routines it became feasible to recover a large number of unknown parameters from the equations of gas exchange and led to the idea of considering the lung as a quasi-continuum. Thus, Wagner et al (29) developed the concept of a lung model consisting of up to one hundred gas exchanging compartments, each compartment receiving a proportion of the

total tidal ventilation and pulmonary blood flow. In order to obtain ventilation perfusion distributions, Wagner et al infused six inert tracer gases into a peripheral vein and, after steady state conditions had been established, mixed arterial and mixed expired gas concentrations were simultaneously measured. The ratios of mixed arterial to mixed venous concentrations (the retention, R) and mixed expired to mixed venous concentrations (the excretion, E) were plotted as a function of the solubility, λ (the Ostwald solubility coefficient), for each gas.

Farhi's steady state equations of inert gas exchange (30) allow the retention R, and excretion, E, of a gas, i, to be expressed in terms of the solubility and the ventilation-perfusion distribution as in equations (2) and (3),

$$R_i = \frac{1}{\dot{Q}_T} \sum_{j=1}^{j=N} \frac{\dot{Q}_j \lambda_i}{\lambda_i + \dot{V}_j / \dot{Q}_j} \quad (2)$$

$$E_i = \frac{1}{\dot{V}_T} \sum_{j=1}^{j=N} \frac{\dot{V}_j \lambda_i}{\lambda_i + \dot{V}_j / \dot{Q}_j} \quad (3)$$

where N is the number of lung compartments, which is large enough such that the distributions approach a continuum.

Consider equation (2) which expresses the retention of a gas of solubility λ_i . If the retention of six inert gases is simultaneously measured, then six experimental data points are available. Corresponding to these six data points are the unknown compartmental values of fractional perfusion and ventilation perfusion ratio. The number of unknowns can be reduced if compartmental values of $(\dot{V}/\dot{Q})_j$ are assumed to be equally spaced on a logarithmic scale, which for one hundred compartments is an accurate approximation. Thus, the final problem is one of recovering one hundred values of \dot{Q}_j/Q_T , corresponding to values of $(\dot{V}/\dot{Q})_j$, from six measured values of retention.

A solution may be found from computer minimization procedures and in this case Wagner et al chose to consider the method of least squares. Initial values of \dot{Q}_j/Q_T and $(\dot{V}/\dot{Q})_j$ are chosen arbitrarily and using equation (2), theoretical values of R_i are calculated. When the distribution of \dot{Q}_j/Q_T as a function of $(\dot{V}/\dot{Q})_j$ is identical to the original, then

$$R_i \text{ (theoretical)} = R_i \text{ (experimental)} \quad (4)$$

Expressing this in terms of the sum of squares, L,

$$L = \sum_{i=1}^{i=m} (R_i \text{ (th)} - R_i \text{ (exp)})^2 \quad (5)$$

and when equation (4) is satisfied, L tends to zero.

Hence, when the sum of squares approaches a minimum the correct distribution is defined. Logical means of approaching a minimum and improving the initial assumed distribution are complex, and Wagner et al chose to use a computerized version of the Newton-Raphson gradient method (35).

More recently, Lewis et al (34) suggested extending the use of Wagner et al's protocol to the non-steady state nitrogen washout test. Using a similar quasi-continuous lung model together with computer minimization techniques, attempts were made to recover distributions of fractional ventilation as a function of specific ventilation.

However, the measurement of continuous distributions of ventilation perfusion ratio by Wagner et al initiated enormous controversy over the validity of their results. In order to test their theory, Wagner et al had demonstrated the recovery of several theoretical distributions from error free data. Later, however, Jaliwala et al (31) determined the recoverability of theoretical distributions when error was present on the data and showed that the accuracy of the

recovered distributions could be severely effected by random experimental error. But the greatest criticism of the method came from Olszowka (32) who reiterated the fact that when the number of data points is less than the number of unknowns, the recovered distributions are not unique. Olszowka classed such systems as underdetermined. An example of an underdetermined system is easily explained. Consider the equation of a straight line,

$$y = ax + b$$

(6)

If only a single value of y is known, corresponding to a certain value of x , then the constants a and b cannot be defined. If, however, two coordinates can be measured then in the absence of experimental error, unique values of a and b can be determined. Olszowka proved mathematically that the remarkable recovery of theoretical distributions by Wagner et al was due to a phenomenon which he referred to as "minimum length solutions". For the recovery of a confident unique solution, the number of data points must outweigh the number of unknown parameters.

This criticism of Olszowka could not be reputed, and in order to partially solve the problem, Evans and Wagner (33) showed that although their solutions were not unique, they were able to assign probabilities for a given set of data coming from a certain distribution. For example, if a well separated bimodal distribution was recovered then the underlying distribution had a high probability of being multimodal.

Alternatively, if a narrow unimodal distribution was observed, then it was very improbable that the true distribution was bimodal with well separated modes. Nevertheless, their recovered distributions are still subject to doubt and one has to observe very marked deviations in the distributions to be able to class normals and abnormals.

It is essential to understand the concept of underdetermined systems in the context of the ventilation-perfusion problem. However, the conclusions are equally applicable to the recovery of ventilation-specific ventilation distributions from nitrogen washout data. It has already been demonstrated with the simple example of the straight line equation that the number of data points must equal, or ideally be greater than the number of unknowns. However, it is not merely sufficient to obtain $N_{\text{data}} \gg N_{\text{unknown}}$, but the data must also be representative. For example, areas of very low \dot{V}/\dot{Q} ratio can only be resolved by fitting data from the retention-solubility curve in the region of very low solubility. Similarly, retention from regions of very high V/Q ratio is only accurately determined from studying gases with very high solubility. Olszowka gave examples of several distributions which are indistinguishable by virtue of the number of data points being less than the number of unknowns. But it is also possible to demonstrate how even with $N_{\text{data}} \gg N_{\text{unknown}}$, the system may still be underdetermined.

Consider non-steady state retention, that is, a curve of

retention as a function of time in the initial stages of Xenon uptake as in Figure 1A. If the total length of observation is ten seconds, and the time interval between measurements of concentration is 0.1 seconds, one hundred data points may be obtained. However, the information is not significantly greater than if only ten data points at one second intervals are observed, since the retention curve is still in the linear stage.

The \dot{V}/\dot{Q} distribution which produced the retention time curve for Xenon in Figure 1A is shown in Figure 2. However, a homogeneous lung with \dot{V}/\dot{Q} ratio equal to 0.01 was found to give an almost identical Xenon retention curve in the first ten seconds of uptake, and which would thus be difficult to distinguish if only data from the linear portion of the curve was obtainable. Figure 1B compares the two retention time curves for the two lung models and demonstrates the importance of obtaining a significant proportion of the uptake curve.

In conclusion, therefore, to obtain sensible recovery of distributions of ventilation, perfusion or lung volume, the number of data points *must* be greater than the number of parameters to be determined. When experimental error is present, the number of data points must be even greater, and it is essential to obtain data which is representative of all regions of the lung.

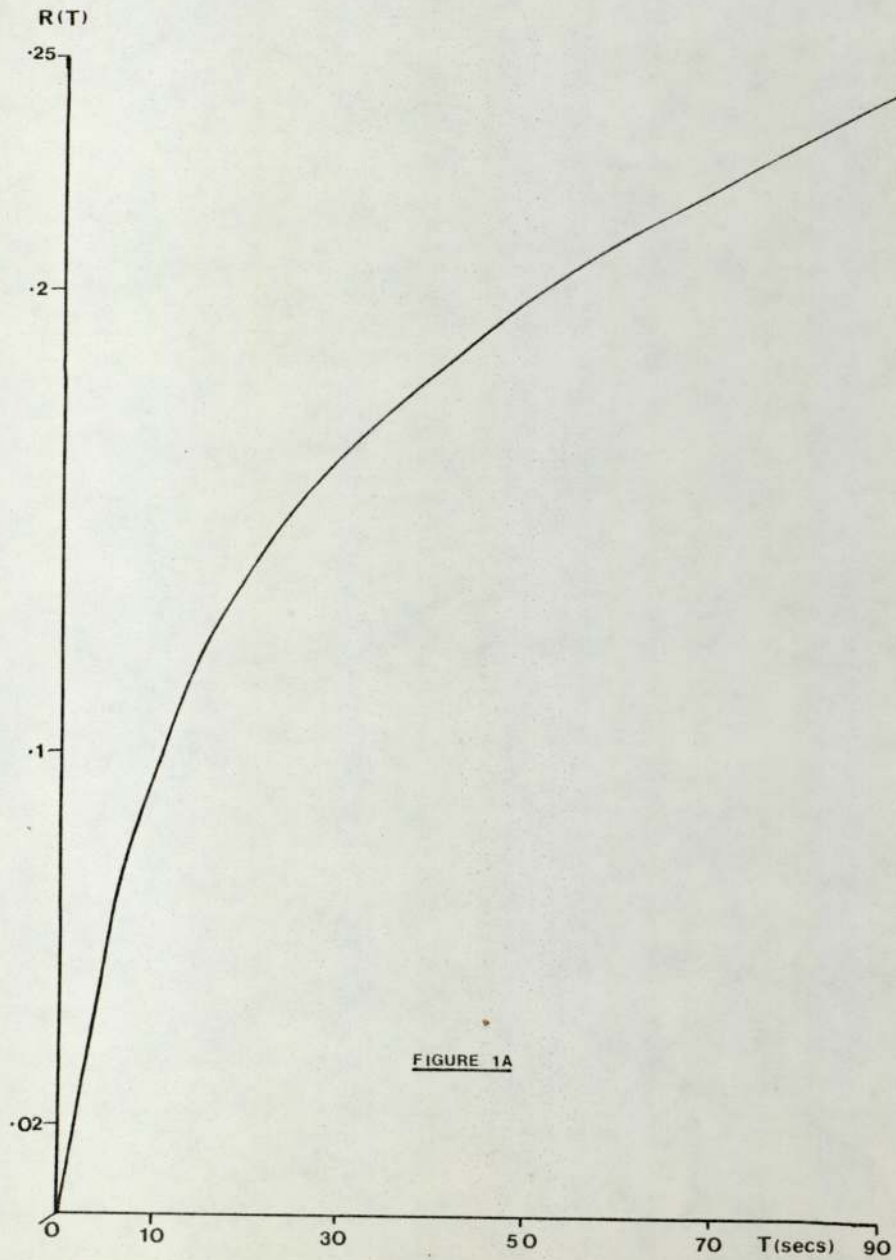


FIGURE 1A

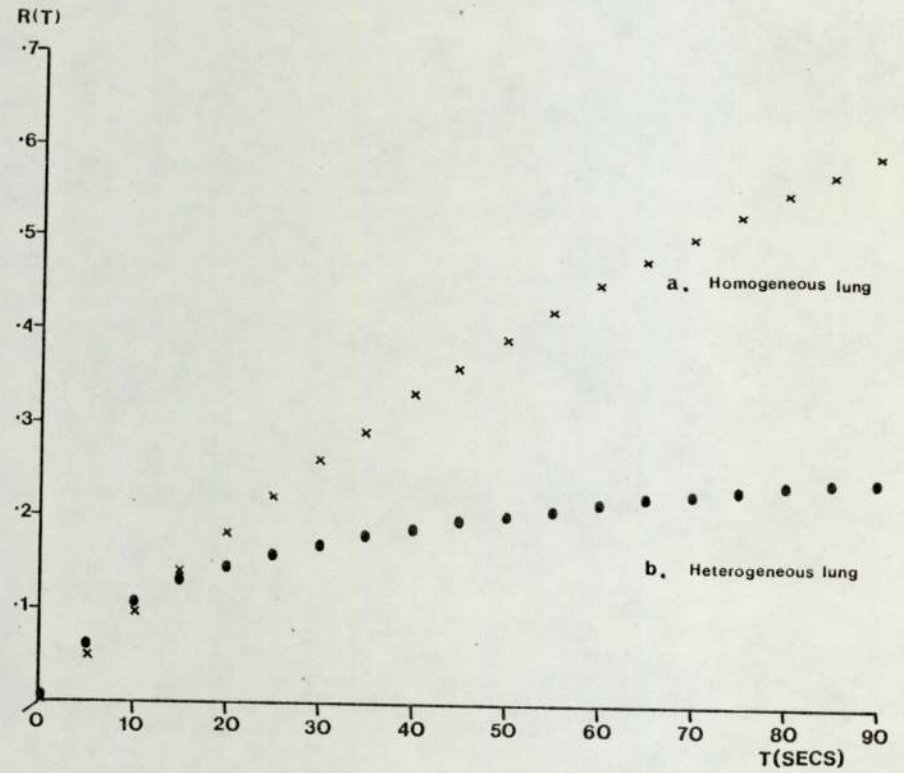


FIGURE 1B

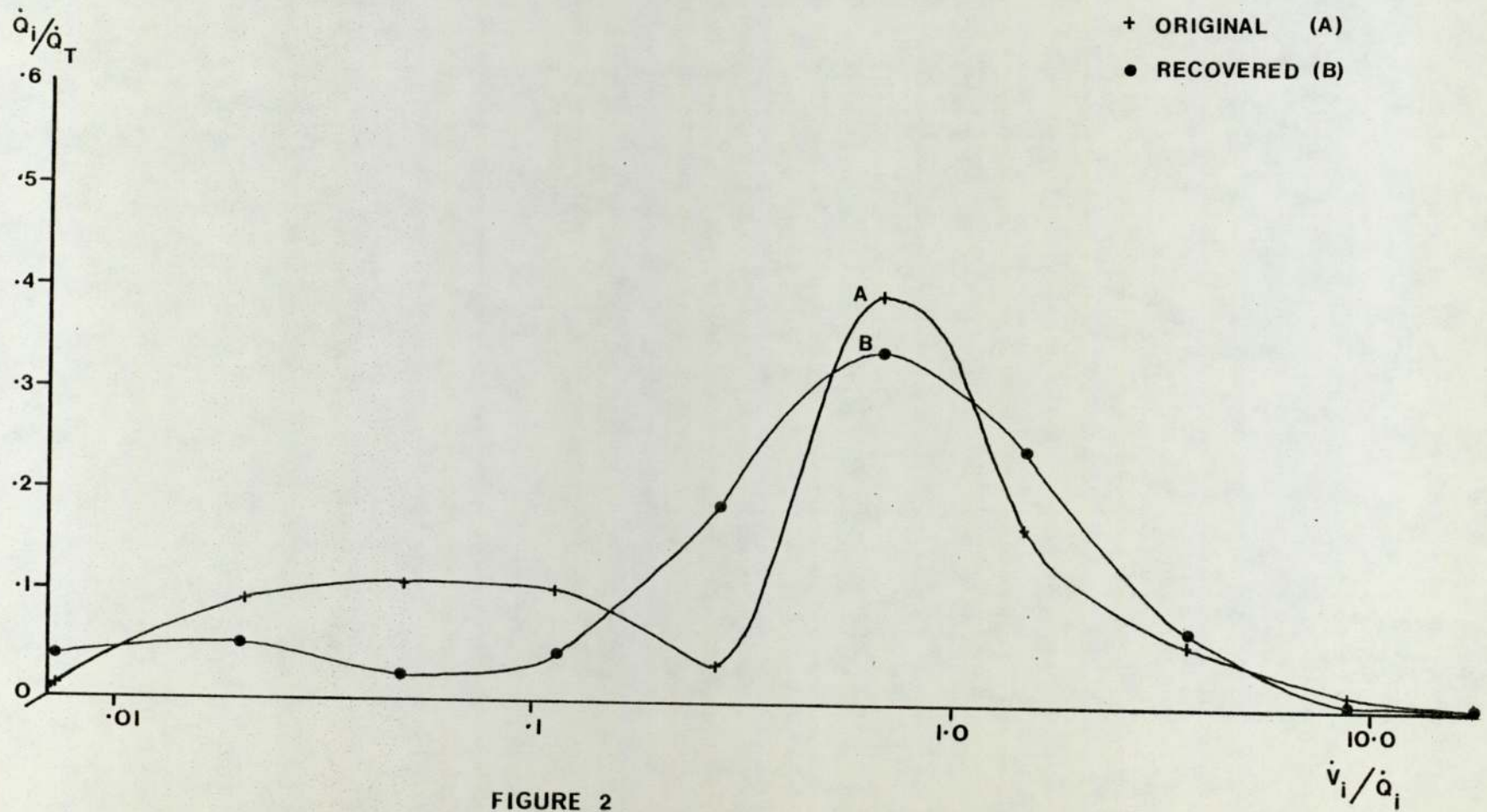


FIGURE 2

CHAPTER 3

A NEW TECHNIQUE FOR OBTAINING UNIQUE DISTRIBUTIONS

3.1 The Lung Model

Before describing the new technique for ensuring the recovery of unique distributions from a nitrogen washout curve, the model of the lung which simulates the theoretical nitrogen washout curves must be described. The lung was assumed to consist of a number of homogeneous compartments ventilated in parallel and each having unique values for volume, specific ventilation and alveolar end-expired gas concentrations. It was assumed that all series inequalities had a parallel equivalent (36), and as such were not specifically included in the model. If the nitrogen concentration through the lung is initially given by C_0 , then after one breath of pure oxygen the concentration in the i^{th} compartment can be expressed as,

$$C_1 (i) = C_0 \cdot V_L (i) / (V_L (i) + V(i)) \quad (8)$$

where $V_L (i)$ is the end-expired volume of the i^{th} compartment, and $V(i)$ is the tidal ventilation to the i^{th} compartmental.

Equation (8) applies to a lung model which makes no account of anatomical dead space or the contribution of nitrogen from the blood. These factors decrease the rate of washout of nitrogen and are therefore defined by a term which represents the "inefficiency" of the system. The inefficiency parameter, E , is assumed to be constant over the period of washout, which over a period of twenty to forty breaths is a reasonable approximation (50). Thus, equation (8) is modified such that,

$$C_1(i) = C_o \left[\frac{V_L(i)}{V_L(i) + V(i)} + E \right] \quad (9)$$

After m breaths of pure oxygen,

$$C_m(i) = C_o \left[\frac{V_L(i)}{V_L(i) + V(i)} + E \right] \quad (10)$$

and the mean expired concentration must be given by,

$$\frac{C_m}{C_o} = \sum_{i=1}^{i=n} \left[\frac{V(i)}{V_T} \frac{V_L(i)}{V_L(i) + V(i)} + E \right] \quad (11)$$

Equation (11) can be further rearranged to give the mean expired nitrogen concentration of the m^{th} breath in terms of the fractional ventilation, $V(i)/V_T$ and specific ventilation, $V(i)/V_L(i)$, as in equation (12).

$$\frac{C_m}{C_o} = \sum_{i=1}^{i=n} \frac{V(i)}{V_T} \left[\frac{1}{1 + S(i)} + E \right] \quad (12)$$

where $S(i) = V(i)/V_L(i)$

and n is the number of lung compartments.

For given distributions of $V(i)/V_T$ as a function of $S(i)$, equation (12) can be used to generate a theoretical nitrogen washout curve. Since an experimental nitrogen washout curve must contain a degree of error, random noise is generated to simulate the experimental situation. Random numbers were generated between ± 1 and the error on each data point was defined as,

$$e_i = 2 r p - p$$

where e_i is the error on the m^{th} data point

r is the random number between ± 1

and p is the percentage noise

The concentration of N_2 in the expirate of the m^{th} breath can then be expressed as,

$$C_i = C_i + e_i$$

3.ii Reducing the Number of Unknowns

Although the N₂ washout enables a larger number of data points to be obtained, unique distributions can still only be recovered if the number of unknowns is less than N_{data}. In the least squares fitting procedure suggested by Wagner et al the number of unknowns equals the number of lung compartments and hence N_{compt} must be less than N_{unknown}. However, a technique is now described with which unique solutions may be recovered and where the number of unknowns is independent of the number of lung compartments. Hence, quasi-continuous, one hundred compartment distributions of ventilation and specific ventilation can confidently be recovered with a limited number of breaths of a N₂ washout curve.

Consider, for example, that the distribution of $\frac{V(i)}{V_T}$ as a function of $(V/V_L)_i$ across the lung is a straight line. The fractional ventilation can now be expressed in terms of the specific ventilation by the function,

$$\frac{V(i)}{V_T} = a (V/V_L)_i + b \quad (13)$$

If it is again assumed that for quasi-continuous distributions $(V/V_L)_i$ are equally spaced on the log of the abscissa, then the only unknowns in equation (13) are a and b.

The number of unknowns is thus reduced to two and more importantly, is independent of the number of lung compartments.

Such a technique for reducing the number of unknowns is termed parametrizing the distribution, but unlike Gomez et al (25), the values of a and b are determined by a computer minimization routine. Thus, a quasi-continuous lung model is used to calculate theoretical values of nitrogen concentration from a continuous parametrization of ventilation as a function of specific ventilation.

3.iii Determining a Suitable Parametric Function
by Compartmental Fitting

Equation (13) is probably not a very realistic description of the distribution of fractional ventilation as a function of specific ventilation in the lung, but is useful for illustration purposes. Since the detailed physiology of the lung has still to be determined, it is not sufficient to merely assume that one general parametric function such as a straight line or a logarithmic normal can represent the distribution of all normal or abnormal lungs. Thus, it is necessary to first determine the type of function which would be most likely to describe the distribution existing in the particular lungs being studied.

The nitrogen washout generally enables a minimum of fifteen data points to be studied and therefore it is possible to determine at least eight unknowns, even in the presence of experimental errors. Hence, if the lungs is considered as a system of seven gas exchanging compartments plus dead space, then these eight unknowns can be determined directly by computer minimization (assuming values of $S(i)$ to be equally spaced on a log scale). Although such a lung model cannot recover detailed information concerning the distributions, the overall structure can be determined and a suitable parametric function chosen. Fitting the data to a small number of lung compartments is termed here as *direct compartmental fitting*.

The model simulating nitrogen elimination from the lung gave an expression for the ratio of end-expired nitrogen concentrations of the m^{th} breath to the initial concentration, as

$$\frac{C_m}{C_o} = \sum_{i=1}^{i=n} \frac{V(i)}{V_T} \left[\frac{1}{1 + S(i)} + E \right] \quad (14)$$

where C_m/C_o is the *theoretical* value of the nitrogen concentration of the m^{th} breath compared to the initial concentration.

That is,

$$C_m/C_o = C_m^{th} \quad (15)$$

Now, the unknowns in equation (14) are the fractional ventilations to n compartments and the inefficiency parameter E . Therefore,

$$N_{\text{unknown}} = N_{\text{compt}} + 1$$

Although the minimization routine, described in detail in Appendix 2, is capable of recovering up to twenty unknowns, the efficiency of the program is greatly reduced as N_{unknowns} is increased. The number of lung compartments was therefore kept as small as possible.

However, it was felt that the minimum number of lung compartments which could feasibly reproduce a continuous distribution was seven, which gave a total of eight unknowns.

The minimization procedure for the recovery of these unknowns is best described as a series of steps (a detailed description of the subroutines SEEK, SIMPLEX and MIGRAD is given in Appendix 2).

1. Read in the experimentally measured values of C_m/C_o and call these values C_{mexp} . Read in the initial

assumed values of fractional ventilation, $\frac{V(i)}{V_T}$
assuming the distribution of $(V(i)/V_T)$ against
specific ventilation to resemble an inverted
parabola. (The starting distribution has no effect
on the recovered distribution.)

2. Calculate corresponding values of specific ventilation, $(V/V_L)_i$ such that they are equally spaced on the log scale of the abscissa.
3. Calculate values of C_{mth} from these compartmental values of fractional ventilation and specific ventilation.
4. Calculate the value of least squares, L , where

$$L = \sum_{j=1}^{j=m} (C_{mexp} - C_{mth})^2 \quad (16)$$

When L equals zero, the values of fractional ventilation and specific ventilation to equal those present in the lung. It is very rare, however, that in a well determined system and with experimental error, L will ever equal zero, and in this program a minimum in least squares is said to have been obtained if the estimated distance to the minimum is less than 10^{-4} .

It is possible to make the test more discriminating if constraints are added to the value for least squares (31). For example, we know that the sum of the fractional ventilations must not be greater than unity, and cannot be negative. Therefore, solutions may be excluded which do not conform to these constraints by including extra terms as in equation (17).

$$\begin{aligned}
 L = & \sum_{j=1}^{j=m} (C_{mexp} - C_{mth})^2 + \sum_{i=1}^{i=n} \frac{V(i)}{V_T} \cdot 10^{12} \\
 & + \sum_{i=1}^{i=n} \left(\frac{V(i)}{V_T} - 1.0 \right)^2 \dots\dots\dots (17)
 \end{aligned}$$

The second term in equation (17) causes L to be very large and is included if the blood flow is negative, forcing the minimization routine away from unphysical solutions.

The third term in equation (17) ensures that the sum of the fractional ventilation is unity in the final solution.

5. Enter *SEEK*. This subroutine uses a Monte Carlo search routine to find a reasonable starting distribution of ventilation and specific ventilation. Random numbers are generated between 0 and 1 and assigned to the compartmental values of fractional ventilation and E. The distribution which gives the lowest value

of least squares from equation (17) is used as the starting point for the next step. Hence, the recovered distributions are independent of the initial guess made in step 1.

6. Enter *SIMPLEX*. This subroutine improves the values of the unknowns such that L approaches a minimum.
7. If $L < 10^{-2}$, simplex is said to have converged and the program is advanced to the next step. If this condition is not met, the program returns to step 6.
8. Enter *MIGRAD*. This subroutine attempts to improve the minimum found by simplex using the Newton-Raphson method.
9. If *migrad* fails to converge re-enter simplex at step 6.
If the value of L found by *migrad* is less than 10^{-4} advance to step 10.
10. Write out the values of the n fractional ventilations and the value of E .
11. STOP

3.iv Recovering Quasi-continuous Distributions:
Parametrization Fitting

Having obtained an overall picture of the distribution from direct compartmental fitting, a suitable parametric function can be chosen. Consider, for example, that the general picture of the distribution resembled that of a straight line, then the n fractional ventilations are related to the n values of specific ventilation by equation (13). The number of unknowns is now given by,

$$N_{\text{unknown}} = N_{\text{para}} \quad (18)$$

where N_{para} corresponds to a and b in equation (13). Since the number of unknowns is independent of the number of lung compartments, quasi-continuous distributions can be recovered. The system contains only two unknowns and at least fifteen data points and therefore unique solutions are now possible.

The minimization routine for parametrization fitting can be summarised by the following procedures:-

1. Read in the experimentally measured values of C_{mexp} . Read in the initial assumed values of a and b .

2. Calculate the values of $(V/V_L)_i$ such that they are equally spaced on the log scale of the abscissa.
3. Calculate corresponding values of fractional ventilation, $V(i)/V_T$ from parametric function (in this case equation (7)) using current values of a and b.
4. Calculate values of C_{mth} from these compartmental values of fractional ventilation and specific ventilation.
5. Calculate the value of least squares, L, from equation (17)
6. Enter *SEEK*. Improve the initial guess of a and b, each time recalculating values of $V(i)/V_T$ and C_{mth} .
7. Enter *SIMPLEX*. Continue to improve the values of a and b such that L approaches a minimum.
8. If $L < 10^{-2}$ advance to step 9, otherwise return to step 6.
9. Enter *MIGRAD*. Improve distribution still further.

10. If migrad fails to converge re-enter simplex at step 6. If the value of L found by migrad is less than 10^{-4} advance to step 11.
11. Write out the values of the parameters a and b and the values of the n fractional ventilations and specific ventilations.
12. STOP.

CHAPTER 4

RECOVERY OF THEORETICAL DISTRIBUTIONS

If any conclusions are to be drawn from distributions recovered from experimental data, the ability to recover theoretical distributions must first be demonstrated. The following distributions were used to generate nitrogen washout curves and from this data attempts were made to recover the original distributions by means of direct compartmental and parametrization techniques. This enabled the efficiency of the two fitting procedures to be estimated.

4.1 Delta Type Function

A delta type unimodal distribution is a difficult function to recover by parametrization techniques owing to its rapid variation over a very small region. Nevertheless, it is an important distribution to recover, since it has been suggested (34) that delta type functions may exist in normal lungs. Therefore, a function as in Figure 3 and defined by one hundred coordinates was used to express the distribution of $V(i)/V_T$ as a function of $S(i)$ in the lung model. A nitrogen washout curve of thirty breaths duration was then generated and used to demonstrate the effects of the following parameters on the recovered distributions.

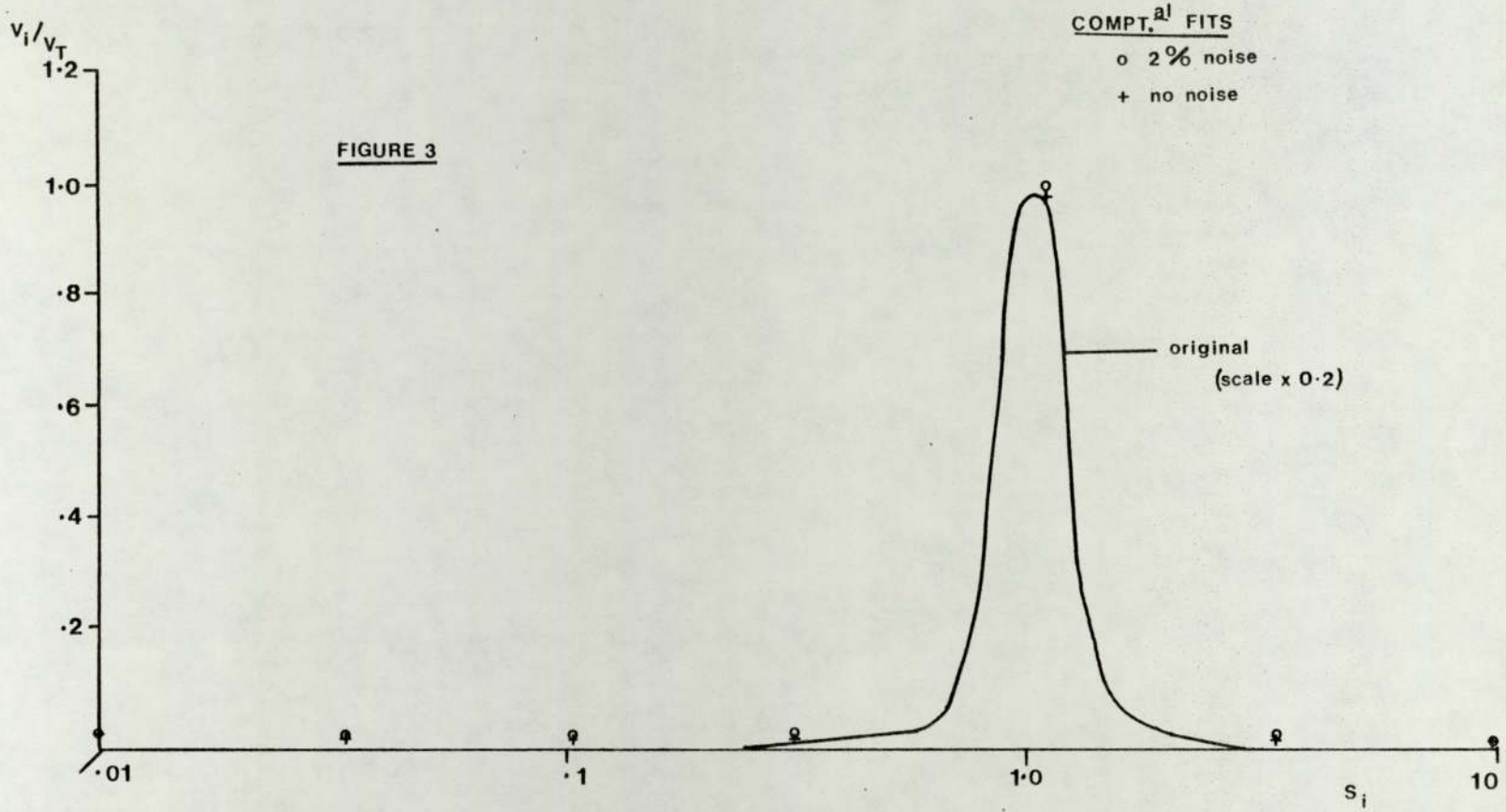


FIGURE 3

4.1 (a) Effect of noise

Experimental error was simulated, as described in section 3.1, and nitrogen washout curves were generated with 0% and 2% random noise. Figure 3 demonstrates the effect of noise on the recovery of a delta type function using a *direct seven compartment fit*. Curve A shows the original theoretical distribution used to generate the washout curves, whilst curves B and C are the recovered distributions with 0% and 2% error respectively. It appears that experimental error has little or no effect on these recovered distributions. The value of the fitted inefficiency parameter E was 0.34 and 0.35 with 0% and 2% noise respectively, compared to the true value of 0.5.

Although the recovered value for E is lower than the true value, it is of the correct order of magnitude.

The reproduction of the original distribution is remarkably good even though only seven lung compartments define the recovered distribution compared to one hundred in the original. The unimodal delta type features have been preserved, with 99.9% of the tidal ventilation directed towards a compartment with specific ventilation 0.53. From these compartmental fits, the following parametrization was chosen to represent the distribution of $V(i)/V_T$ as a function of $S(i)$,

$$V(i)/V_T = a \exp \left[- b (c - \log S(i))^2 \right] + d \exp \left[- e (f - \log S(i))^2 \right] \quad (19)$$

Using equation (19), therefore, to express fractional ventilation in terms of specific ventilation, Figure 4 illustrates the distributions recovered by the one hundred compartment *parametrization fit*. Curve A is the original distribution, and B and C are the fits to data with 0% and 2% noise respectively. When no noise was present in the data, the fitted distribution was a remarkably accurate reproduction of the original. The maximum fractional ventilation, $V(i)_{\max}$ of 0.174 occurred at a specific ventilation $S(i)_{\max}$ of 0.85, compared to the original $V(i)_{\max}$ and corresponding specific ventilation of 0.178 and 0.95 respectively. On the addition of 2% noise, the amplitude and width of the distribution were affected, but the position of the curve was virtually unaltered with $S(i)_{\max}$ equal to 0.8. Thus, Figures 4b and 4c demonstrate that the main features of the delta function can be recovered by a parametrization fit even in the presence of noise.

4.i (b) Effect of the number of compartments, N_{compt}

The above delta type distributions recovered by parametrization methods all assumed one hundred lung compartments. By coincidence, this was the number of lung compartments used to generate the theoretical nitrogen washout curves. It was

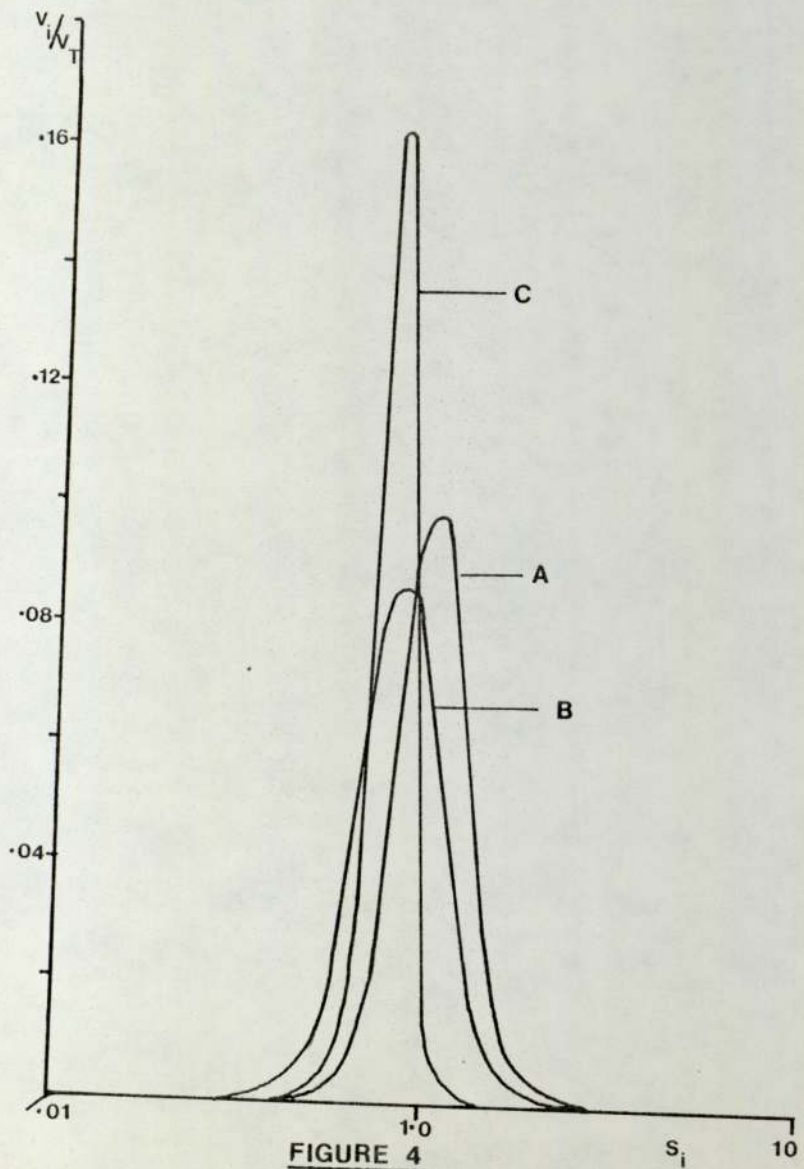


FIGURE 4

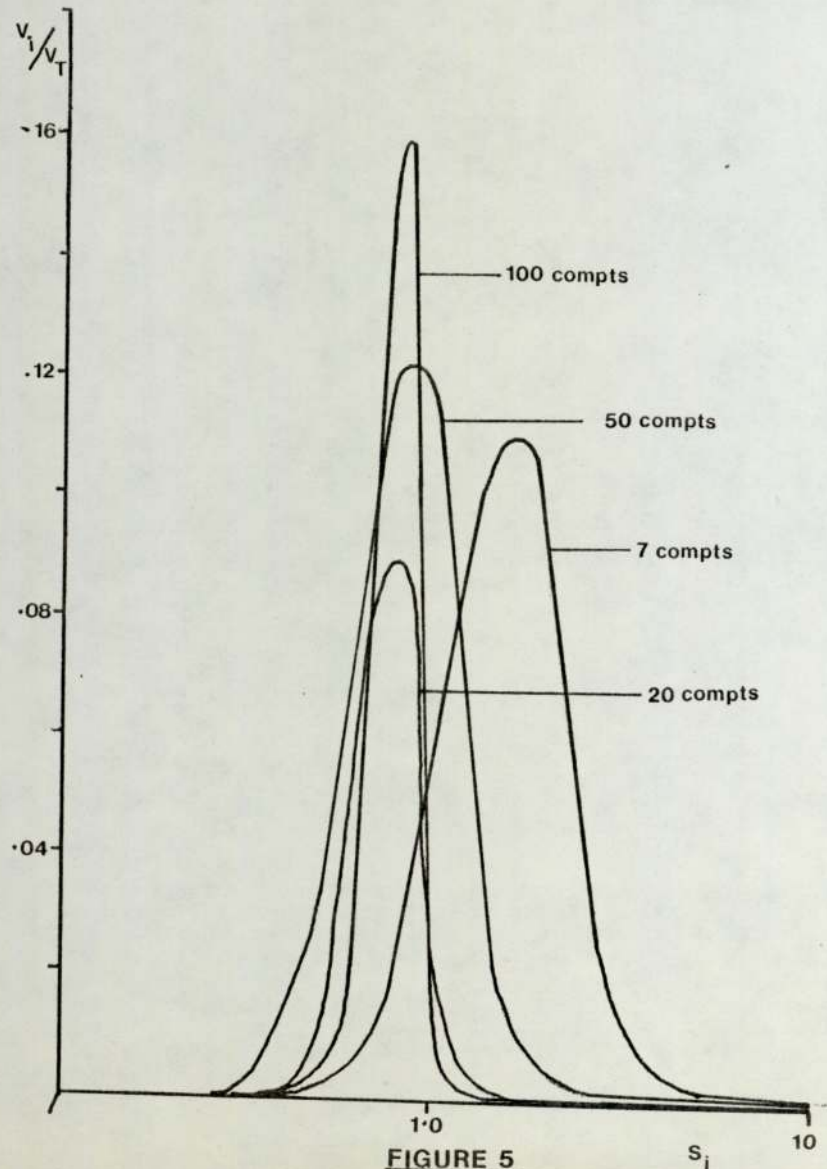


FIGURE 5

essential, therefore, to assess the effect of varying the number of compartments assumed by the fitting procedure.

Figure 5 shows distributions recovered with 100, 50, 20 and 7 lung compartments and demonstrates how the position on the x axis and the shape of the distribution is not affected by N_{compt} . Comparison of the amplitudes of the distributions is not really feasible since $V(i)_{\text{max}}$ is a fraction and indirectly dependent on the number of compartments. However, the values of $S(i)_{\text{max}}$ can be compared and are seen to remain virtually constant except for when N_{compt} is reduced to seven. However, this latter shift can be largely attributed to the limitations of available values of $S(i)$, due to the assumption that they are equally spaced on the x axis.

4.i (c) Effect of the number of data points, N_{data}

Olszowka clearly demonstrated the need for *the number of data points to be greater than the number of unknowns* for the recovered distribution to be *unique*. When noise is present on the data, even more data points are required to cancel the effects of random error. In general, the degree of cancellation of noise is proportional to the square root of the number of data points.

It has also been demonstrated that another essential consideration is that the analysis is performed over a significant portion of the washout or retention curve. Using data with 2% random error, figure 6 shows curve A recovered from data over 30 breaths and curve B from 20 breaths using the parametric function of equation (19) and one hundred lung compartments. The effect of reducing N_{data} on the recovered distribution was minimal. (Reducing N_{data} by ten was a choice made after experimental trials for which approximately 30 ± 10 breaths were obtained from each subject).

A direct compartmental fit was also performed with N_{data} equal to 20, but the effect was so small that it was not possible to discriminate between the two distributions graphically.

4.i (d) Effect of the Inefficiency Parameter, E

The value of E determined from the compartmental fit to data with 2% noise was 0.35 compared to the true value of 0.5. Since under experimental conditions the true value of E is unknown, it was crucial to demonstrate the effect of maldetermining E on the recovered distributions. Figure 7 illustrates distributions found from a parametrization fit, having assumed values for E of 0.5 and 0.0. It is immediately apparent that if E is ignored or underestimated, the recovered distribution shifts to areas of higher volume in order to

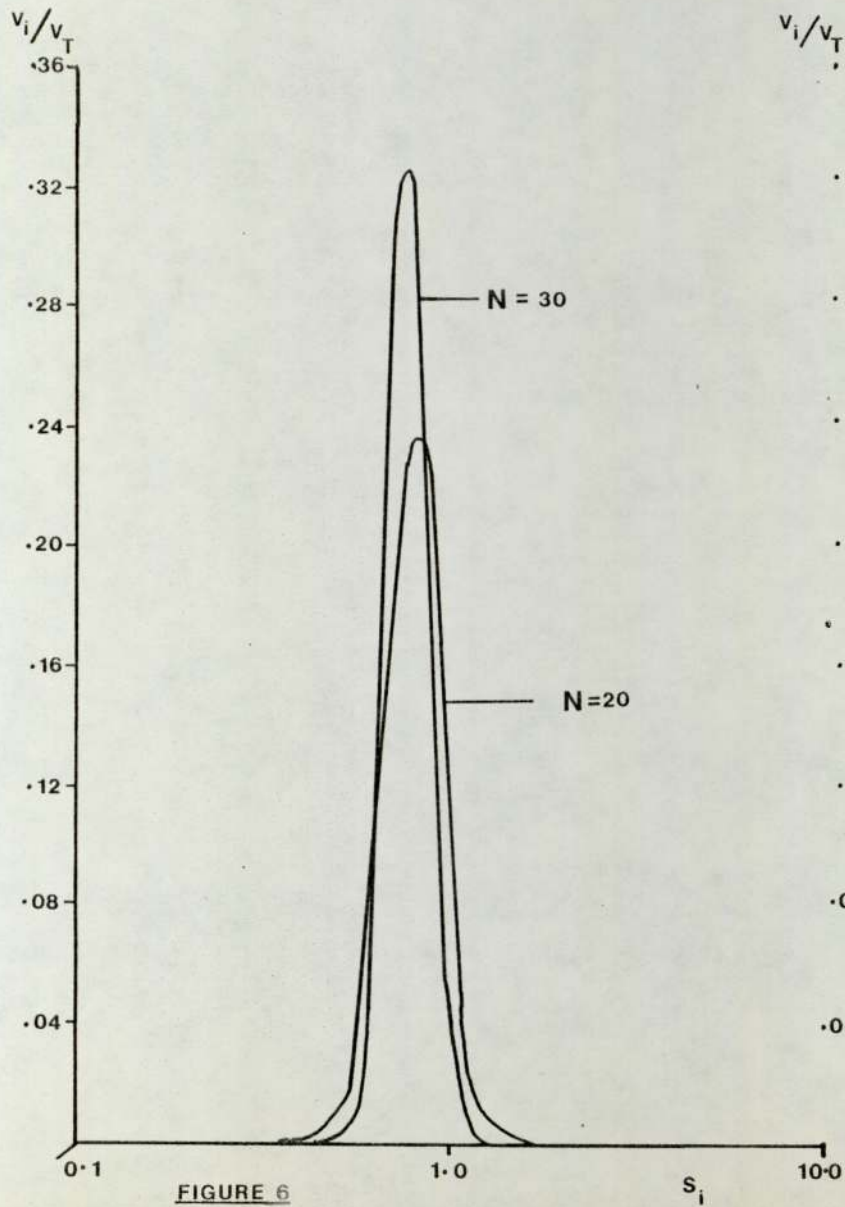


FIGURE 6

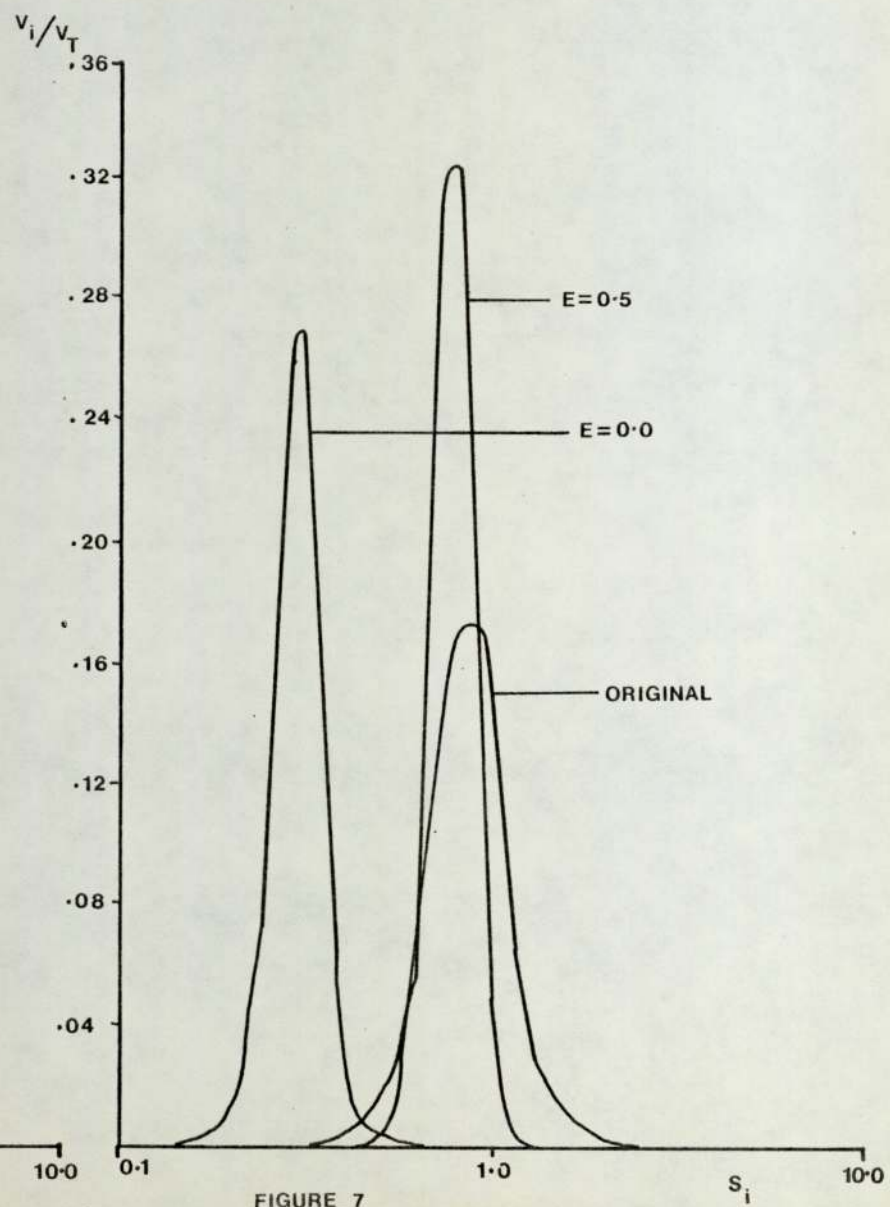


FIGURE 7

Table 1: Recovering a delta type function by parametrization fitting techniques

RECOVERED DISTRIBUTIONS

	N_{compt}	N_{data}	E	$S(i)_{\text{max}}$	$V(i)_{\text{max}}$
Original Distribution	20	30	0.5	0.95	0.196
0% noise	100	30	0.5	0.85	0.174
2% noise	100	30	0.5	0.8	0.326
"	50	30	0.5	0.8	0.246
"	20	30	0.5	0.78	0.9
"	7	30	0.5	1.5	1.11
"	100	20	0.5	0.8	0.234
"	100	30	0.0	0.3	0.27

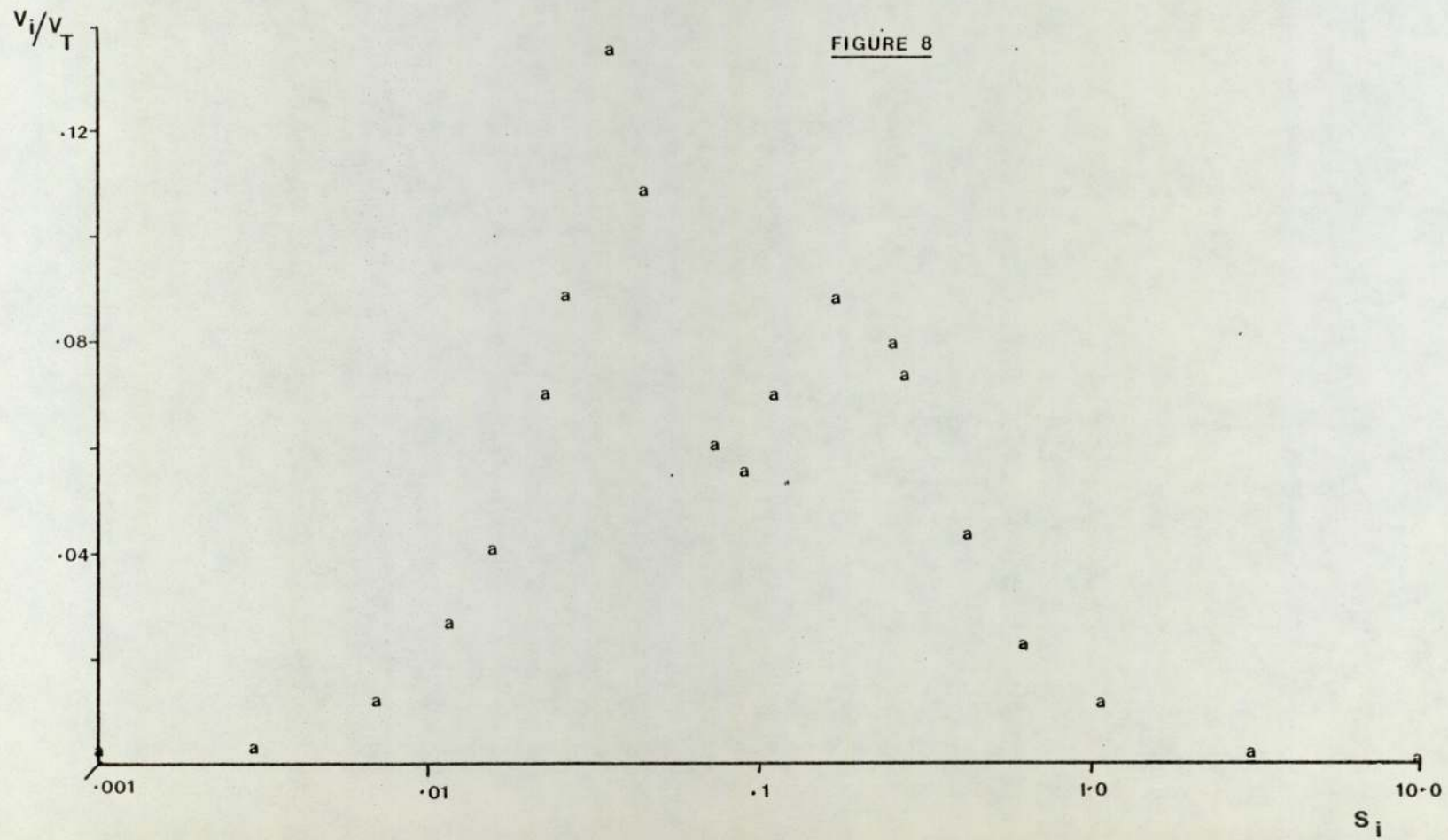
decrease the rate of N_2 washout normally accounted for by E. It is interesting, however, that the principle features of the distribution remain, and the distribution merely shifts to areas of lower specific ventilation.

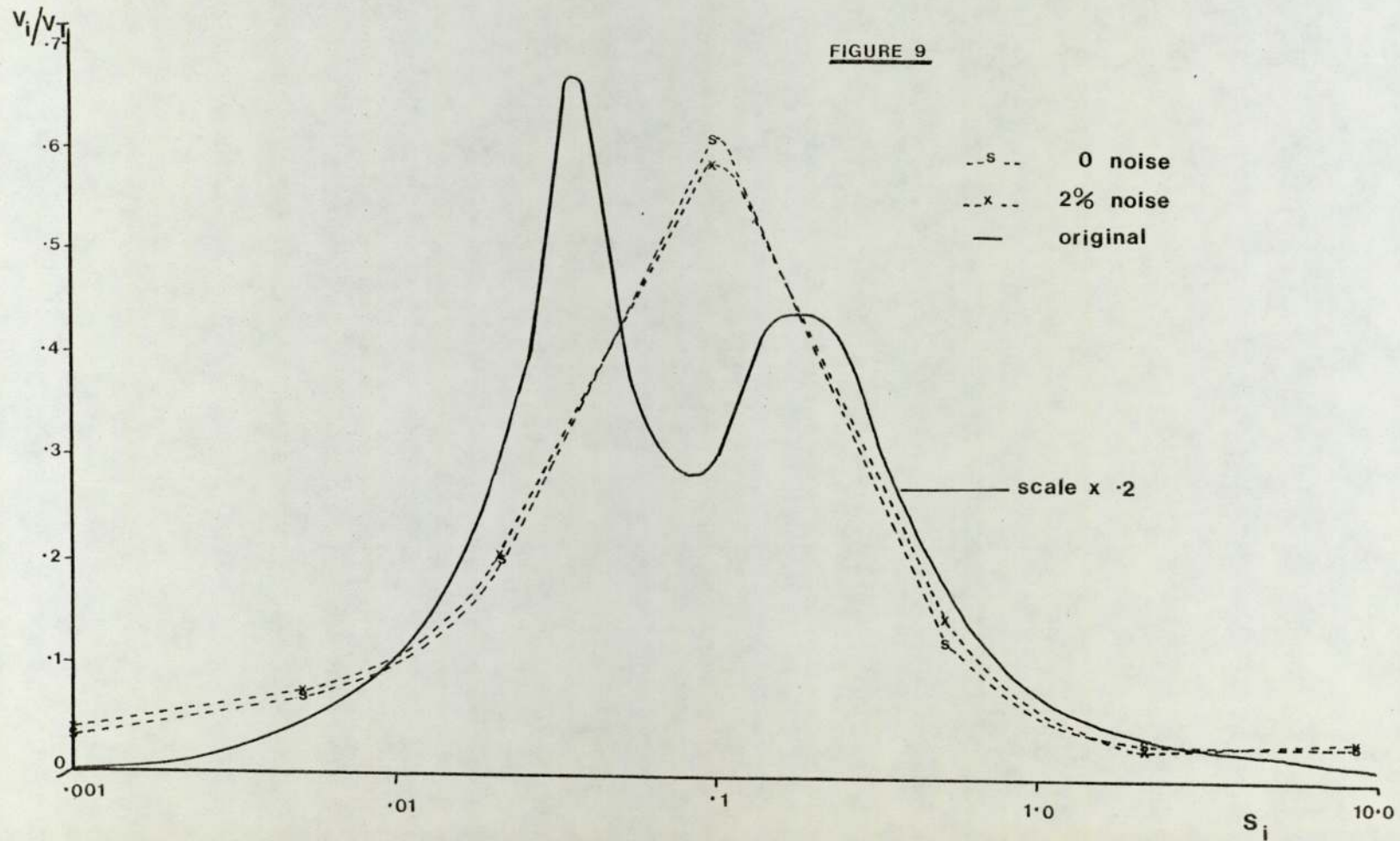
4.ii Bimodal Distribution

It is highly probably that the distributions existing in normal and particularly abnormal lungs are multi-modal. Figure 8 shows a 'hand drawn' bimodal distribution defined by twenty compartments with narrowly separated modes. In the practical situation it may not be feasible that values of specific ventilation are equidistant and hence a deliberate attempt was made to arbitrarily spread the values of $S(i)$, used to generated theoretical data.

4.ii (a) Effect of Noise

Data was generated from the above *bimodal* distribution with 0% and 2% noise. Figure 9 summarises the results of the *compartmental fit* to both sets of data. In both cases, a broad *unimodal* distribution was recovered, confirming previous results (29) which show how multi-modal features can be obscured if the number of recovered lung compartments is small. As with the delta type function, the *effect of noise was minimal for the compartmental fit*. The determined value of





E was 0.32 both with 0% and 2% noise in the data. The specific ventilation corresponding to the single peak ventilation was 0.1, and was unaffected by noise. Only the amplitude varied slightly from 0.6 to 0.57 with the addition of noise.

Although the compartmental fit remains a useful technique for determining the overall pattern of the ventilation-specific ventilation distribution, the broad underlying features cannot be reproduced. It is particularly in the case multi-modal distributions that it is essential to consider a relatively large number of compartments.

The original distributions consisted of twenty lung compartments randomly spaced on the $\log S(i)$ axis, and Figure 10 shows the distribution recovered using the *parametrization* of equation (19) with one hundred lung compartments equally spaced on the $\log S(i)$ axis. The recovered distributions are clearly bimodal for both error free data and data with 2% noise, and Table 2 lists the positions and heights of the two modes. Reproduction of the original features is not exact, the modes are narrower and more widely separated but the general features of the distribution have been preserved. In particular, the heights and position of the modes are of the correct order of magnitude even in the presence of noise, and the recovered function is certainly a more informative representation of the original distribution than that recovered from the compartmental fit.

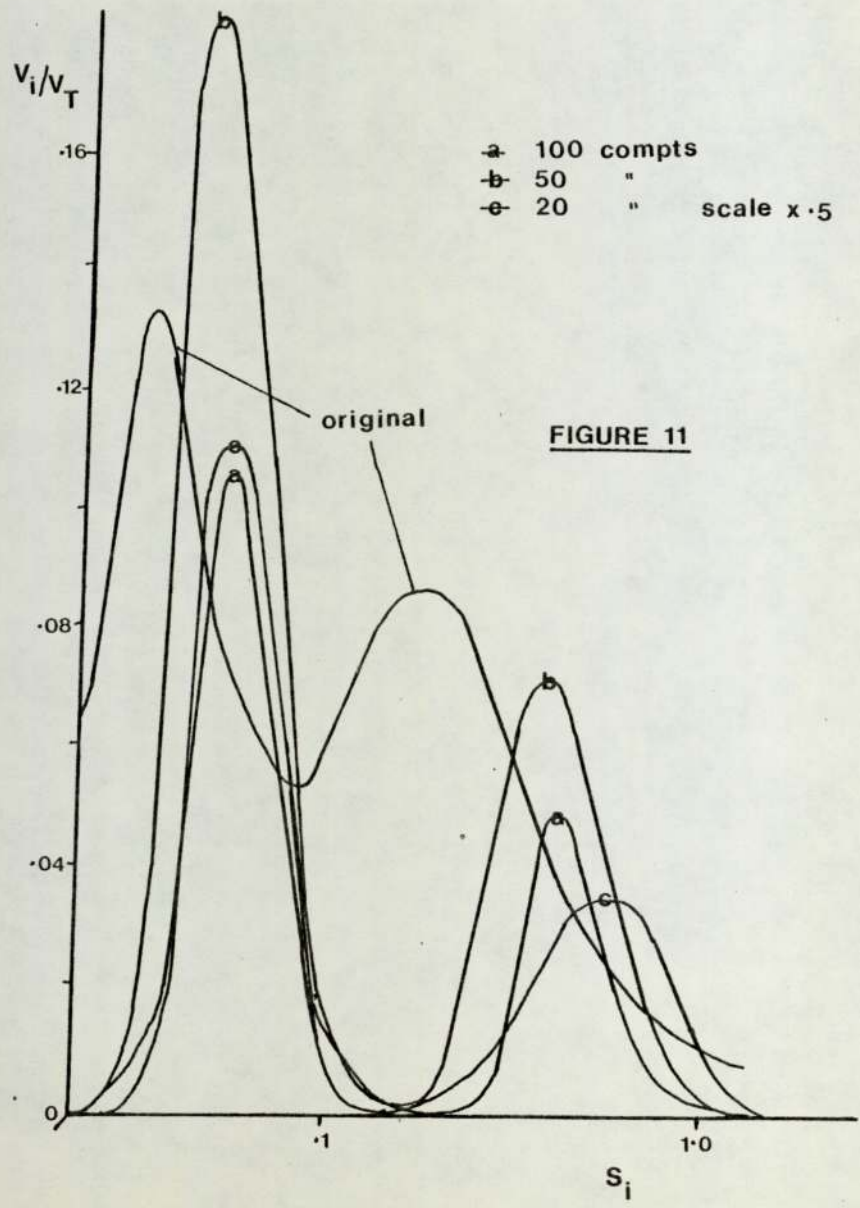
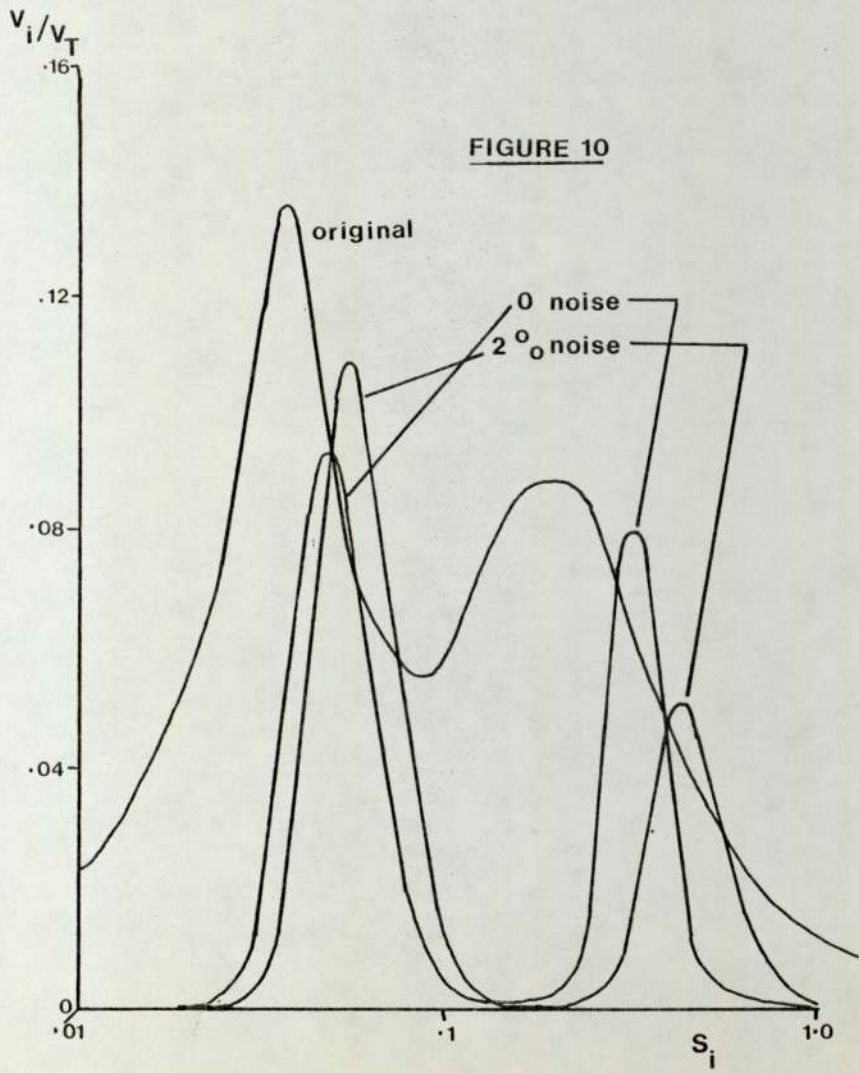


Table 2: Recovering a bimodal distribution by parametrization fitting techniques

N_{compt}	N_{data}	E	$S(i)_{\text{max}}$ (LH mode)	$S(i)_{\text{max}}$ (RH mode)	$V(i)_{\text{max}}$ (LH mode)	$V(i)_{\text{max}}$ (RH mode)
20	30	0.5	0.034	0.175	0.134	0.088
100	30	0.5	0.052	0.34	0.092	0.079
100	30	0.5	0.063	0.45	0.11	0.05
50	30	0.5	0.056	0.464	0.185	0.072
20	30	0.5	0.06	0.46	0.56	0.16
7	30	0.5				
100	20	0.5	0.047	0.34	0.094	0.058
100	30	0.0	0.026	0.16	0.12	0.047

Original
Distribution

0% noise

2% noise

"

"

"

"

"

RECOVERED DISTRIBUTIONS

4.ii (b) Effect of Number of Compartments

The number of lung compartments defining the original fit, and hence the nitrogen washout data, was twenty, whereas one hundred compartments was to be used in the recovery of distributions from experimental nitrogen washout curves (Chapter 5). Therefore, using *standard parametrization fitting techniques*. Figure 11 shows the effect of N_{compt} on the recovered distributions and Table 2 summarises the principle features. As with the delta type function, it is not very instructive to compare the heights of the peak ventilations for distributions with different numbers of compartments. However, one interesting observation can be seen in Figure 11 (A) which shows the recovery of two modes even with N_{compt} reduced to seven. This must be compared to the unimodal distribution recovered with the direct compartmental fit.

4.ii (c) Effect of the Number of Data Points

On reducing the number of data points from thirty to twenty, the distribution recovered by *parametrization fitting* remained virtually unchanged, as shown in Figure 12 except for a slight shift towards areas of higher lung volume. The 'fast' lung compartments, that is compartments with relatively low $S(i)$, which quickly exhaust their nitrogen are predominant in the early stages of the washout and hence explain the shift of the distribution when N_{data} is reduced.

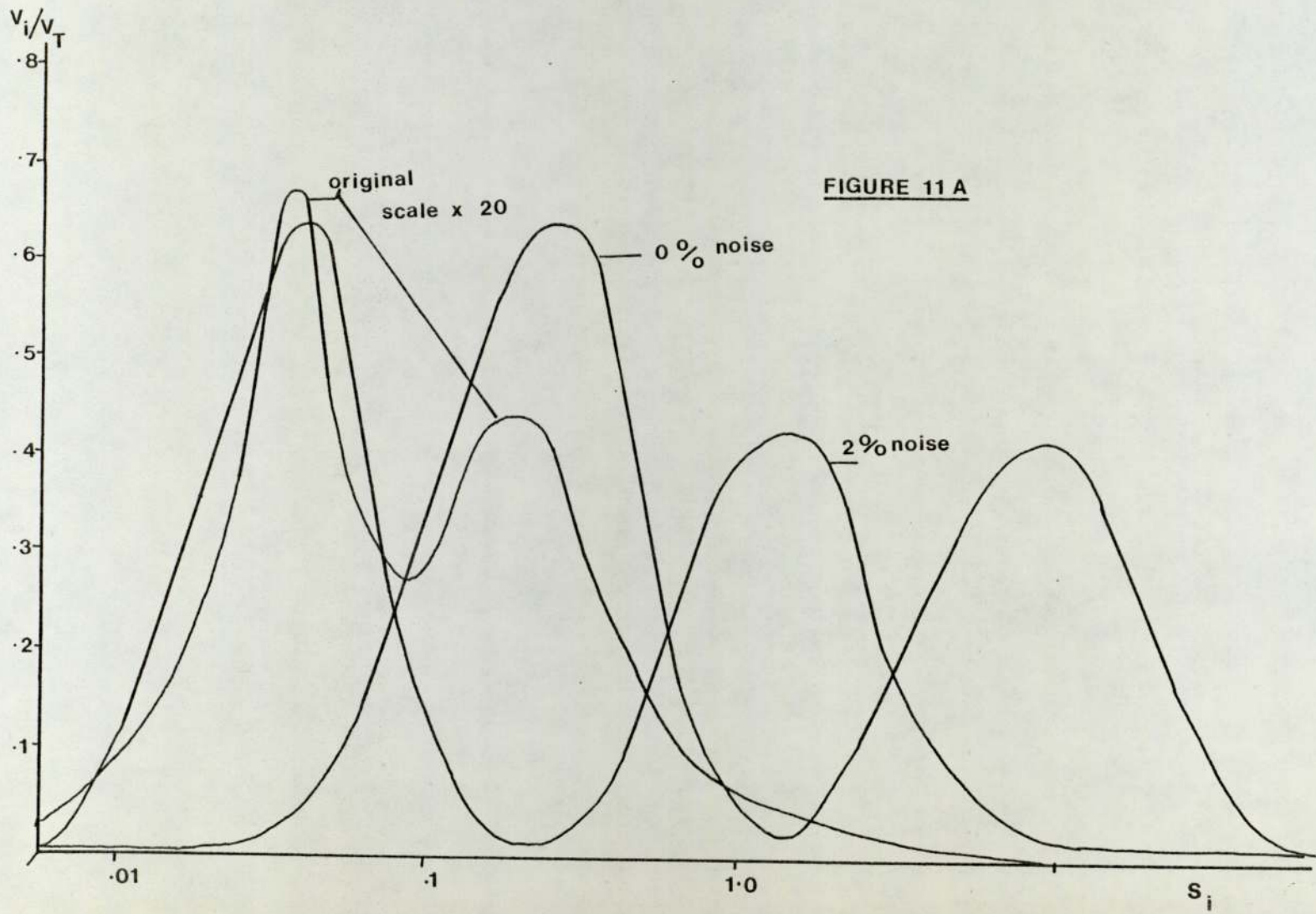
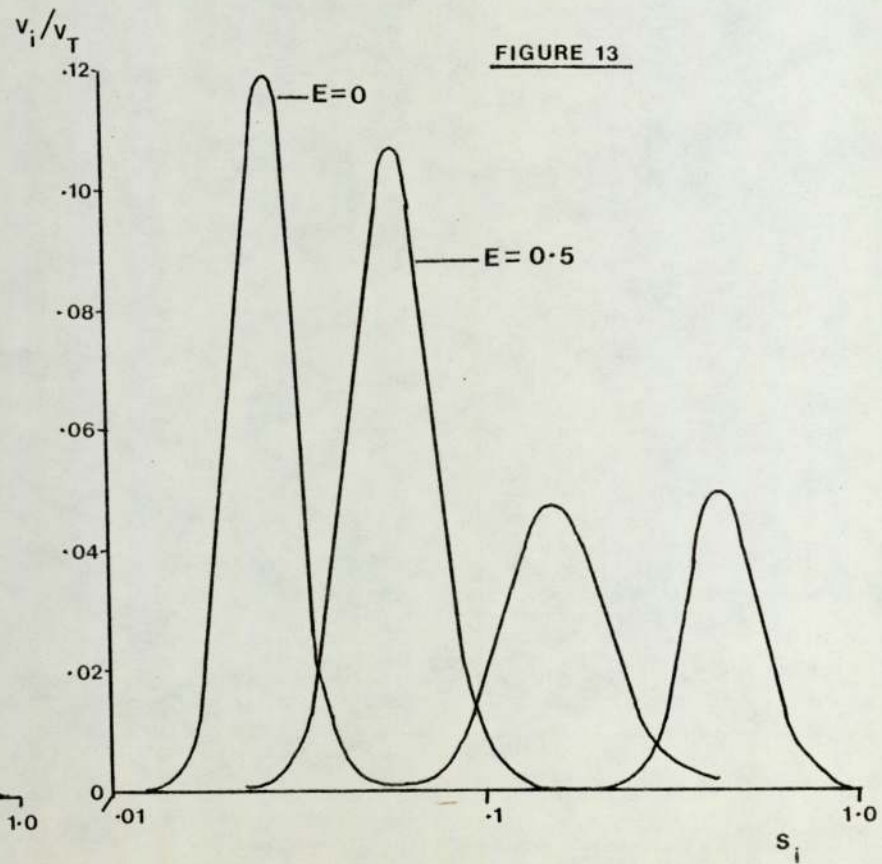
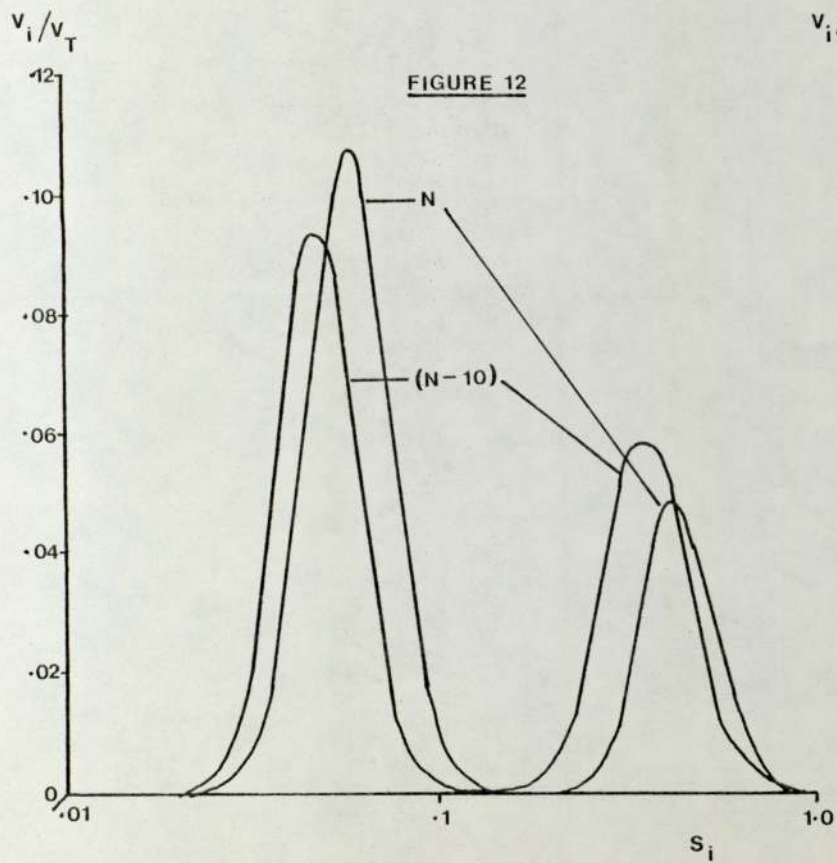


FIGURE 11 A

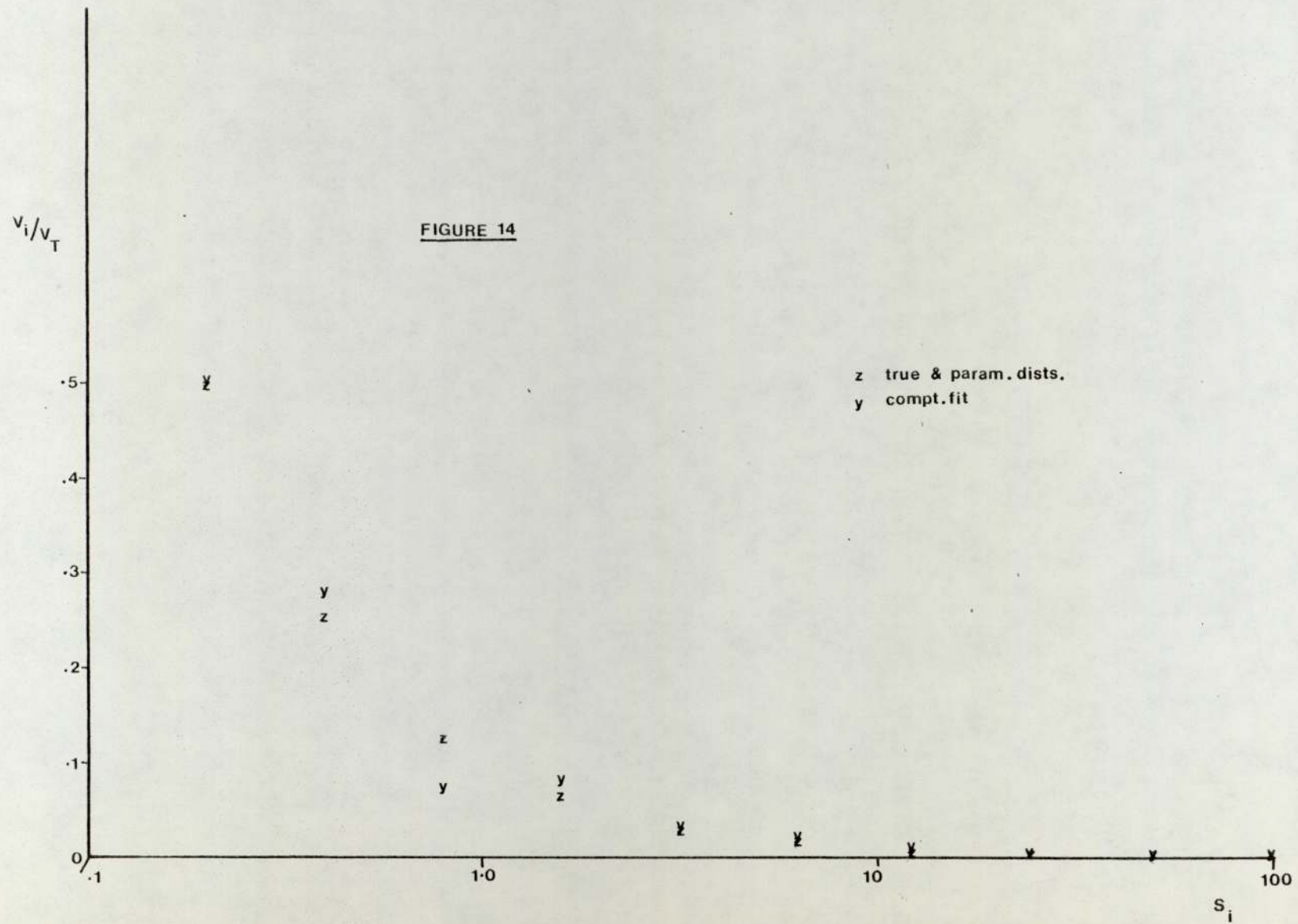


4.ii (d) Effect of the Inefficiency Parameter, E

As expected, the result of underestimating E is to cause the resultant distribution to move towards areas of higher lung volume in order to reduce the rate of nitrogen washout. This is clearly shown by Figure 13.

4.iii Recovery of Further Distributions

Having studied, in detail, the recovery of delta type functions and bimodal functions the recoverability of other probable distributions was also considered. It has been demonstrated that regional inequalities in the lung may resemble a geometric progression (37). Although experimental results appear (Chapter 5) to recover more delta type, bimodal functions this may be due to the modelling of series as parallel inequalities. If true regional inhomogeneities could be recovered they may in fact resemble the geometric progression. Figure 14, curve B, illustrates the results of a *direct compartmental fit* to a nitrogen washout curve (error free data) produced from a *geometric progression* (curve A). It is obvious from the direct compartmental fit, that the parametrization of equation (19) will not fit this data, and on attempting to use such a parametric function an error message, "function will not converge", was recorded from the computer. This is encouraging since if an unrealistic parametric function is chosen from the compartmental fit, it appears that the minimization routine will merely fail to



converge. In order to fit the geometric progression, a Padé Approximate of the form,

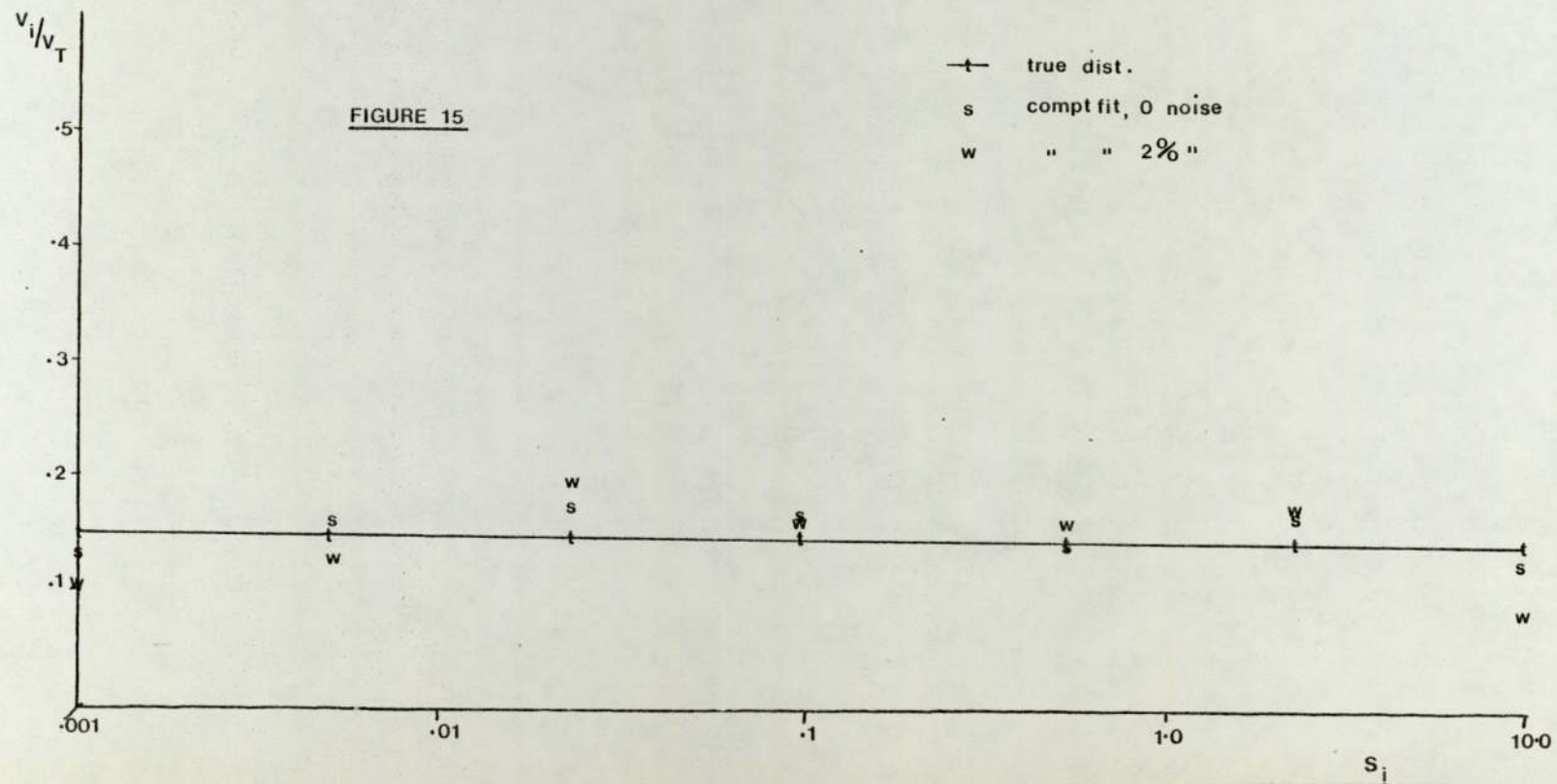
$$\frac{V(i)}{V_T} = \frac{1}{a + b \log S(i)} \quad (20)$$

was used; a and b being the parameters to be recovered. Curve C shows the resulting fitted parametrized distribution.

Figure 15 shows a *straight line* distribution together with the corresponding *direct compartmental fit*. Again, the results of the compartmental fit would have been enough to show that the exponential parametrization could not have easily expressed the distribution function. If the parametrization of equation (19) was used, however, the function would fail to minimise. Nevertheless, figures 16, 17 and 18 show three very different distributions which did minimize using equation (19) as the parametric function.

Discussion

Modelling the lung as a group of parallel constantly ventilated compartments is a gross oversimplification. However, such a lung model has been used by numerous groups and must discussion has centred about the validity of the major assumptions. The effects of collateral ventilation, often termed series gas exchange, has been studied recently by Wagner and Evans (38).



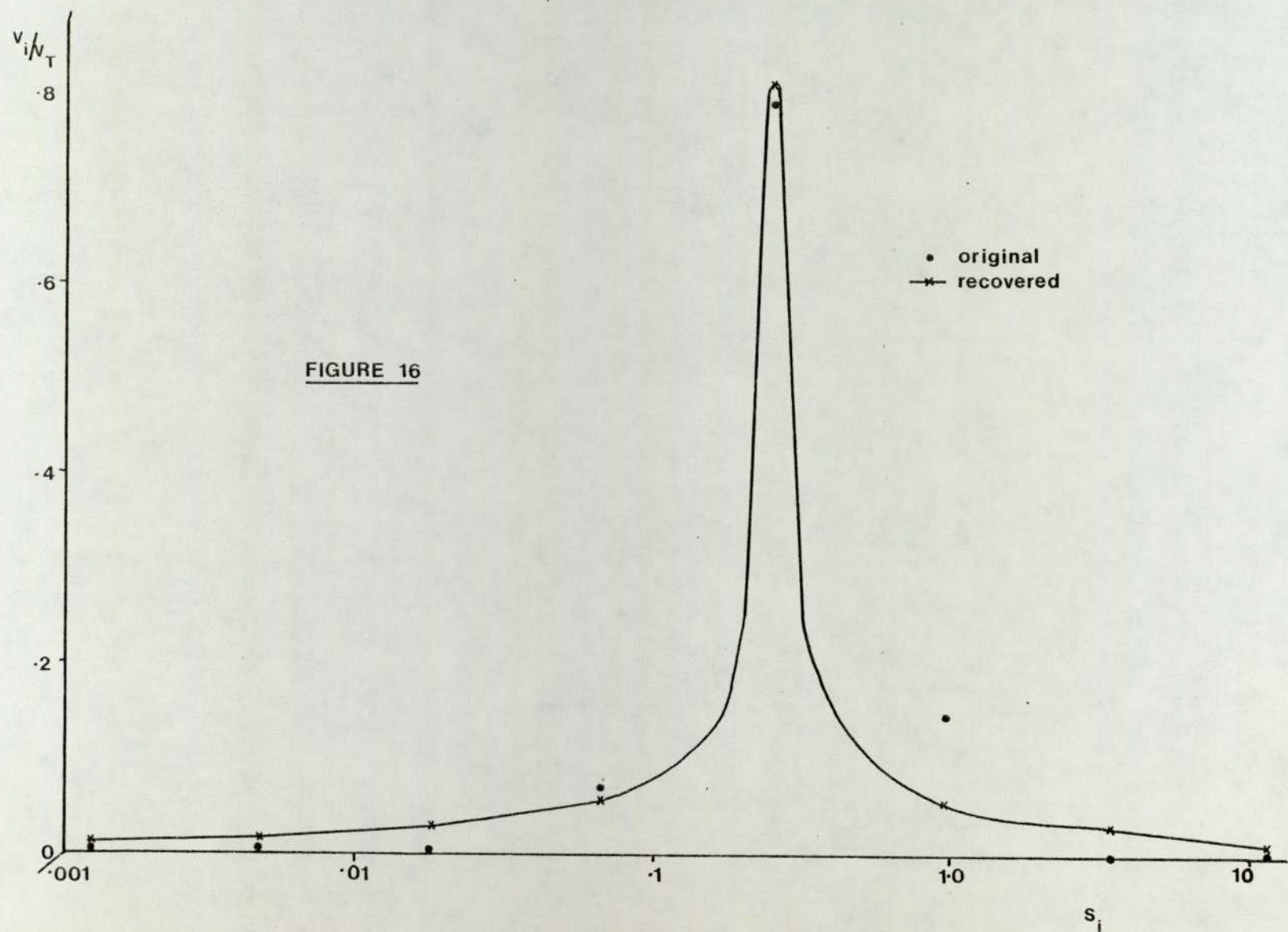


FIGURE 16

FIGURE 17

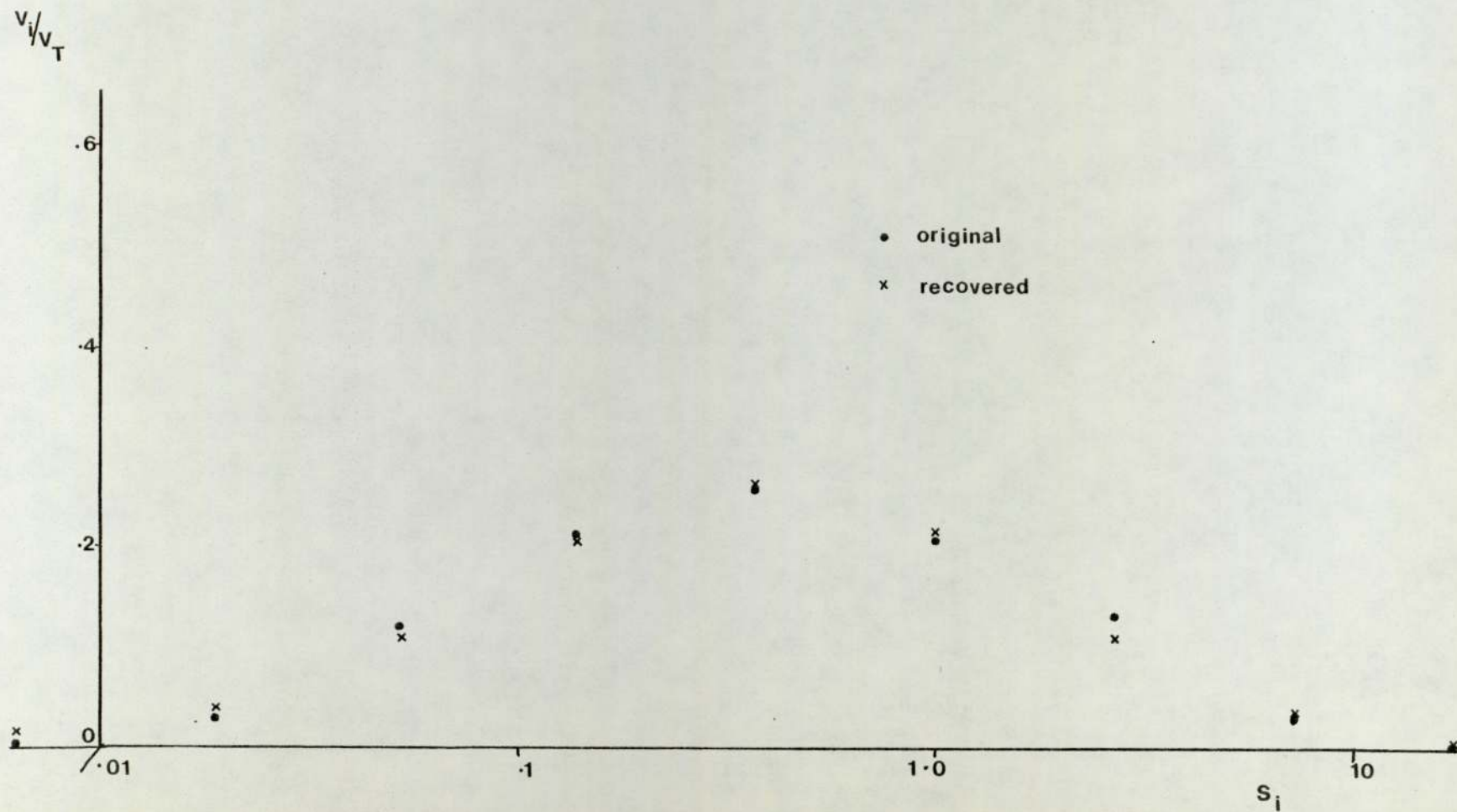
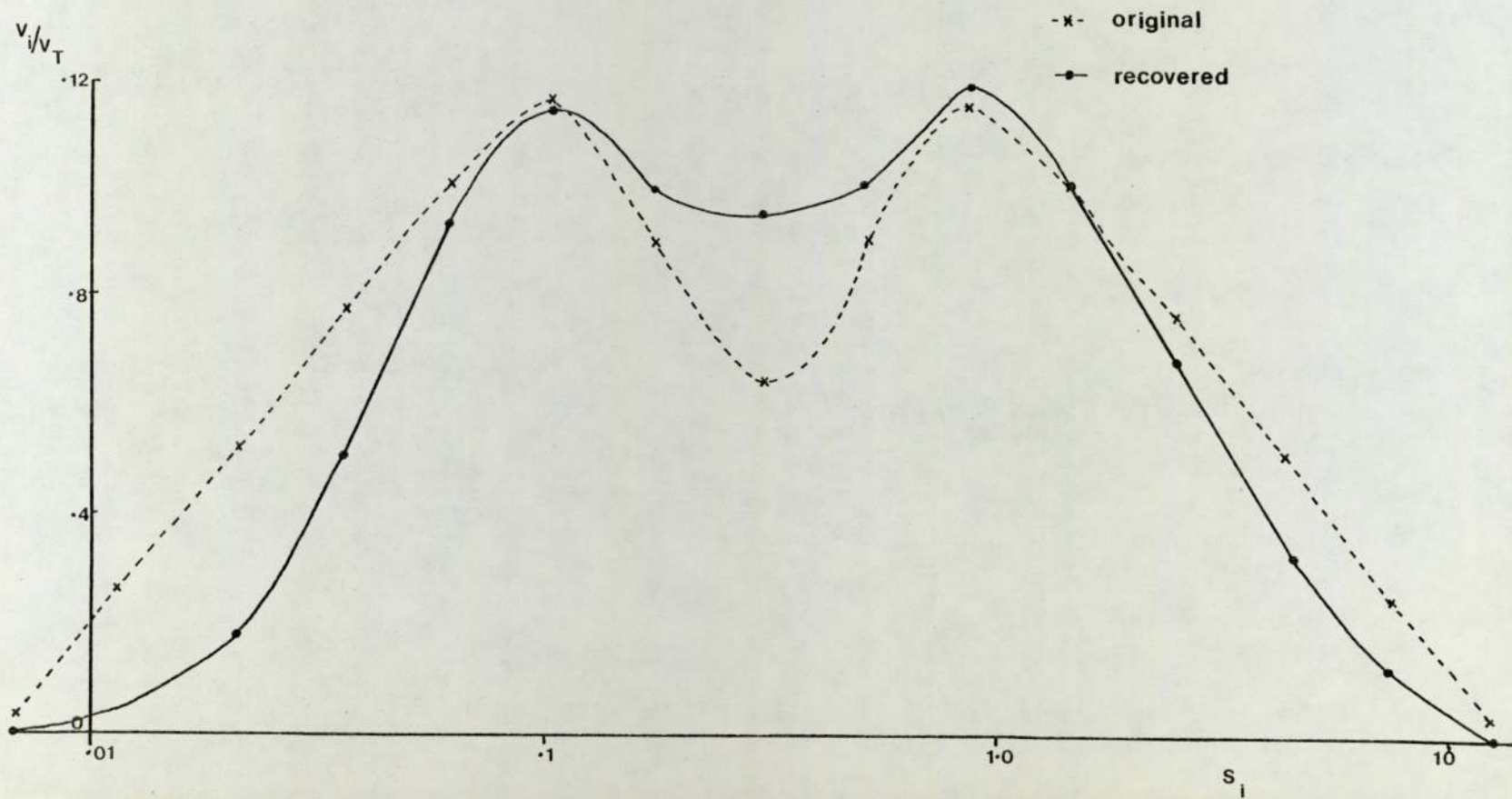


FIGURE 18



Using the Fick principle applied to series and parallel compartmental lung models, they have demonstrated how series inequalities always have a parallel equivalent. Although this work concentrated on steady state gas transfer, it confirms the previous work of Evans (39) who showed that series and parallel models are also indistinguishable when describing a nitrogen washout.

Lewis et al reiterated the assumptions necessary for series and parallel models to be regarded as equivalent, namely, all breaths of the washout are identical, and inspired and expired volumes of tracer take the same path through the lungs. These assumptions certainly apply well to diffusion and convection, and cardiogenic mixing will meet them in a statistical sense. However, it must be stipulated that where series compartments are modelled as parallel compartments, the distributions recovered cannot correspond to true anatomic sites.

The recovery of theoretical distributions is the only method of determining how successful the distributions recovered from experimental data will be in describing certain lung features. Reproduction of the original distributions described here may not appear as impressive as those obtained by previous groups. However, it must be stressed that these previous methods using computer minimization routines have never been able to recover *unique* solutions. Although Wagner et al, and Lewis et al, demonstrated remarkably good reproduction of theoretical

distributions, their results cannot be given much credance. They attempted to recover more parameters than data points, and under such conditions an infinite range of solutions exist, as was so convincingly shown by Olszowka. The one hundred compartment parametrization fit has more data points than unknowns, as does the direct 7 compartment fit. Hence, even in the presence of experimental error, the recovered distributions are unique, within a certain *tolerance* level.

This *tolerance* level is the largest value of least squares for which a minimum is said to have occurred. This was given a value of 10^{-4} and was found to offer a good compromise between accuracy and computer execution time. Thus, it can be confidently stated that the recovered distributions are unique within the estimated distance to the minimum.

CHAPTER 5

Recovery of fractional ventilation to specific ventilation distributions from experimental N₂ washout curves

5.1 Introduction

Theoretical N₂ washout data has demonstrated the accuracy by which compartmental and parametrization techniques recover the features of continuous distributions of fractional ventilation to specific ventilation. Although the fitting of data to a small number of compartments recovers the overall structure of the distribution, bimodal features can be lost and the distributions appear much broader. Parametrization techniques offer more detailed information and have been shown to recover the number of modes, and the separation of the modes with a certain degree of accuracy, but the forcing of the distribution into a particular functional form can cause some important features to be lost. With this knowledge in mind, distributions are now recovered from experimental N₂ washout curves by the compartmental and parametrization methods described in Chapter 3 in an attempt to compare both the results from the two minimization methods as well as the distributions from the three subject groups.

Group I consisted of seven young normals whose ages ranged from 23 to 31 years and who were not known to be suffering from any respiratory symptoms at the time of the washout tests.

Group II consisted of three subjects whose ages were 45, 57 and 60 years and who were all very heavy smokers. Finally, Group III included two patients (subjects 11 and 12) who complained of chest pains and were expected to display abnormal distributions. The N₂ washout data for these two subjects was taken from a Centronic publication (38). Subject 11 was 38 years of age and complained of vague chest pains on exercise, although during an exercise study, subsequent to the N₂ washout test, the patient did not feel any discomfort, and there were no electro-physiological changes indicative of myocardial ischaemia. The N₂ washout curve had originally been analysed (38) by considering the curve to compose of two exponential terms of the form,

$$C_t = X \exp (- (V_1 / V_{L1}) b) + Y \exp (- (V_2 / V_{L2}) b) \quad (21)$$

where X and Y are constants determined from the intercepts on the ordinate and b is the number of breaths. The N₂ washout had been found to be indistinguishable from those obtained from normal patients.

Subject 12 was 48 years of age, a former coal miner, was quite severely exercise limited, showing a very high V-A CO₂ difference. Using curve stripping techniques, the washout was found to be monoexponential and of the form,

$$N_t = 37 \exp (- 0.05 b)$$

The half-life of the curve was found to be far greater than observed in normal patients, the washout being ten times slower than for normals.

Having obtained data from three different groups of subjects, it was hoped to relate the recovered distributions to progressively increasing pulmonary abnormalities through the three groups. Using N_2 washout concentrations from each subject as data for the minimization routines described in Chapter 3, distributions corresponding to a seven compartment lung model (and dead space) and a hundred compartment lung model were recovered, the latter distribution formed by parametrizing the fractional ventilation as a function of specific ventilation. Not only did this enable a comparison of distributions recovered for the different groups of subjects, but it also allowed the two methods of recovery to be compared.

5.ii Experimental Method

The multi-breath N_2 washout has long been used as a lung function test (39, 40), although recently its use has largely been superceded by the single breath N_2 washout (41), partly due to the difficulties in obtaining a uniform curve from patients with severe pulmonary abnormalities. In this experimental set-up, figure 19, the subject was asked to test breathe through a valve from an ordinary air source.

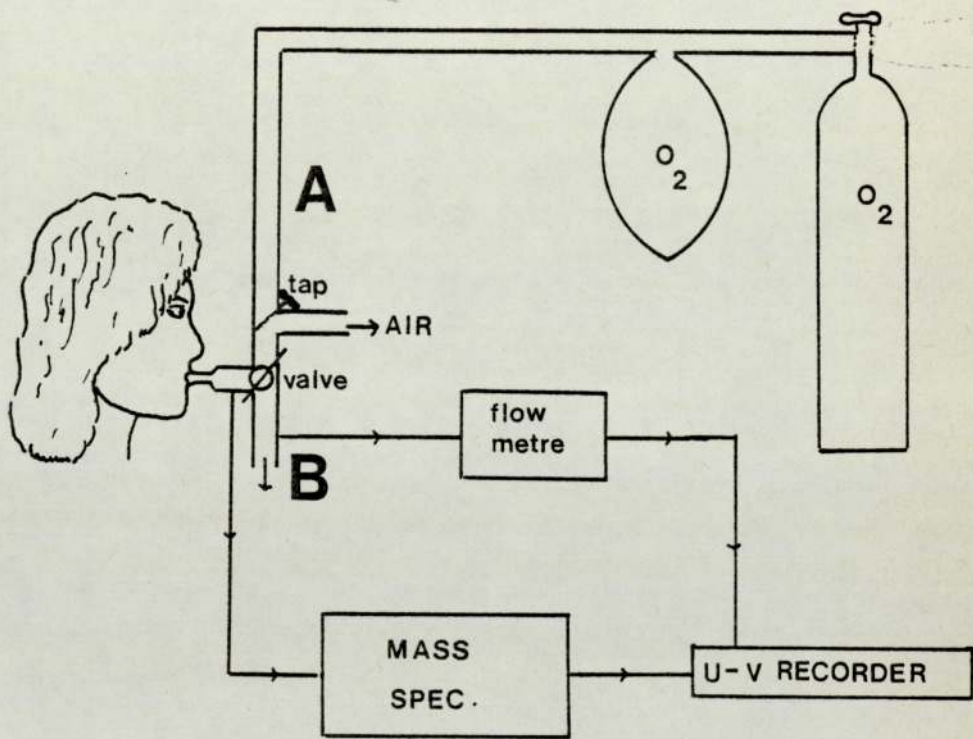


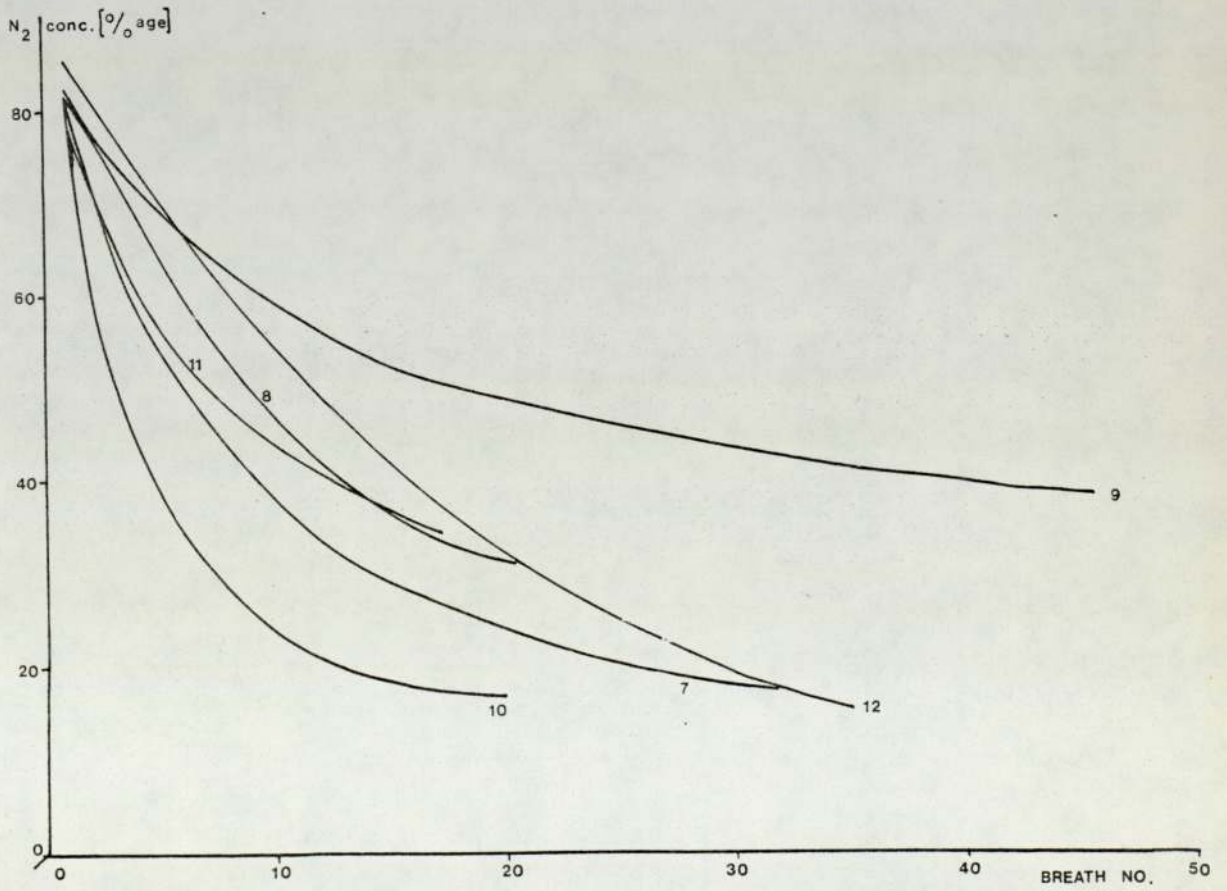
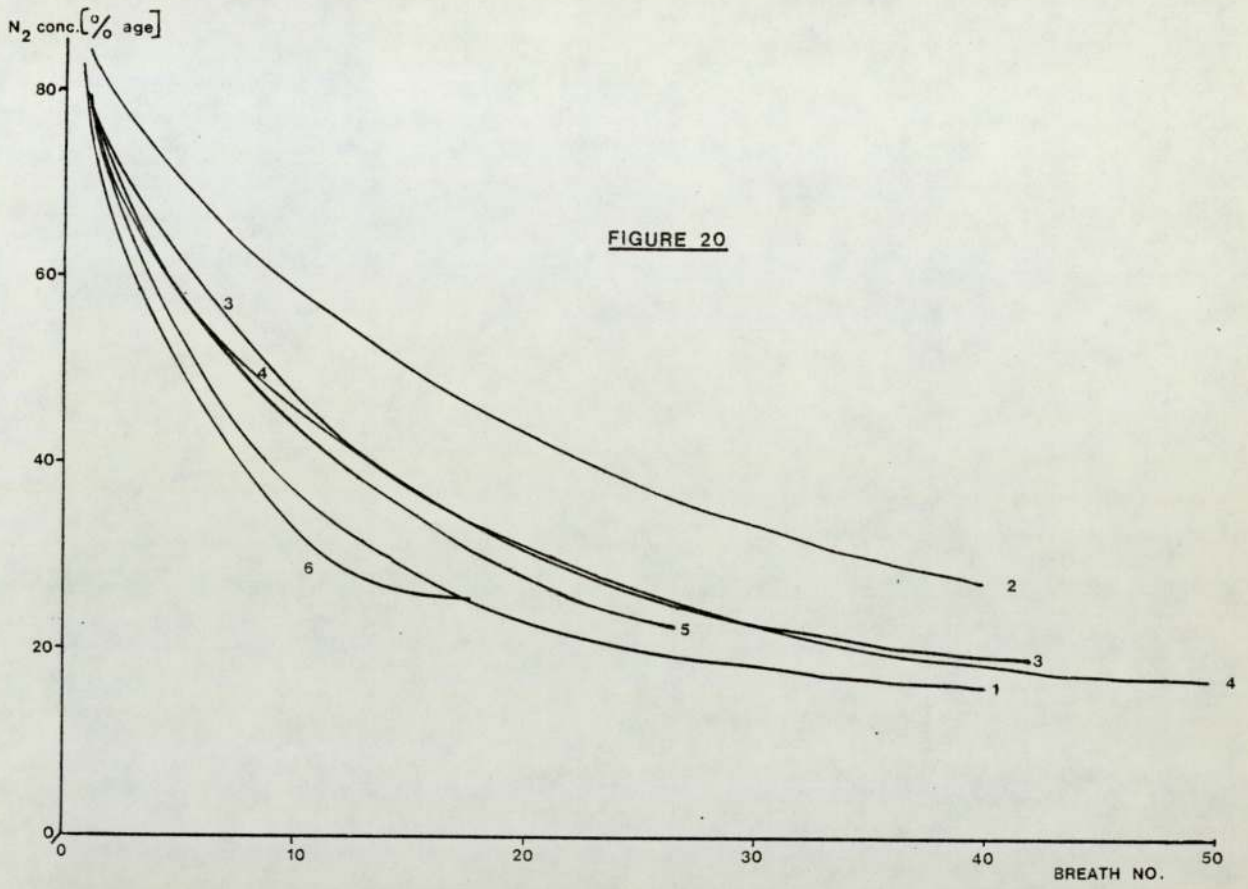
FIGURE 19

During inspiration, the valve allowed the subject to breathe only from line A, but at end-inspiration the valve closed forcing the expirate to flow along line B.

The subject took a number of test breaths in order to obtain uniformity of both tidal volume and flow. The volume metre was placed in front of the subject so that the subject could easily regulate his breathing. When regular breathing was thought to have been attained the operator switched the tap to pure O₂ breathing, without the subjects knowledge. Nitrogen concentration was recorded using a mass spectrometer, the concentration and tidal volume being continuously and simultaneously registered on an ultra-violet 'pen' recorder. Figure 20 shows end-expired N₂ concentration as a function of breath number for all twelve subjects.

5.iii Compartmental fitting: 7 compartmental lung model

Briscoe and Cournand (17-19) made a comparison of normal and emphysematous lungs, by assuming a N₂ washout curve to have arisen from two groups of alveoli, one well ventilated and the other poorly ventilated. This approach proved highly successful in describing general features of normal and abnormal lungs, but failed to reveal inhomogeneities present in each group of alveoli. Wagner et al (29) showed how, in order to distinguish narrowly separated modes and recover



underlying structure, the lung must be considered as a large number of gas exchanging compartments and ideally, a quasi-continuous distribution should be produced.

In Chapter 4, it was clearly demonstrated how fitting the data to a small number of compartments was a successful means of illustrating general unique features of the distribution. Although multi-modal features may not be recovered, such a compartmental fitting procedure may prevent the use of an unrealistic parametrization and also gives a reasonable estimate of the inefficiency parameter, E. With eight unknown parameters representing E and seven lung compartments, and a minimum of 19 data points the system was well determined, even allowing for experimental error. Using the compartmental minimization procedure outlined in Chapter 3, the seven values of $V(i)/V_T$ and E for the following subject groups were recovered.

(a) Compartmental fits for Young Normals-subjects 1 to 7:Group I

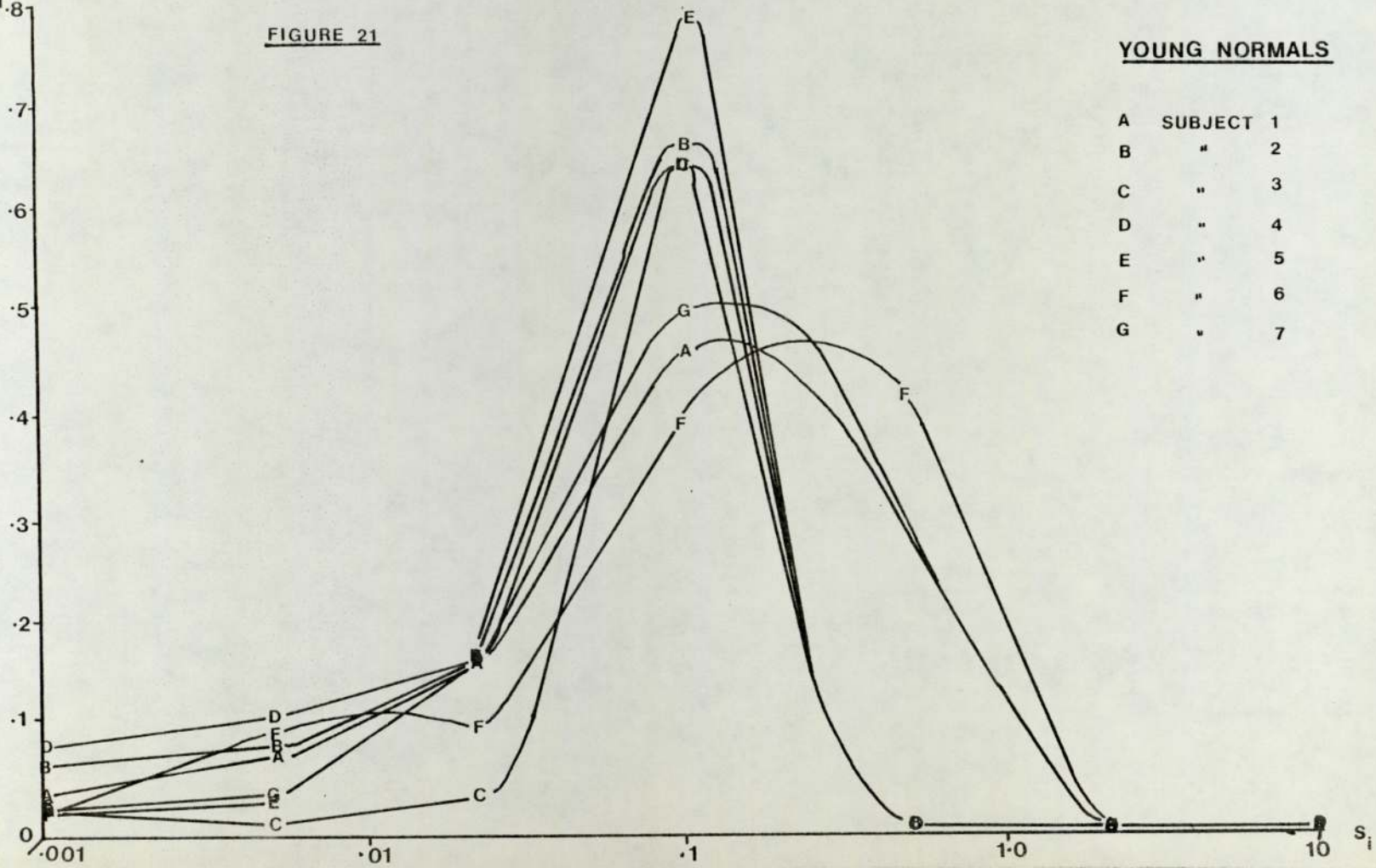
These subjects, whose ages ranged from 23 to 31 years of age, had no respiratory symptoms. There were no heavy smokers amongst the group, although subjects 2, 7 and 5 were occasional smokers. In all instances, the compartmental fitting routine converged rapidly with assumed values of $S(i)$ ranging from 0.001 to 10.0. Figure 21 illustrates the compartmental fits of the seven N_2 washout curves from these young normals and illustrates the

$v_i/v_{T.8}$

FIGURE 21

YOUNG NORMALS

A	SUBJECT	1
B	"	2
C	"	3
D	"	4
E	"	5
F	"	6
G	"	7

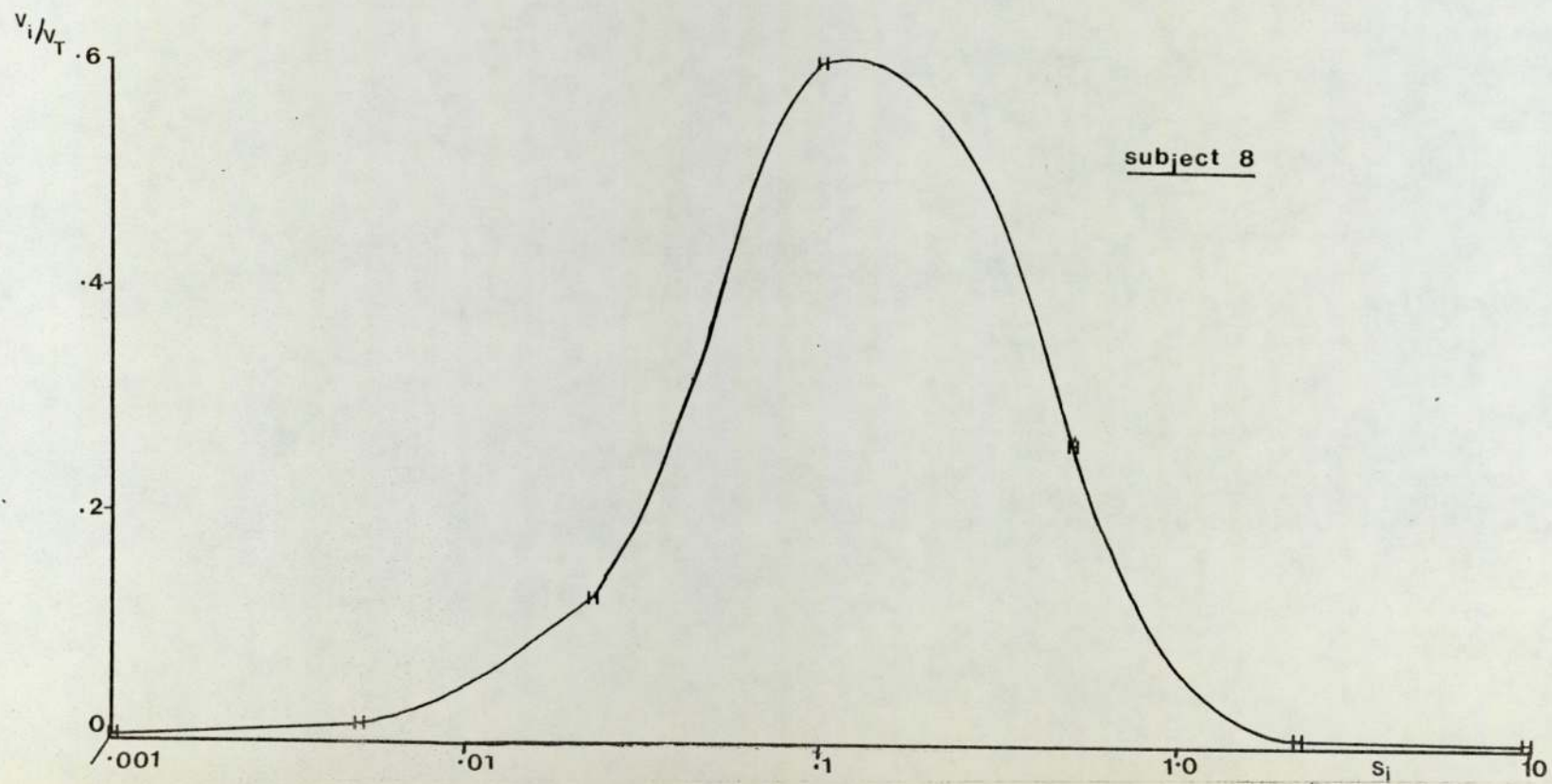


similarity and reproducibility of the recovered distributions. Except for subject 6, the maximum ventilation in young normals occurred at a specific ventilation of 0.1. However, subject 6 had a slightly higher proportion of ventilation directed towards a compartment of specific ventilation 0.53. All the recovered distributions showed a marked degree of symmetry about the peak ventilation. The mean value of the inefficiency parameter E for young normals was found to equal $0.33 (\pm 0.11)$ which seems to suggest that it is principally a measure of anatomical dead space which is usually assumed to be approximately one third of the tidal ventilation.

(b) Older Normals-subjects 8,9 and 10: Group II

This group of subjects, aged from 45 to 60, were not known to have any serious respiratory complaints, although all were heavy smokers and prone to attacks of bronchitis. The seven compartment distribution for subject 8, as illustrated in figure 22, was very similar to those demonstrated by young normals, with a peak ventilation occurring at a specific ventilation of 0.1, within the range of $S(i)$ between 0.001 and 10.0. However, when the minimization procedure was applied to nitrogen washout data from subjects 9 and 10, the least squares function, L , either failed to converge, or unphysical values of E , such as $E=0$, were recovered. In an attempt to obtain convergence, the range of $S(i)$ was changed from $(0.001 \rightarrow 10.0)$ to $(0.0001 \rightarrow 1.0)$, but satisfactory solutions

FIGURE 22



could still not be obtained. However, when the range of specific ventilation was reduced to (0.01 → 10.0), solutions were found for both subjects 9 and 10, as in figure 23, with values found for E of 0.474 and 0.384 respectively. The distributions recovered for these two subjects can be seen to vary considerably from those recovered from the young normals in group I. Unlike the symmetrical, unimodal distributions of group I, subjects 9 and 10 show a marked degree of assymetry, with the distribution from subject 9 being bimodal. Subject 8 showed a predominance of compartments with higher specific ventilation than seen in group I whereas subject 9 appeared to have a high proportion of the total ventilation directed towards areas of lower specific ventilation.

(c) Compartmental fits for diagnosed abnormals -
subjects 11 and 12: Group III

Both subjects 11 and 12 complained of chest pains on exercise, and were severely exercise limited. Subject 12 had been diagnosed as suffering from some type of obstructive lung disorder. As with subjects 9 and 10, the minimization routine failed to converge for specific ventilations in the range 0.001 to 10.0. However, without reducing the range of specific ventilation, it was found possible to obtain convergence in the range 0.0001 to 1.0. The distributions recovered are illustrated in figure 24 and are obviously very different from those seen

FIGURE 23

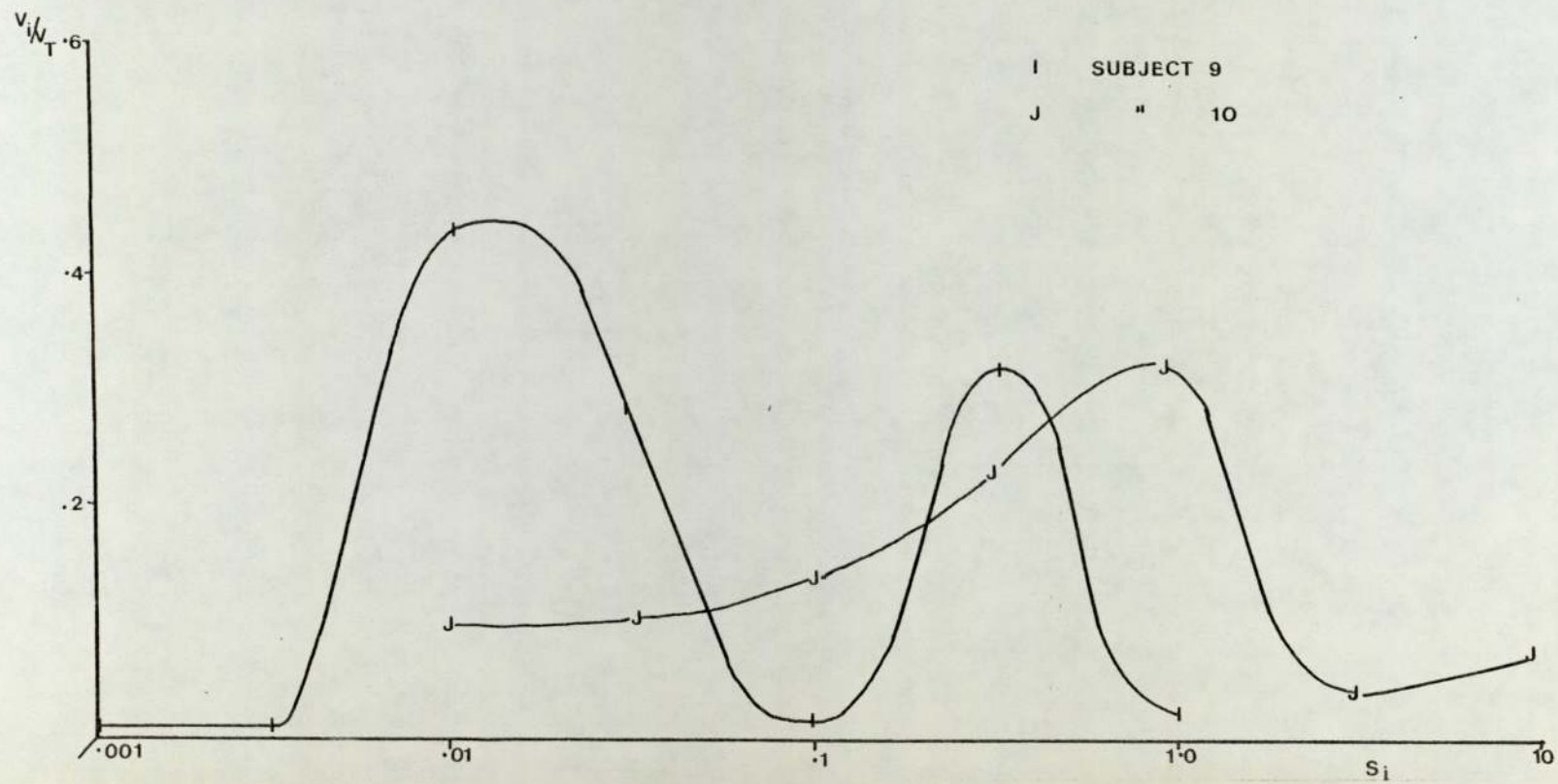
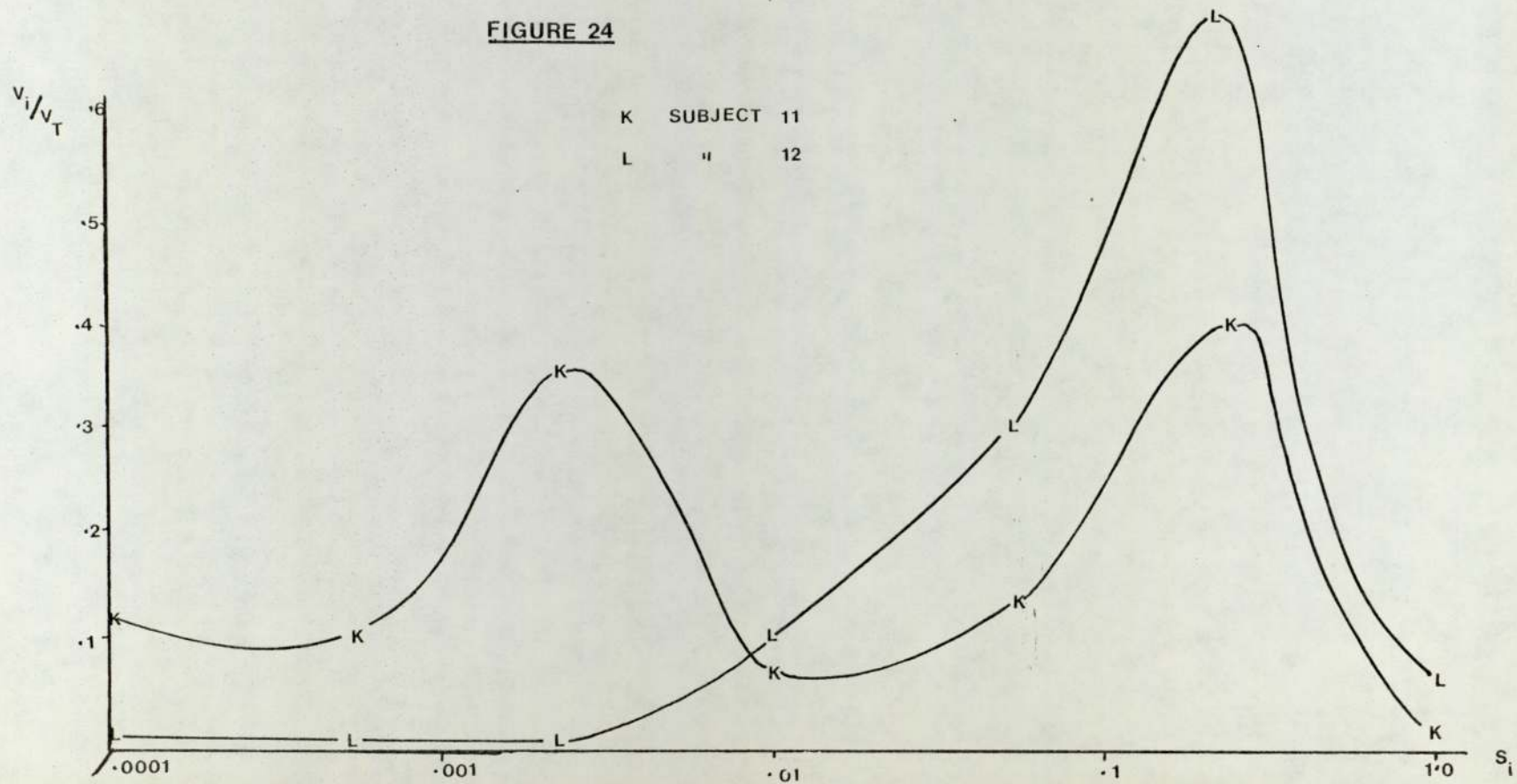


FIGURE 24



in the young normal group. Subject 12 bears some resemblance to the distributions recovered from young normals, but subject 11 shows two well separated modes illustrating the ability of the compartmental fit to recover bimodality in certain extreme cases. The inefficiency parameter E for subjects 11 and 12 was found to equal 0.28 and 0.5 respectively.

5.iv Conclusions from the compartmental fit

Although these distributions cannot reveal the detailed structure existing in the lungs, they appear to have highlighted very important differences in the distributions from the three groups of subjects. The pattern for young normals appears very uniform with an almost symmetric distribution centred around a peak ventilation corresponding to a specific ventilation between 0.1 and 0.53.

There is a distinct difference in the recovered distributions from group I and the older normals and abnormals. This was initially evident from the failure of the least squares function to converge in the normal range of specific ventilation. For subjects 11 and 12 it was merely necessary to increase the range of $S(i)$ to cover areas of lower specific ventilation. However, it was obvious that for subjects 9 and 10, that a distribution could not be found to satisfy the data with such a small number of compartments spanning four logarithmic cycles of specific ventilation. When the

range of $S(i)$ was reduced to three cycles, the difference between adjacent compartmental values of $S(i)$ was reduced and hence it became easier to describe marked localised changes in the distributions. The failure of the fitting routine to converge in the four cycle range of specific ventilation appears to suggest a large degree of variation in fractional ventilation over a small range of specific ventilations. If the spacing of adjacent compartments on the $S(i)$ axis is too large not enough variation can be produced by the seven compartment lung model. Thus, in order to obtain a general picture of the distributions by means of considering a small number of lung compartments equally spaced in $\log S(i)$ space, it is sometimes necessary to either change or reduce the range of $S(i)$. It may even prove more realistic to plot $S(i)$ rather than $\log S(i)$.

Having recovered all the distributions, the major differences between the groups can be summarised as follows. Whereas young normals and subject 8 show unimodal symmetric distributions centred around a specific ventilation of 0.1, the distributions for subjects 10 and 12 are assymmetric with a peak ventilation occurring at higher specific ventilations than in Group I. Subject 9 and 11 have outstanding distributions because they are bimodal with a high proportion of the tidal ventilation directed at areas of lower specific ventilation. In conclusion, therefore, it appears that abnormalities of some

description are being observed by the compartmental fits for groups II and III and moreover, the delta type and bimodal patterns observed lend themselves to the parametrization of equation (19).

5.v Parametrization fitting: 100 compartment lung model

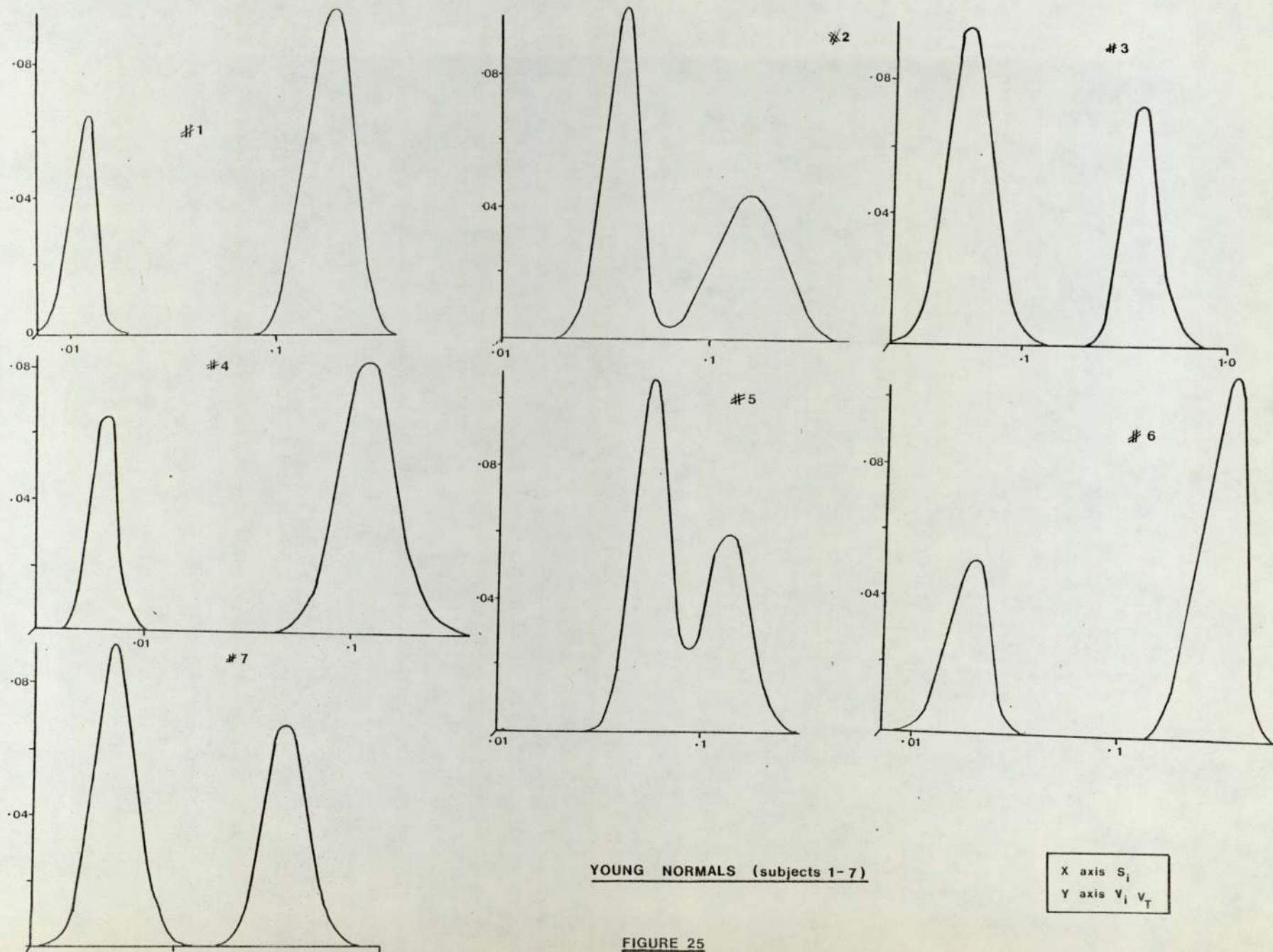
Methods for recovering information concerning a small number of lung compartments are well documented and have been used extensively as a means of detecting pulmonary abnormalities. However, the complex effects of lung disease on respiratory behaviour necessitate the recovery of more detailed information of the ventilation and lung volume inhomogeneities present in certain classes of disease. For the recovery of such information, it has been suggested that the lung be treated as a very large number of compartments approaching a continuum. Thus, a lung model has been described with one hundred compartments each having a particular fractional ventilation which is related to a value of specific ventilation by the parametrization, chosen from the compartmental fits to be that of equation (19). The number of unknowns in such a parametrization is six and since the minimum number of data points is nineteen, N_{data} is very much greater than N_{unknown} . The assumption that the values for $S(i)$ are equally spaced along the $\log S(i)$ axis was not very realistic for the seven compartment lung model, but for one hundred compartments the assumption is good and a more representative positioning

of the distribution on the x axis can be expected with a parametrization fit.

It is only by expressing some functional relationship between $V(i)/V_T$ and $S(i)$ that a one hundred compartment quasi-continuous distribution may be recovered from nitrogen washout curves having at the most sixty data points. Thus, the following results, detailed in Table 3, describe distributions recovered from each of the subject groups using such a parametrization technique (the parametrization chosen for all subjects being that of equation (19)).

(a) Group I

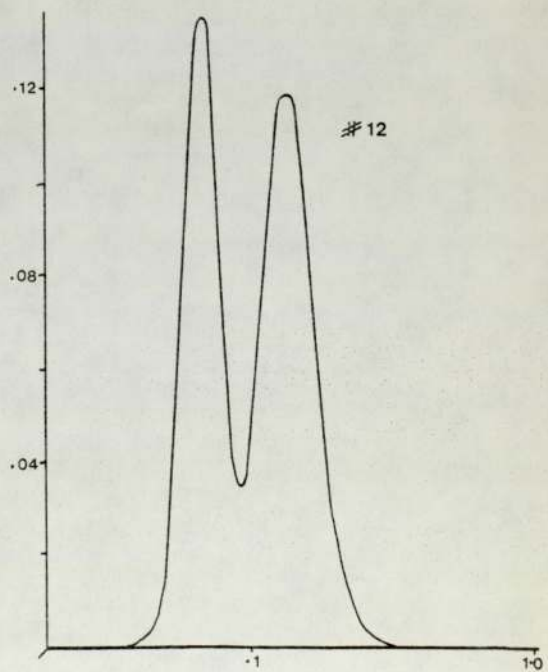
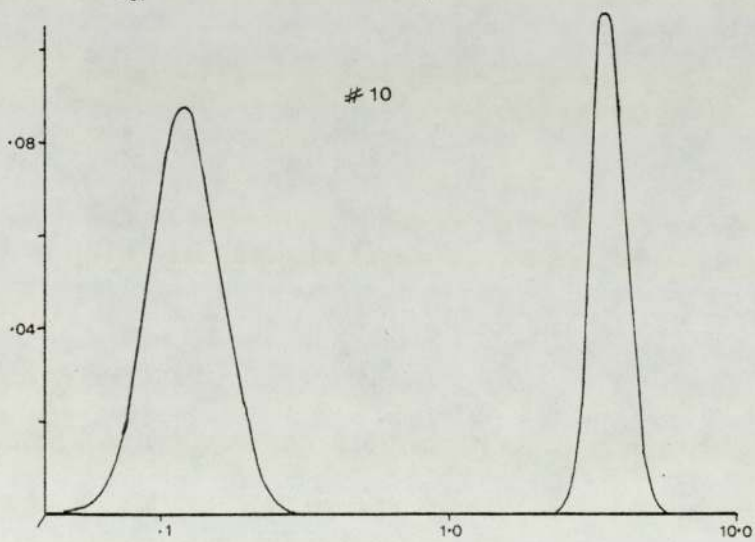
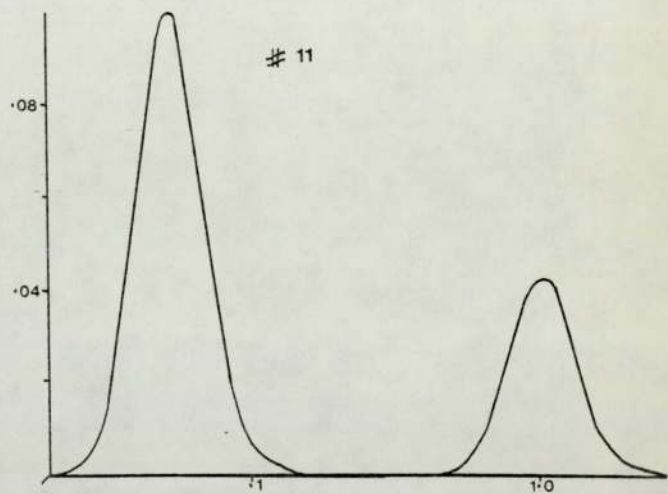
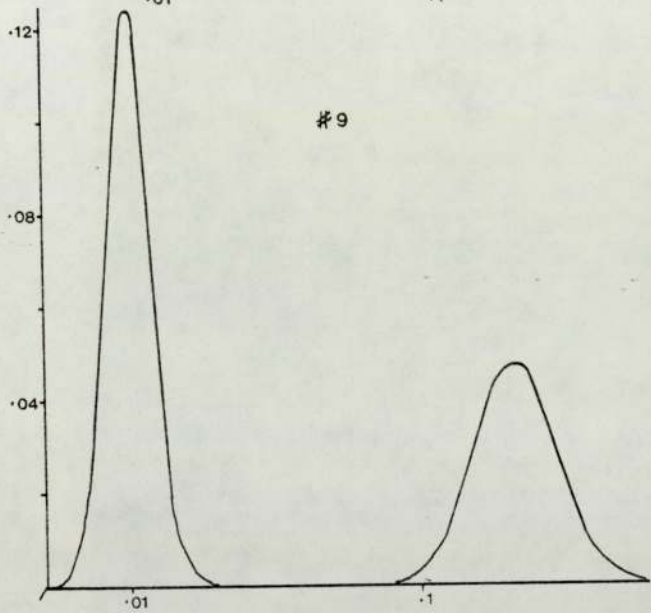
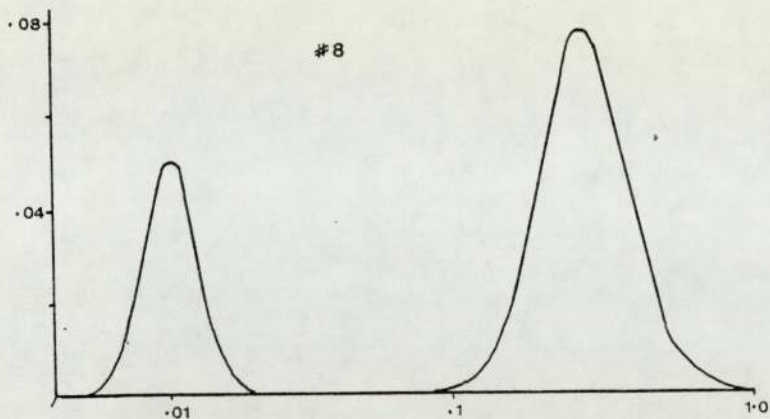
The recovered distributions for this group of young normals are illustrated in Figure 25. All the recovered distributions can be seen to be bimodal which is not merely a feature of the parametric function since it has already been shown to be capable of recovering unimodal distributions (Chapter 4). Owing to the large number of compartments there is an increased sensitivity both in the shape and the positioning of distributions, but for quantitative comparison of curves the effect of tidal volume is an important consideration. If a subject breathes more deeply than another subject with identical lungs, the nitrogen washout will be necessarily faster. Thus, it is difficult to make quantitative comparison between subjects of the actual positioning of the modes, S_1 and S_2 (the specific ventilations corresponding to peaks



YOUNG NORMALS (subjects 1-7)

X axis S_i
Y axis $V_i V_T$

FIGURE 25



OLDER NORMALS (subjects 8-10)

ABNORMALS (subjects 11 & 12)

FIGURE 25
contd.

TABLE 3

Subject	Age	E	S ₁	S ₂	S ₁ /S ₂	ΣS ₁	ΣS ₂	ΣS ₁ /ΣS ₂	V _{L1} /V _{L2}	$\frac{\Sigma V_1}{V_T}$	$\frac{\Sigma V_2}{V_T}$	R'	h ₁	h ₂
1	23	0.175	0.012	0.174	14.53	0.139	4.3	30.9	5.7	0.273	0.715	11.8	0.24	0.32
2	23	0.446	0.030	0.121	4.03	0.396	3.6	9.09	4.9	0.540	0.460	10.7	0.25	0.46
3	24	0.499	0.057	0.373	6.54	1.098	5.87	5.35	7.6	0.640	0.360	9.5	0.31	0.23
4	24	0.264	0.007	0.121	17.29	0.075	2.96	39.5	6.6	0.253	0.696	14.4	0.19	0.39
5	24	0.314	0.052	0.133	2.56	0.624	2.21	3.54	3.6	0.587	0.407	5.1	0.24	0.33
6	28	0.250	0.018	0.281	15.61	0.264	5.3	20.08	5.0	0.294	0.710	8.3	0.26	0.29
7	31	0.344	0.052	0.373	7.17	0.977	7.03	7.2	8.9	0.565	0.434	9.4	0.29	0.3
		0.327	0.033	0.225	9.67	0.51	4.47	16.52	6.04	0.45	0.54	9.86	0.25	0.33
		±.113	±.021	±.115	±5.99	±0.4	±1.7	±14.04	±1.79	±.169	±.159	±2.9	±.009	±.03
8	45	0.454	0.011	0.281	25.55	0.176	9.89	56.19	10.3	0.290	0.711	22.95	0.38	0.36
9	57	0.474	0.009	0.212	23.56	0.150	5.21	34.73	24.3	0.590	0.410	49.78	0.22	0.41
10	60	0.381	0.121	3.556	29.39	2.610	38.65	14.81	54.8	0.640	0.360	26.33	0.34	0.15
11	38	0.280	0.052	1.048	20.15	1.420	22.66	15.96	48.5	0.710	0.280	40.46	0.33	0.32
12	48	0.500	0.069	0.133	1.93	0.579	2.12	3.66	1.5	0.450	0.490	3.36	0.29	0.37

Mean
and
S.D.

N.B. Symbols are defined in Appendix 1

of ventilation) without an accurate estimate of the tidal volume. However, the ratio of S_2/S_1 is independent of V_T , as is $\Sigma S_2/\Sigma S_1$ ⁽¹⁾ and V_{L1}/V_{L2} ⁽²⁾. The half widths of the modes are also independent of the tidal volume and hence only these parameters are used for quantitative comparisons. The relative separation of the two models, S_2/S_1 , is not very consistent amongst the young normal group, and hence is not a particularly useful parameter by which to define abnormalities. Nevertheless, the ratio of the lung volumes enveloped by each mode and the half widths of the modes appear remarkably well defined.

In general, it appears that the normal lung behaves as two well-ventilated compartments, the ratio of volumes of the two compartments being approximately 6.04 (± 1.79). The width of the modes seems to represent the dispersion of $V(i)/V_T$ about the peak ventilation within a particular lung region, and is seen to be virtually constant throughout the group with values of 0.25 (± 0.009) and 0.33 (± 0.03) for the two modes respectively.

(1) the sum of specific ventilations enveloped by each mode

(2) the volumes of lung represented by a mode

(b) Group II

Group II consists of three subjects, two of which have already displayed some form of abnormality in the seven compartment fit. Of this group, subject 9 appeared to have a distinct bimodal distribution, whereas the distribution for subject 10 was an asymmetric bimodal function with an absence of ventilation to poorly ventilated regions. From the parametrization fits, it is obvious that whereas subject 8 is again very similar to a typical 'normal' distribution, subjects 9 and 10 have abnormally high values for V_{L1}/V_{L2} . Subject 10 has a predominance of compartments with very high specific ventilation and the value of V_{L1}/V_{L2} of 54.8 which is 27 s.d. from the mean for young normals. This enormously high value of V_{L1}/V_{L2} must be significant of some abnormality which it is hoped to identify with future work. The very narrow half width, 0.15, of this second region in subject 10 must also be noted. Subject 9 also showed a significant increase in V_{L1}/V_{L2} but the dispersion of fractional ventilation around the peak ventilation as measured by the half width was within the normal range.

(c) Group III

The two subjects in this group included two patients who were suspected as having some form of pulmonary abnormality prior to the nitrogen washout test. Subject 12 was severely exercise limited. The seven compartment fits revealed distributions quite obviously different from Group I and these abnormalities again revealed themselves in the

parametrization fits. Subject 11 showed two well separated modes ($S_2/S_1 = 20.15$) representing two compartments with very high volume ratio ($V_{L1}/V_{L2} = 48.5$). Subject 12, however, appeared to have very narrowly separated modes ($S_2/S_1 = 1.93$) and a volume ratio of 1.5, suggesting that the lung could be represented by one compartment. Clearly the distribution from subject 12 displayed features very different from both groups I and II, although the half widths of the two distributions appeared normal. The original analysis (38) compares favourably with these results which showed the lungs of subject 11 to act essentially as two compartments, but those of subject 12 to be acting as a single compartment.

5.vi Conclusions from the parametrization fits

It is always essential to remember that when series compartments are modelled as parallel units, the units in the model may not strictly correspond to any anatomic site. However, correlation of the recovered distributions to specific lung sites is not necessarily a requirement for the model to describe or make useful statements concerning gas exchange in the lungs. *The only requirement for diagnosis and therapy is that normal and abnormal distribution characteristics can be correlated to certain diseased states.* Examples of such disturbances from the norm in the patterns recovered for group II and group III were clearly evident.

Although it was not possible to distinguish normals and abnormals by direct inspection of the fitted distributions, certain calculated parameters such as V_{L1}/V_{L2} and R' ⁽¹⁾ showed marked increases with age and appeared very sensitive to abnormalities, such as those thought to exist in subjects 11 and 12. Both the volume ratio V_{L1}/V_{L2} and R' increased rapidly with age amongst the normals of groups I and II. Although more sample points would be necessary to determine the exact dependence of volume ratio on age, Figures 26 and 27 illustrate the general recovered trend and it is of particular interest that subjects 11 and 12 who were diagnosed as having some form of respiratory complaint bore no correspondence to the pattern observed for normals.

Thus, recovery of distribution of fractional ventilation to specific ventilation by parametrization methods appears to be a positive test for abnormalities which may in future be classified by extensive clinical trials.

(1)
 $R' = (\Sigma S_2 / \Sigma S_1) / (\Sigma V_2 / \Sigma V_1)$

FIGURE 26

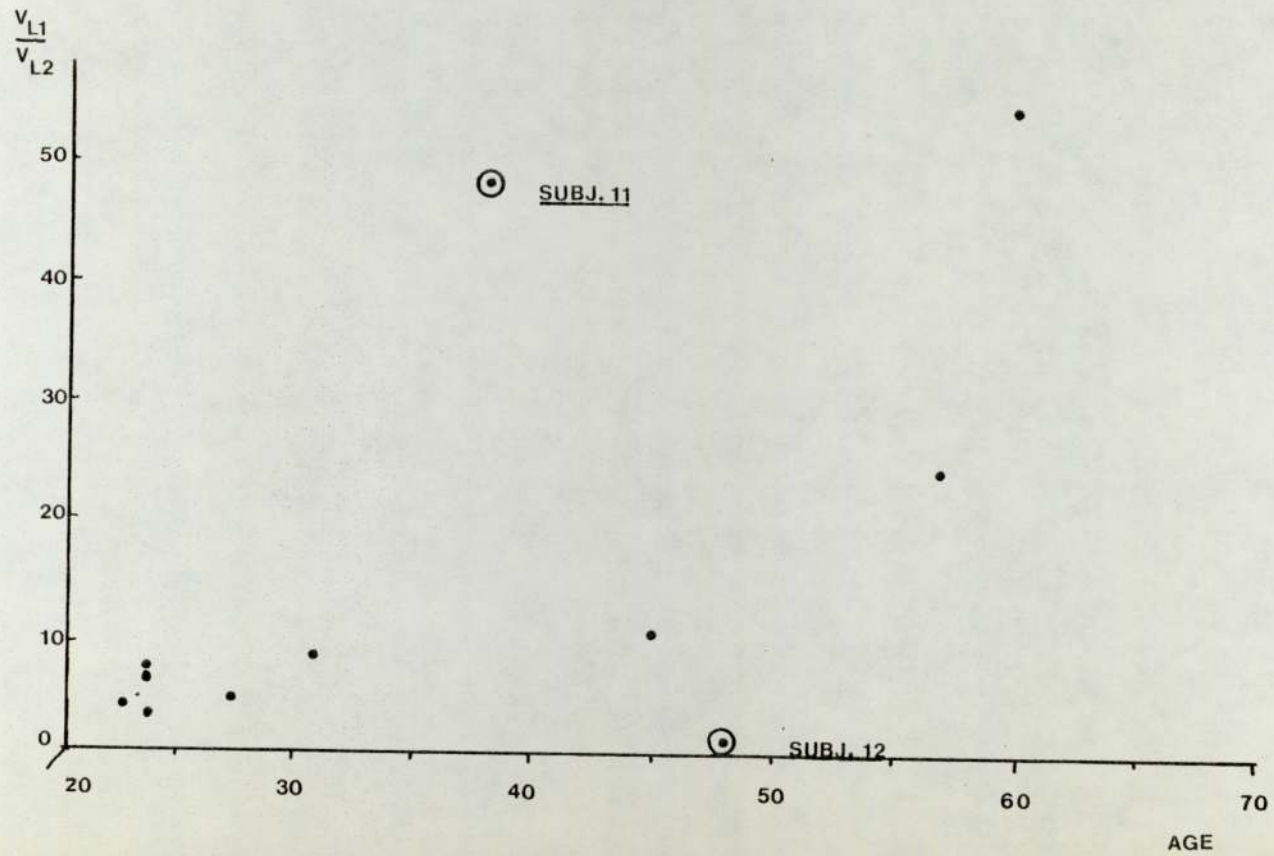
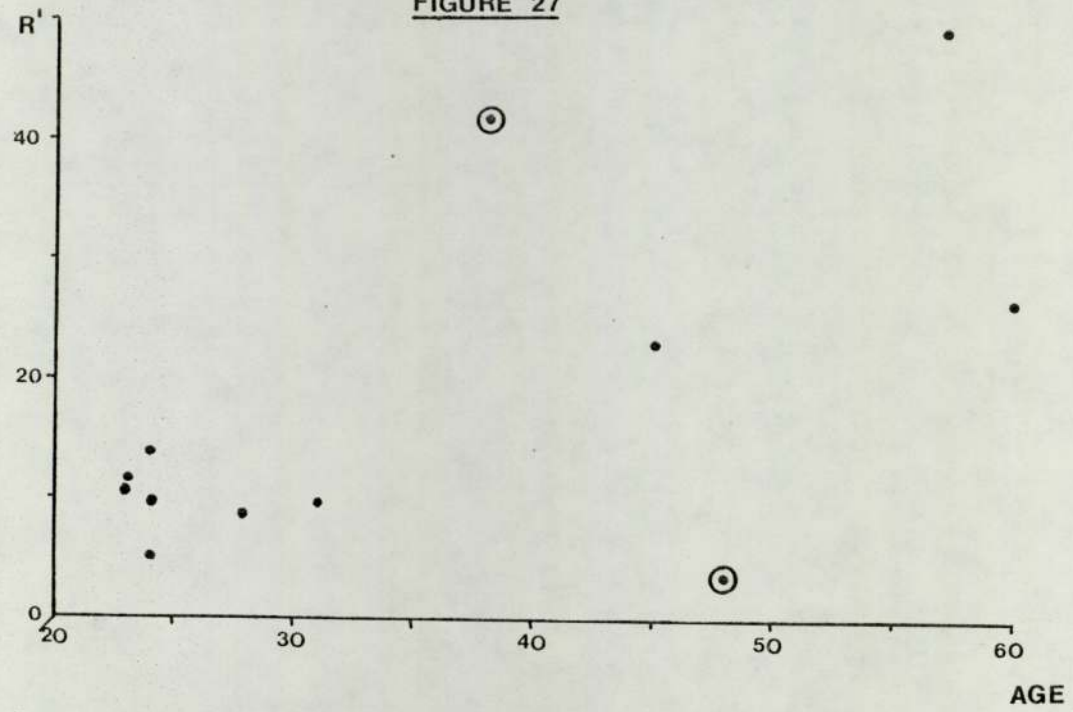


FIGURE 27



CHAPTER 6

CONCLUSIONS

6.i Recovery of theoretical distributions

Consider the *direct compartmental fit* recovered from nitrogen washout data generated by a *delta type* function in Chapter 4.i. The recovered distributions were remarkably accurate, even in the presence of simulated experimental error, with 99.9% of the total ventilation being direct towards a single compartment. Although the specific ventilation corresponding to this peak ventilation was 0.53 compared to the true value of 0.95, some discrepancy between recovered and original values of $S(i)_{\max}$ must be expected since the seven compartment fit recovered a true *singularity* whereas the original distribution, although narrow, was made up of a large number of compartments constituting a spread of ventilations around the peak. However, it is encouraging that the values of $S(i)_{\max}$ are of the correct order of magnitude irrespective of noise on the data. It can be concluded, therefore, that a direct compartmental fit is capable of recovering the principle features of a delta type function from nitrogen washout data.

When the *direct compartmental fitting* routine was applied to nitrogen washout data generated from a *bimodal distribution* (Chapter 4.ii), the recovered distributions remained unimodal.

The only distinguishing feature which suggested the envelopment of a multi-modal structure was the direction of significant proportions of ventilation towards a larger number of compartments. This cannot be said to be an identification of multi-modality, since a similar distribution may represent a broad unimodal function (Chapter 4.iii) as in figure 17. Nevertheless, direct compartmental fitting to a small number of compartments can reveal very significant information. It is certainly possible to distinguish narrow and broad distributions even if it is not always possible to estimate the number of modes present in the original distribution. Such a technique gives a good approximation to the true distribution, from which a suitable mathematical function can be chosen to describe the distribution.

In an attempt to recover continuous distributions of fractional and specific ventilation, a technique was utilized by which a mathematical function was chosen to represent the distribution. That is, the fractional ventilation was *parametrized* as a function of specific ventilation and the unknown constants of the parametrization determined. This meant that the number of parameters to be determined was independent of the number of lung compartments and therefore *continuous unique distributions* could be obtained from nitrogen washout curves.

Similar techniques have long been successfully used in related sciences (42a).

Obviously the forcing of all the lung compartments to relate to the chosen parametric function may cause certain original features to be lost. However, the requirement that the least squares function, L , must be approximately zero can only be satisfied if the most important characteristics of the distribution are maintained. If a totally unrealistic parametrization is used, the program will merely fail to minimize. Certainly, in the recovery of bimodal distributions and particularly in the recovery of delta type functions (Chapter 4) the principle features of the distributions are satisfactorily retained even with 2% experimental error.

6.ii Recovery of distributions from experimental N₂ washout curves

The results of both the *direct compartmental* and the *parametrization* fits to the experimental N₂ washout data obtained from the twelve subjects have previously been discussed in detail (Chapter 5). However, a number of the more important conclusions arising from this study must be briefly reiterated.

- (a) Direct compartmental fitting not only recovered remarkably uniform distributions amongst the young normals, but appeared very sensitive to any pulmonary abnormalities and may in future preclude the need to obtain continuous distributions.

- (b) All twelve distributions recovered by means of the parametrization fitting were *bimodal*, even though the parametric function of equation (19) was capable of reproducing a unimodal distribution. It is impossible at this stage to hypothesis as to the meaning of such bimodality, but possible means of identifying the cause of the peaks are suggested in the section on Future Work.

- (c) The lungs of young normals appear to behave "as if" they consist of two principle respiratory regions of volume ratio equal to six

- (d) This volume ratio, and the parameter R_1' , increased rapidly with age and it is tentatively suggested that this ratio together with the parameter R_1' may be a very sensitive indication of abnormalities.

With a sample of twelve nitrogen washout curves, no definite conclusions can be drawn which would aid diagnosis. However, the results provide a clue to the recovery of unique distributions of V_i/V_T and S_i and suggest the need for future extensive experimental and theoretical trials since there appear to be very definite analytical responses to pulmonary abnormalities.

It was inherent from the increased computing time (approximately ten times greater), that *parametrization fitting* is a far more complex process than *direct compartmental fitting*. It is hoped that the results gained from expressing the distributions as parametric functions may be improved by further studies. However, it may prove that the process becomes so complex as to exclude it from routine clinical use. Alternatively, the recovery of *unique* distributions by direct compartmental fitting restricts the analysis to a small number of lung compartments with which multi-modal features do not become apparent.

Although both procedures have disadvantages, nevertheless, it is felt that the data which can be already obtained from the two processes regarding the true existing distributions may well be sufficient to define and identify diseases of the lung. It is also envisaged that if sufficient experimental data is analysed and the results from the two types of fit

correlated, the seven compartment fit may in future be the only test required to detect pulmonary abnormalities. If the minimization routine was converted for use on a "mini" computer, the analysis could be fully automated for clinical use. This would lead the way to a truly informative and readily applied lung function test which, above all, would have the advantage of simplicity.

PART II

DETECTING AND QUANTIFYING PULMONARY

ARTERIOVENOUS BLOOD SHUNTS

PART II: Detecting and quantifying pulmonary
arteriovenous blood shunts

CHAPTER 7

Background

A pulmonary-arteriovenous blood shunt may be defined as that proportion of cardiac output which drains directly into the mixed arterial circulation without taking part in gas exchange. The concept of venous admixture is simple since it is merely the contamination of arterial blood by deoxygenated blood, but the mechanisms responsible for this entity are complex (6, 14, 44, 16). Numerous pathways exist by which venous blood may reach the peripheral circulation. Typical examples are congenital anomalies of the heart and great vessels; bronchial, Thebesian and anterior cardiac veins; portal-mediastinal-pulmonary venous anastomoses; and pulmonary arterio-venous shunts.

The latter channel for venous admixture, which will be referred to as a true blood shunt, is very important since it is believed to occur in a number of diseases and in some cases even during anaesthesia, (45). True intrapulmonary blood shunts are thought to be small in normal man, a typical quoted value being less than 1% of the total pulmonary blood flow. An increase in the blood flow traversing the shunt causes severe oxygen depreciation in arterial blood and limits the essential supply of oxygen to the tissues. True blood shunts are known

to occur in certain chronic lung disorders (45, 46, 47) such as bronchiectasis, tuberculosis, carcinoma of the bronchus and, most frequently, emphysema. Considerable increases in collateral flow, that is blood from the systemic (bronchial) arteries which bypasses the bronchial capillary bed and reaches the pulmonary veins, may often be found in patients with congenital heart disease. In such cases, blood flow in the pulmonary arteries is severely reduced often to the extent of complete absence of blood. Other examples of true shunt have been reported during anaesthesia or in situations of severe surgical shock (50).

Conventionally, a blood shunt is measured using the oxygen method together with classical gas mixing equations (46). However, whilst it is a simple test to perform, it has two major disadvantages. First, steady state conditions are difficult to establish, particularly in subjects having chronic pulmonary disfunctions. Second, the high pulmonary O_2 tension required to ensure saturation may cause regional lung collapse in areas of low \dot{V}_A/\dot{Q} thereby increasing the size of the initial shunt (48).

This phenomenon is particularly noticeable in patients with emphysema in whom the administration of oxygen may cause severe disturbance of the blood flow distribution in the lungs.

Thus, in an attempt to find an alternative to the standard oxygen method, research concentrated on the possible use of inert tracer gases. Inert tracer gases are particularly useful for pulmonary tests because a number of radioisotopes can generally be found which are relatively harmless, and have longer half lives than those of the respiratory gases such as O_2^{15} . Detection and measurement of a radioisotope concentration is readily performed 'in situ' with a very concise clinical arrangement (49, 50).

The basic hypothesis behind the use of inert tracer gases is relatively simple, and applies to all the so-called double indicator techniques. If an inert gas of very low solubility is intravenously injected and subsequently arrives at the site of a ventilated alveolus, it will be rapidly expelled from the blood, whereas blood traversing a shunt pathway, say an atelectatic area of the lung will retain the gas. Thus, if the amount of gas introduced into the pulmonary arteries is known, the amount of gas measured in arterial blood leaving the lungs can be related to the amount of blood passing ventilated alveoli. Fritts et al (51) developed this fundamental idea into a method, now generally known as the double indicator technique, which could quantitatively measure true pulmonary blood shunts. Although numerous techniques have since followed and some typical examples are quoted in references 52 to 55, all are variations of the basic principles pioneered by Fritts et al and are compared in detail by Spry (50).

The double indicator technique involves the simultaneous intravenous infusion of two inert tracers, one readily expelled from the blood in contact with air, and one which is retained. Fritts et al (51) chose to use Kr⁸⁵ and T-1824 dye as the gaseous and retained tracers respectively. However, Xe¹³³ (55) and more recently SF₆ (52) have been substituted for Kr⁸⁵, whilst Tc^{99m} has been shown to be a very useful cardiac output tracer (50). As the volatile tracer gas will tend to be excreted via ventilated alveoli, the majority of the gas subsequently appearing in arterial blood must be contributed by the shunt flow. Unfortunately, any gas having a finite solubility will not be completely cleared from capillary blood during the first circulation and even in the complete absence of shunt, an estimation of this normal retention is a 'sine qua non' in all of the proposed tests. Fritts et al for example, assumed end-capillary gas concentrations to be a linear function of time in an attempt to assess the contribution of non-shunted blood to the mixed arterial blood concentration. An alternative approach suggested by Copley et al (52) was to use an extremely low solubility tracer gas to ensure that most of the gas is eliminated from capillary blood perfusing functional alveoli. Here, any tracer gas detected in arterial blood must be predominantly due to a shunt. Whilst errors introduced by this assumption may be small (50), this experimental protocol does not lend itself easily to routine clinical application.



Moreover, the only gas which can realistically be utilized is SF₆ which requires elaborate equipment for detection in arterial blood and cannot be measured in situ. It is therefore necessary to reappraise experimental protocols involving *higher solubility* tracers for purely practical reasons.

By simulating the double indicator techniques using a mathematical model of non-steady state inert gas exchange, it was possible to study the effects of abnormal distributions of \dot{V}_A , \dot{Q} and V_L on the measurement of true shunt (50). It was found that the experimental protocols using the more soluble tracers Kr⁸⁵ or Xe¹³³ failed to distinguish between true pulmonary blood shunts and oxygen deficiency due to abnormal distribution of \dot{V}_A and \dot{Q} , referred to as apparent shunts. In addition, the theoretical analysis employed by Fritts et al was found to always underestimate the value of true shunt whereas the method developed by Copley et al was prone to overestimation. Moreover, this was shown to be a method in itself of discriminating true from apparent shunt. Figure 28 illustrates the effects of various pulmonary abnormalities on the size of the measured shunts by the basic methods of Fritts et al (51), method A, and Copley et al (52), method B, and the average of the two methods.

The trends summarized in Figure 28 were found to be

Pulmonary Abnormality	Effect on evaluation of shunt by method A	Effect on evaluation of shunt by method B	Effect on ave. value of shunt by methods A & B
TRUE SHUNT ↑	↑	↑	↑
\dot{V}_A scatter	↑	↓	↑
\dot{Q} scatter	↓	↑	↓
\dot{V}_A ↑	↑	↓	↑
\dot{Q} ↑	↓	↑	↓
v ↑	↑	↓	↑

FIGURE 28

extremely useful in distinguishing various apparent shunts from true shunt. This was evident in the experiments on beagle dogs, using Xe^{133} and $\text{Tc}^{99\text{m}}$ as the radiotracers, under conditions of deep anaesthesia with the addition of P.E.E.P. and negative phase. Although these results were very valuable, the quantitative measurement of true shunt was still subject to a large degree of error. This was partly attributed to the errors in estimating the point of recirculation together with the known inaccuracy of estimating the amount of Xe^{133} in blood passing ventilated alveoli. It was found possible however to reduce this error by evaluating the shunt by both methods A and B and taking the average value. Nevertheless, it was felt necessary to search for a more efficient means of evaluating true shunt.

The most interesting conclusion, from the mathematical modelling of the double indicator technique, was that the size of the apparent shunt was dependent on the time of measurement. In the non-steady state, it was concluded that apparent shunt was time variant. Therefore, the aim of this present research was to explain and exploit these time variant characteristics of apparent shunt in an attempt to discover a means of rapidly identifying apparent from true shunt. The more soluble tracers such as Xe^{133} are extremely valuable radiotracers owing to their availability and good detection properties. Thus a further aim was to design a

basic protocol to enable the use of a more soluble tracers such as Xe^{133} .

With these objectives in mind, an extensive study is now made of non-steady state mixed arterial and mixed venous concentrations of inert tracers of varying solubilities under different conditions of true and apparent shunts.

Use is made of a mathematical model which describes the non-steady state pulmonary exchange processes of a physiologically inert gas in terms of its arterial levels, following infusion into the mixed venous blood stream, prior to recirculation. The basic model is adapted to simulate situations in which both true and regional inequalities are present in the lungs enabling a comprehensive study of inert pulmonary gas exchange.

In all cases of non-steady state gas exchange, retention ($P_{\bar{a}G}/P_{\bar{v}G}$) is observed to rise exponentially to a constant steady state value. In cases where true shunt was absent, the retention curve rises from the origin, but where a true shunt exists, the curve cuts through the y axis (the retention axis) at a value of retention equal to the fractional blood flow through the true shunt pathway.

This result is found to be general and independent of the gas solubility, enabling the use of higher solubility tracer gases such as Xe^{133} . The method offers rapid *in situ* determination

of true shunt. Moreover, the shape of the retention-time curve is a function of the ventilation, perfusion and lung volume distributions in the lungs. Therefore, together with the N₂ washout analysis described in Part I, most of the important features of the lung can in future be recovered. Not only is the recovery of the information an essential aid to diagnosis and therapy but will hopefully add considerably to our detailed understanding of pulmonary function.

CHAPTER 8

The Mathematical Model

8.i Non-steady state inert gas exchange

In order to simulate the initial stages of inert gas elimination from mixed venous blood, a continuous non-steady state gas exchange equation was required. The following derivation extends the earlier work of Scrimshire et al (56) who employed a finite state approximation to gas exchange under transient conditions.

Consider the lung to be a single well-ventilated compartment, and suppose an inert tracer gas is introduced into mixed venous blood. The subsequent increase in the alveolar tension due to gas exchange can be expressed as,

$$\frac{d}{dt} (V_L P_{AG}) = V_L \frac{d}{dt} (P_{AG}) \quad (22)$$

where V_L is mean lung volume.

Since the rate of change in the amount of gas G in the lungs must equal the rate of gas uptake from the capillary bed, minus the rate of gas expired from the lungs, then we can write,

$$V_L \frac{d}{dt} (P_{AG}) = V_{BG} - V_A P_{AG} \quad (23)$$

where V_{BG} is the amount of gas G transferred from blood to the

lungs per unit time.

From Fick we have,

$$V_{BG} = \lambda \dot{Q} (P_{VG} - P_{cG}) \quad (24)$$

where λ is the Ostwald Partition Coefficient and P_{cG} is the end-capillary concentration of gas G. If end-capillary blood is assumed to be in equilibrium with the alveolar gas then $P_{cG} = P_{AG}$ and therefore,

$$V_L \frac{d}{dt} (P_{AG}) = \lambda \dot{Q} P_{VG} - [\lambda \dot{Q} + \dot{V}_A] P_{AG} \quad (25)$$

Equation (25) is a homogeneous first order linear differential equation which can be solved in the form,

$$P_{AG} (t) = \frac{K}{C} + \left[P'_{AG} - \frac{K}{C} \right] \exp (- Ct) \quad (26)$$

where P'_{AG} is defined as the alveolar partial pressure of the gas at time $t = 0$, and

$$K = \frac{\dot{Q} \lambda P_{VG}}{V_L}$$

and,

$$C = \frac{\dot{Q} \lambda + \dot{V}_A}{V_L}$$

Although equation (26) describes non-steady state inert gas exchange, it is important to note that as t tends to infinity, it reduces to the steady state equations previously developed by Farhi (30). The ability to solve equation (25) analytically requires that the coefficients are time independent, however, an iterative approach was devised to enable solutions to be obtained with time variant coefficients. If one considers very small time intervals such that the coefficients are approximately constant, then the analytic solution of equation (25) is valid. Equation (26) is therefore modified as in equation (27) to allow for repeated calculations over small time intervals. Hence, the value of P_{AG} at any time τ is given by,

$$P_{AG}(\tau) = \frac{K(\tau)}{C(\tau)} + P_{AG}(\tau - T) - \frac{K(\tau)}{C(\tau)} \exp(-CT) \dots\dots\dots(27)$$

where T is the short time interval which in the present studies was fixed at 0.1 seconds.

Having produced a basis for a simulation of non-steady state gas exchange in a homogeneous lung, attention can now be given to the modelling of true shunt, regional \dot{V}_A and \dot{Q} inhomogeneities and combinations of both phenomena.

8.ii Homogeneous lung with true shunt

Figure 29 shows a schematic representation of a simple lung model having a true blood shunt and no \dot{V}_A/\dot{Q} inequalities. \dot{Q}_T , \dot{Q}_P and \dot{Q}_S represent the total pulmonary blood flow, the flow past ventilated regions of the lung, and the shunted blood flow respectively. P_{VG} , P_{CG} and P_{aG} are the partial pressures of the inert gas in mixed venous, end-capillary and mixed arterial blood respectively at any time t , and P_{AG} is the corresponding alveolar partial pressure. Mixed arterial blood is formed by the confluence of shunt and non-shunt pathway contributions and may be expressed mathematically as,

$$P_{aG}(t) = \frac{\dot{Q}_P}{\dot{Q}_T} P_{CG}(t) + \frac{\dot{Q}_S}{\dot{Q}_T} P_{VG}(t) \quad (28)$$

Since the model has only one homogeneous ventilated compartment P_{CG} can again be assumed to equal P_{AG} , and is therefore evaluated directly from equation (27).

8.iii Heterogeneous lung with no true shunt

The concept of a lung being totally homogeneous is obviously over simplified and we must begin to consider means of allowing for regional variations of \dot{V}_A and \dot{Q} which are known to exist even in normal lungs. The accepted method for

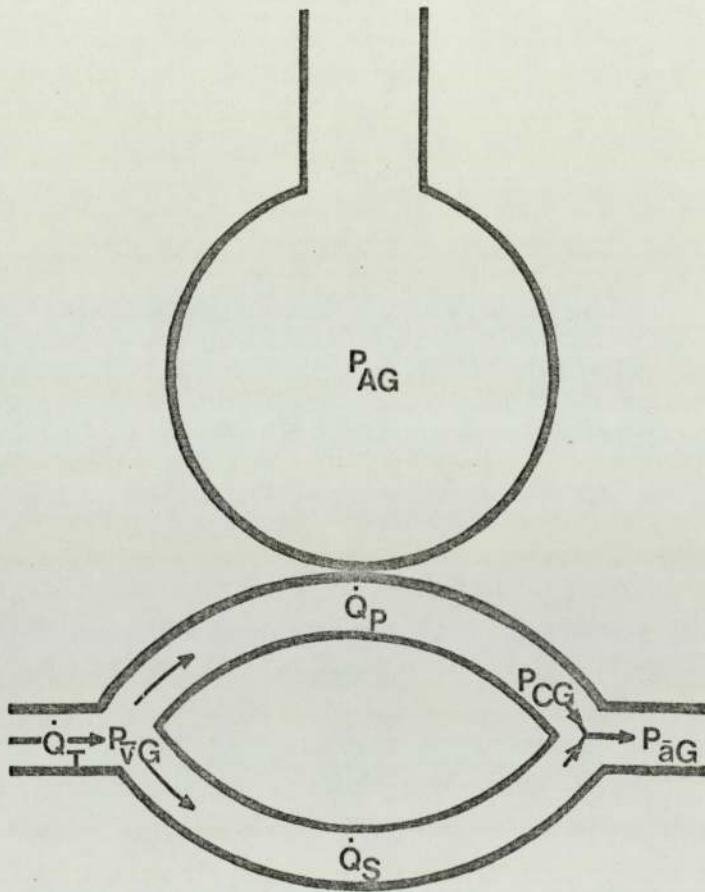


Figure 29

Intra-pulmonary blood shunt

simulating regional inequalities of \dot{V}_A and \dot{Q} is to treat each region of the lung as an individual simple gas exchanger, expressing the gas concentrations relating to each compartment by equation (27). Figure 30 illustrates how the lung is modelling as 'n' well mixed compartments, each having a particular proportion of the total ventilation and blood flow which may be specified by theoretical distributions (57, 37). Since the contribution of each compartment must be proportional to the volume of blood flow from that compartment, the mixed end-capillary gas tension is given by,

$$P_{\bar{C}G}(t) = \sum_{j=1}^{j=n} \frac{\dot{Q}_j}{\dot{Q}_T} P_{cGj}(t) \tag{29}$$

Thus, expressing P_{cGj} by equation (27) we have,

$$P_{\bar{C}G}(t) = \sum_{j=1}^{j=n} \frac{\dot{Q}_j}{\dot{Q}_T} \left[\frac{K_j}{C_j} + \left[P'_{cGj} - \frac{K_j}{C_j} \right] \exp(-C_j t) \right] \dots\dots\dots (30)$$

where $K_j = \frac{\dot{Q}_j \lambda P_{\bar{V}G}}{V_{Lj}}$

and $C_j = \frac{\dot{Q}_j \lambda + \dot{V}_{Aj}}{V_{Lj}}$

Therefore, by means of equation (30) we are able to simulate the behaviour of gas exchange in a non-uniform lung.

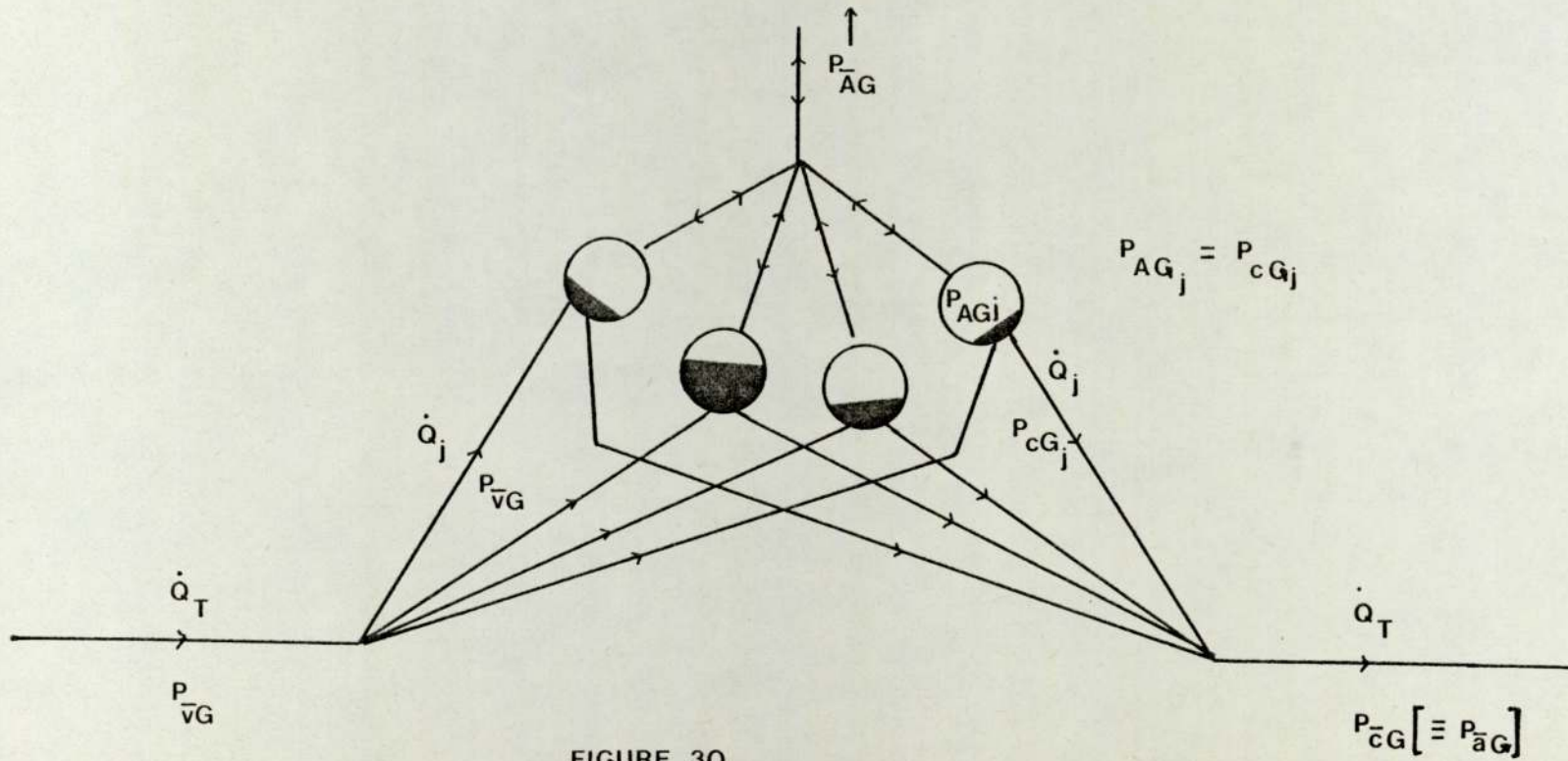


FIGURE 30

8.iv Heterogeneous lung with true shunt

In any real situation, both true shunt and regional inhomogeneities of \dot{V}_A and \dot{Q} are thought to co-exist. Such a case is illustrated in figure 31, and mixed arterial blood composition must now be expressed as,

$$P_{\bar{a}G}(t) = \frac{Q_S}{Q_T} P_{\bar{V}G}(t) + \left[1 - \frac{Q_S}{Q_T} \right] P_{\bar{c}G}(t) \quad (31)$$

where $P_{\bar{c}G}(t)$ is defined in equation (30).

It is now possible to undertake a detailed simulation of gas exchange in both normal and abnormal lungs, and study the simultaneous effects of true shunt and regional \dot{V}_A/\dot{Q} inequalities on the retention of an inert tracer gas.

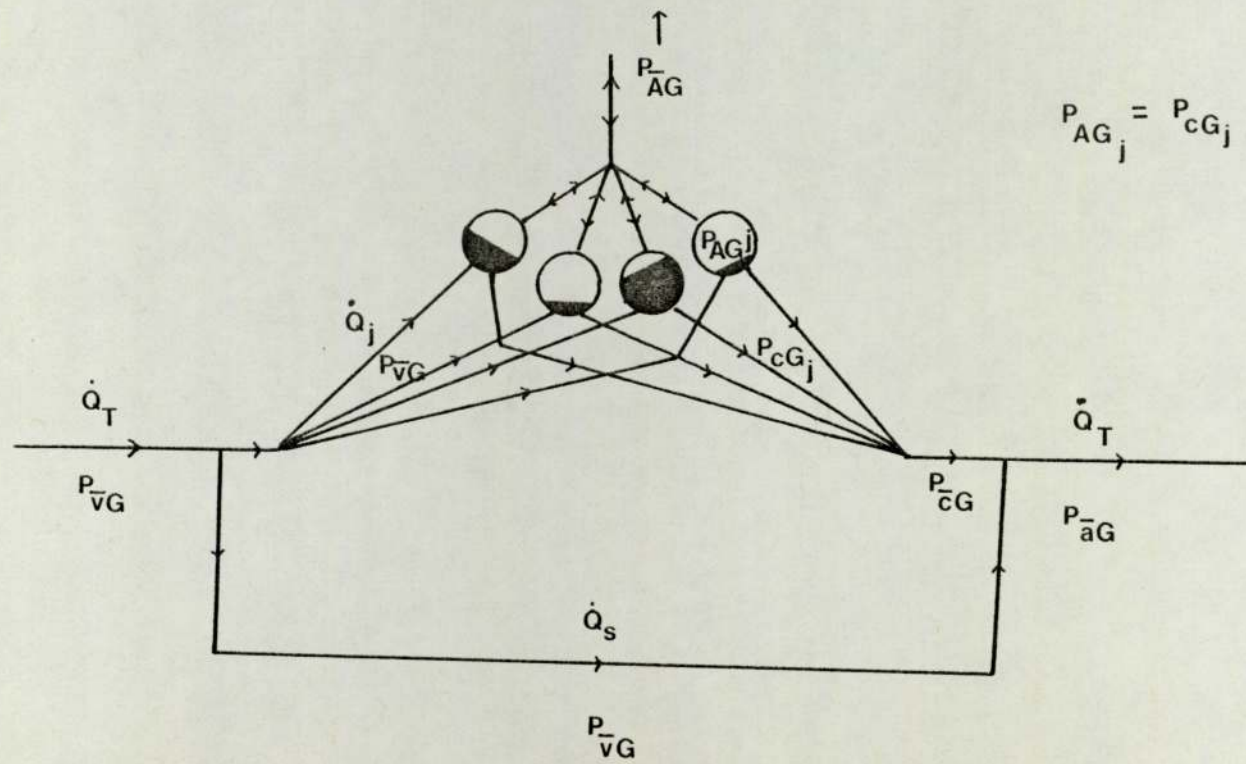


FIGURE 31

CHAPTER 9

Results of simulation

The retention of an inert gas is generally regarded as a steady state measurement (29). Since it is a comparison of arterial to venous gas concentrations, it serves as a good indication of the inefficiency of gas exchange created by regional inequalities of \dot{V}_A and \dot{Q} together with any shunting of blood. However, as ensuing discussion will show, retention could also be measured under *non-steady state conditions*. Thus, simulations of non-steady state inert gas exchange in the previously described lung models were performed in order to study retention as a function of time in the initial stages of gas uptake. The tracer gas Xenon is assumed to be infused at a constant rate into the mixed venous circulation and values for the transient state retention as a function of time are calculated from the respective gas exchange equations.

9.1 Homogeneous lung with no true shunt

This lung model is totally free of any \dot{V}_A or \dot{Q} inequalities, or any true shunt. Thus, optimum gas exchange properties can be expected to exist for any particular value of total ventilation and perfusion. The non-steady state retention as a function of time for a tracer gas, with an Ostwald partition coefficient of 0.5, is illustrated in figure 32. The function rises exponentially from the *origin* to a steady state retention value of 0.33.

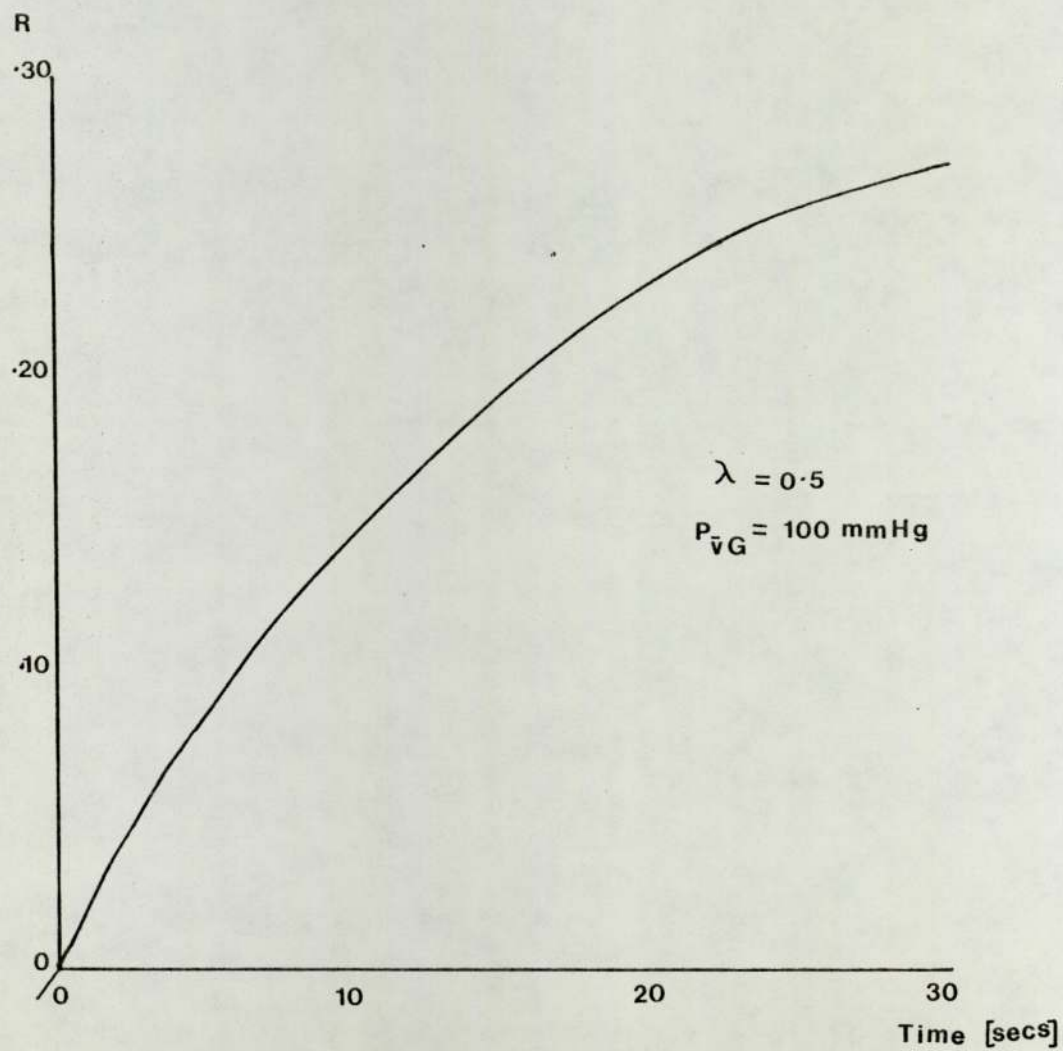


FIGURE 32

9.ii Heterogeneous lung with no true shunt

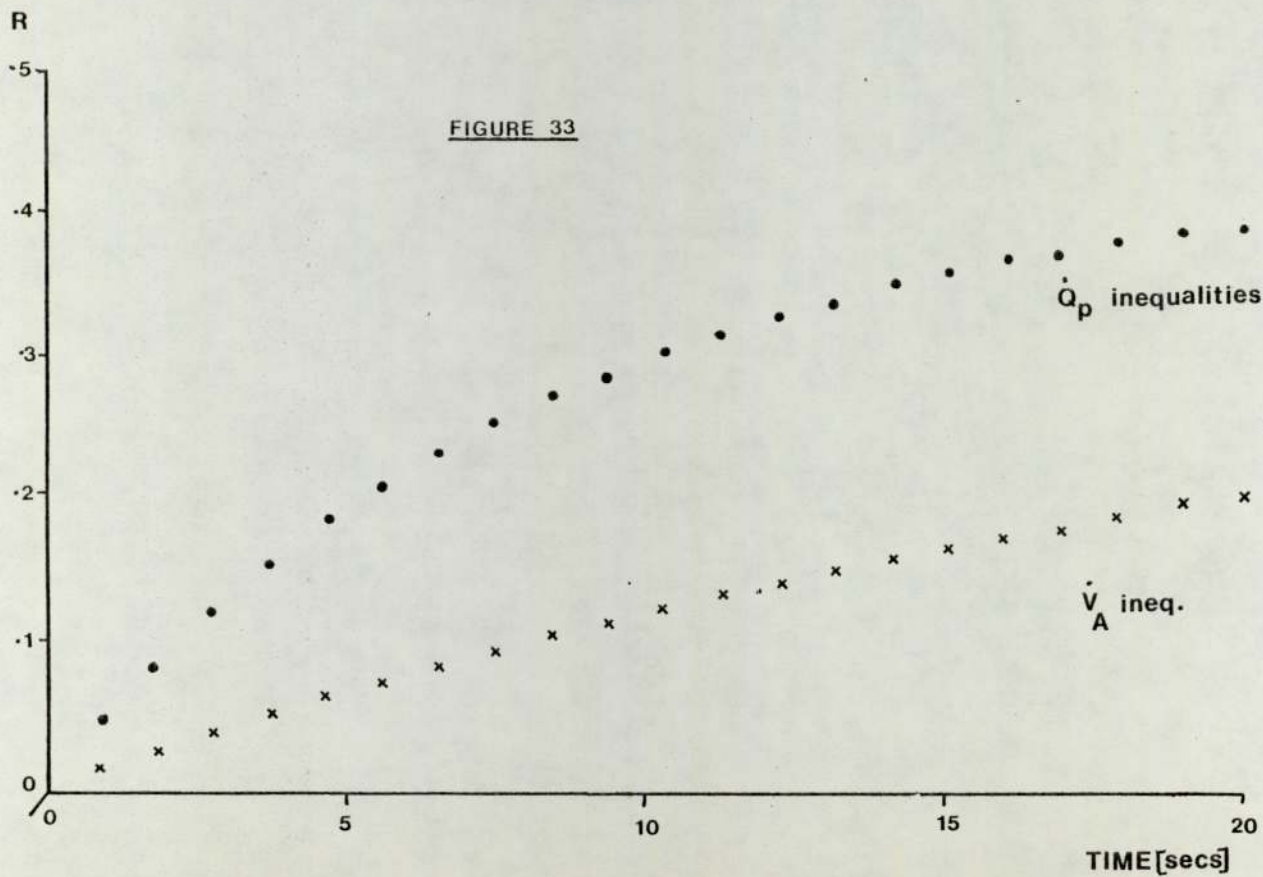
Figure 33 describes the retention of the same gas as a function of time with \dot{V}_A and \dot{Q} inhomogeneities but no true shunting of blood. The distributions of \dot{V}_A and \dot{Q} were simulated by means of a geometric progression as specified by Scrimshire (56). As for the homogeneous lung with no true shunt, the curve rises exponentially from the *origin*. The functional form of the retention curve is dependent on the distribution of \dot{V}_A and \dot{Q} . However, the point from which the curve rises (i.e. at $t = 0$) is independent of the type of distribution or extent of the scatter of regional inequalities and is always at zero coordinates.

9.iii Homogeneous lung with true shunt

When non-steady state retention was calculated for a lung with no inequalities of \dot{V}_A and \dot{Q} but with 10% of the total pulmonary blood flow traversing an arteriovenous blood shunt, *the curve no longer rose from the origin*. Instead, the curve consistently cut the retention axis ($t = 0$), *at a value equal to the fractional shunt blood flow*. However, the rate of increase of retention was identical to that seen in the homogeneous lung with no shunt. These results are demonstrated in figure 34.

9.iv Heterogeneous lung with true shunt

Figure 35 describes non-steady state retention in the presence



$\lambda = 0.5$
 $P_{\bar{V}G} = 100 \text{ mmHg}$
 $\bar{V}G$ [constant]

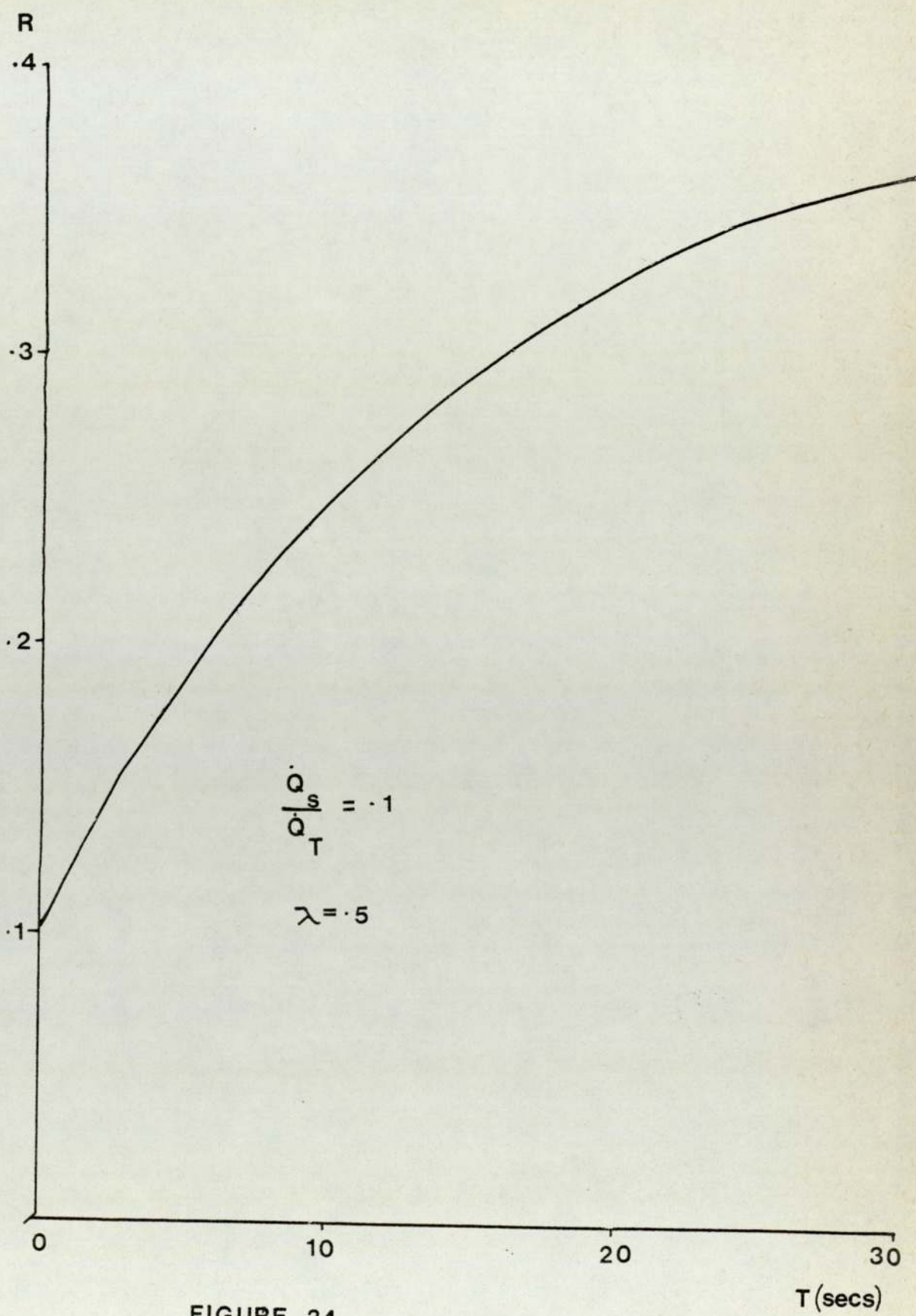
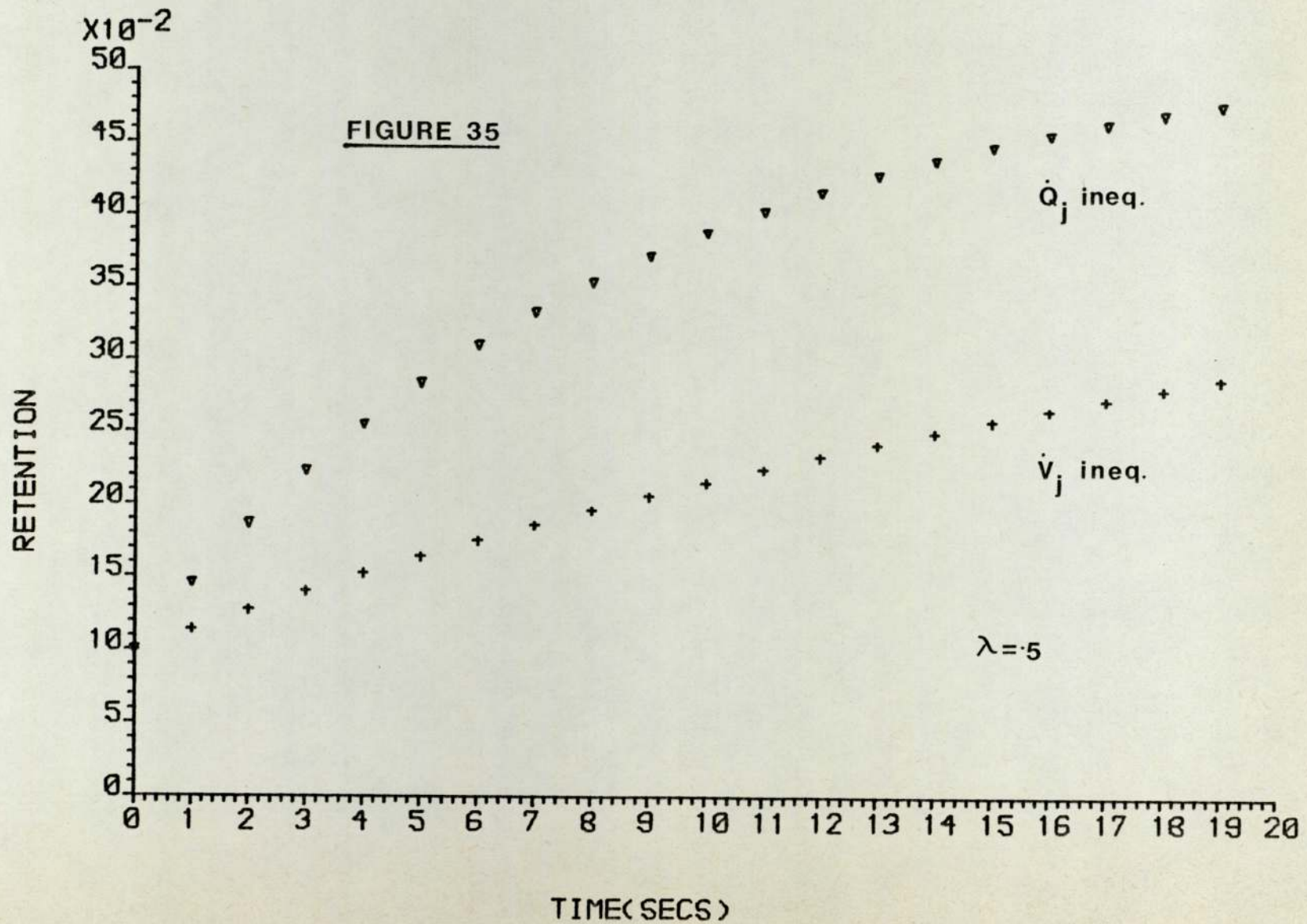


FIGURE 34



of \dot{V}_A and \dot{Q} regional inequalities in addition to a 10% shunt blood flow. These results again suggest that the *value of R at t = 0*, is a direct indication of the presence and size of any *true* blood shunt, whereas the *rate of increase* of the curve is dependent on the properties of the *apparent* shunt.

Thus, the measurement of R at "t = 0" is theoretically a new means of detecting and quantifying true pulmonary arteriovenous blood shunts.

CHAPTER 10

Practical applications of theory

It is evident, that even under conditions of regional scatter of \dot{V}_A and \dot{Q} , retention as a function of time yields the fractional shunt blood flow at time $t = 0$.

This may be demonstrated mathematically by rearranging equation (28) to give an expression for the fractional shunt for a homogeneous lung. That is,

$$\frac{\dot{Q}_S}{\dot{Q}_T} = \frac{P_{\bar{a}G}(t) - \frac{\dot{Q}_P}{\dot{Q}_T} P_{CG}(t)}{P_{\bar{V}G}(t)} \quad (32)$$

For a heterogeneous lung with regional inequalities in V_A and Q , we may also write,

$$\frac{Q_S}{Q_T} = \frac{P_{\bar{a}G}(t) - \frac{\dot{Q}_P}{\dot{Q}_T} P_{\bar{C}G}(t)}{P_{\bar{V}G}(t)} \quad (33)$$

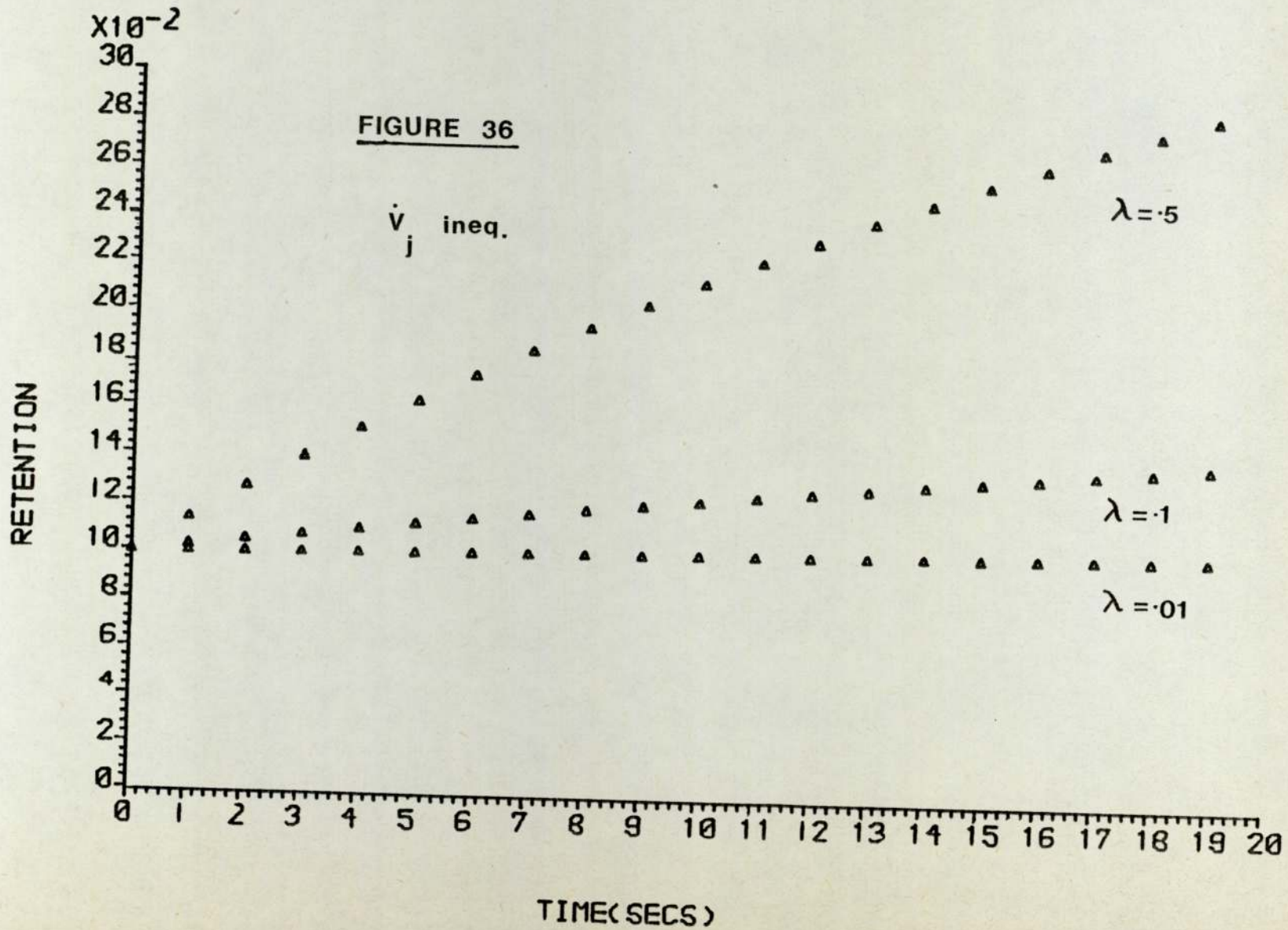
where $P_{CG}(t)$, is given by equation (26) (for constant coefficients), and mixed end-capillary gas concentrations $P_{\bar{C}G}(t)$ by equation (30). Obviously, end capillary gas concentrations throughout the lung must initially be zero, since no tracer is present in the lungs prior to its introduction via mixed venous blood. Substituting $P_{\bar{C}G} = 0$

into equation (33) yields the result that the fractional shunt equals $P_{\bar{a}G}(t=0) / P_{\bar{v}G}(t=0)$ which expresses mathematically the results previously obtained for both a homogeneous and heterogeneous lung under various conditions of true or apparent shunt.

Thus, after extensive theoretical trials, the measurement of true shunt by the retention of an inert gas in the initial stages of gas exchange has been shown to be a general result, independent of the solubility of the tracer, (Figure 36) or the size of the blood shunt (Figure 37).

10.1 Recovering true shunt with a bolus of tracer gas

All the simulations performed so far have assumed $P_{\bar{v}G}$ to be constant. However, in a practical sense, it is simpler to inject a single bolus of the tracer, and particularly in the case of radioactive tracers, this allows higher initial concentrations. Thus, gas exchange was simulated with $P_{\bar{v}G}$ no longer constant. A beta function was used to simulate $P_{\bar{v}G}$ as a function of time after a single injection of the tracer gas. Figure 38 describes the effect on the subsequent retention of an inert tracer gas after a bolus of Xenon ($\lambda = 0.18$) is injected into mixed venous blood, in a lung with regional \dot{V}_A and \dot{Q} inequalities and a 10% true blood shunt. It is clear that the retention at $t = 0$ again gives an exact measure of the true shunt present, even though $P_{\bar{v}G}$ is initially zero.



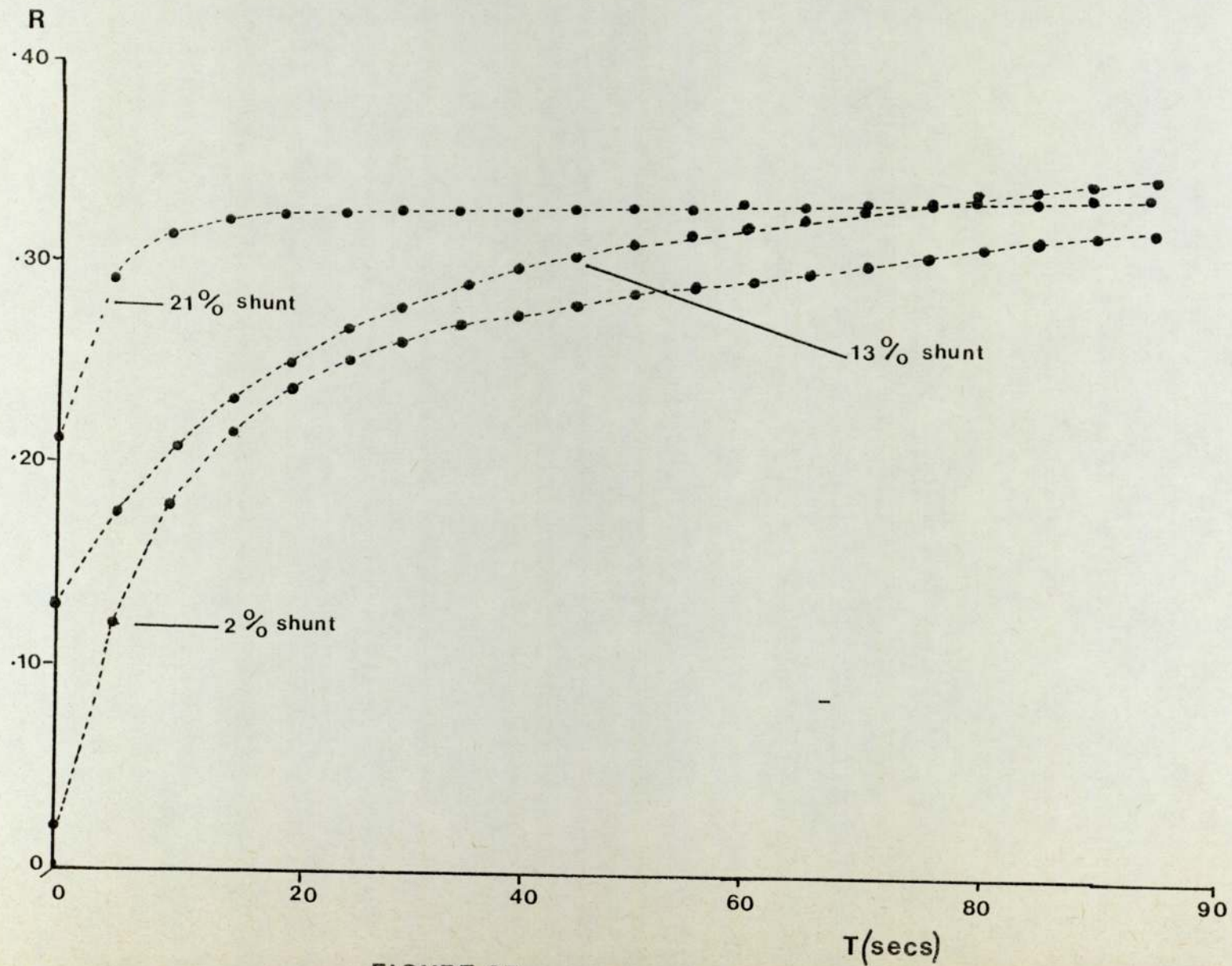


FIGURE 37

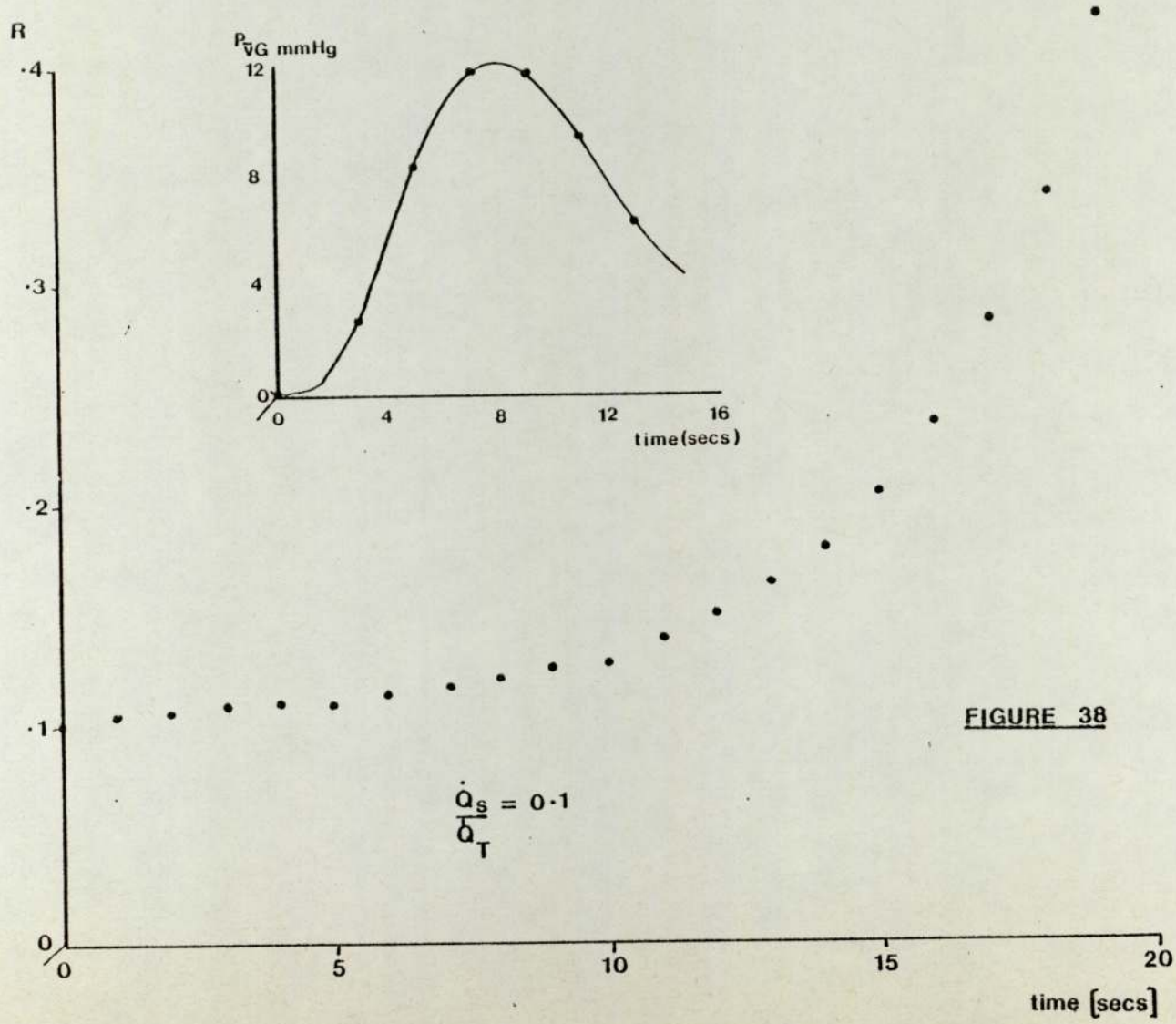


FIGURE 38

10.ii Experimental measurement of non-steady state retention

In the theoretical examination of pulmonary gas exchange it is possible to simulate mathematically the composition of a tracer gas in blood directly as it arrives and leaves the lungs. Experimentally, however, it is impossible to sample blood in the immediate vicinity of the pulmonary capillaries where gas exchange takes place. If the true blood shunt is defined as the retention of an inert tracer gas at $t = 0$, the experimental meaning of " $t = 0$ " must be specified. Consider a volume of blood containing the inert tracer gas arriving at the lungs (and assume that no amount of tracer is present in blood previously arriving at the lungs). A proportion of this blood Q_1 proceeds via *ventilated alveoli* and the remainder Q_2 passes through the *shunt pathway*. Assuming the time taken to travel both pathways is equal, *vide infra*, then for the purpose of *simulation*, $t = 0$ is taken to be the time of confluence of Q_1 and Q_2 .

From the point of view of *experiment*, however, the time of sampling will be *after* the time of confluence of Q_1 and Q_2 , thus when Q_1 and Q_2 arrive at the sample point some dilution of the concentration curve can be expected to have taken place. Similarly, it is only experimentally convenient to measure injectable concentrations yet theory requires us to relate these concentrations to mixed venous concentrations at the site of the lungs.

Sample concentration curves may be related to those at the site of the lungs, however, by the simultaneous introduction of a cardiac output tracer such as Tc^{99m} (50).

Since both tracers follow identical paths and thus undergo the same dilution,

$$\frac{C_{VG} (Xe)}{C_{VG} (Tc)} \Big|_{\text{lungs}} = \frac{C_I (Xe)}{C_I (Tc)} \quad \text{where } C_I = \begin{array}{l} \text{injectate} \\ \text{concentration} \end{array} \quad (34)$$

and,

$$\frac{C_{aG} (Xe)}{C_{aG} (Tc)} \Big|_{\text{lungs}} = \frac{C_{aG} (Xe)}{C_{aG} (Tc)} \Big|_{\text{sampling point}} \quad (35)$$

Hence,

$$\frac{C_{aG} (Xe)}{C_{VG} (Xe)} \Big|_{\text{lungs}} = \frac{C_{aG} (Xe)}{C_{aG} (Tc)} \Big|_{\text{sampling point}} \cdot \frac{C_{aG} (Tc)}{C_{aG} (Tc)} \Big|_{\text{lungs}} \cdot \frac{C_I (Tc)}{C_I (Xe)} \quad (36)$$

But since no cardiac output tracer is lost on passing ventilated or non-ventilated alveoli, then it can be assumed that at the site of the lungs,

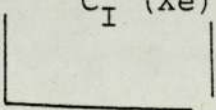
$$\frac{C_{aG} (Tc)}{C_{VG} (Tc)} \Big|_{\text{lungs}} = 1.0 \quad (37)$$

Hence,

$$R_{xe} = \frac{C_{aG} (Xe)}{C_{VG} (Xe)} \Big|_{\text{lungs}} = \frac{C_{aG} (Xe)}{C_{aG} (Tc)} \cdot \frac{C_I (Tc)}{C_I (Xe)} \Big|_{\text{sampling points}} \quad (38)$$

and "t = 0" is defined for the arterial blood sample as the arrival of the tracers at the sampling point, and for the injected tracers as the time of injection. Thus, in practice,

$$\frac{Q_S}{Q_T} = \frac{C_{aG} (Xe)}{C_{aG} (Tc)} \cdot \frac{C_I (Tc)}{C_I (Xe)} \quad (39)$$



 sampling points at
 respective values
 of "t = 0"

Due to increased experimental errors at low tracer concentrations it will almost undoubtedly be necessary to extrapolate the retention curve back to "t = 0" rather than rely on a single measurement of R(t = 0).

10.iii Conclusions

A new experimental protocol has now been suggested for a rapid and accurate quantitation of any true shunt present in the lungs. The experimental technique used by Spry (50), to continuously monitor Xe^{133} and Tc^{99m} levels in sampled arterial blood could be extended to simultaneously monitor injectate concentrations, and the true shunt calculated from the concentrations by an "on-line" processor.

The calculation of true shunt from the non-steady state retention of an inert gas relies on the validity of certain assumptions, namely, the time taken for blood to travel shunt and non-shunt pathways is equal, the magnitude of the shunt remains constant, and there is no loss of either tracer by tissue absorption. These assumptions are necessary for the general mixing equation to be applicable. However, they are also inherent in previous inert tracer gas methods (52, 51, 54) and are generally accepted as being reasonable assumptions.

Since regional \dot{V}_A and \dot{Q} abnormalities must effect end-capillary tracer gas concentrations it is impossible to estimate P_{CG} yet previous methods rely on precisely such an estimation. Consequently, the use of more soluble tracers such as Xe and Kr^{85} to measure true shunt have been unsuccessful, although they are particularly suited to continuous *in situ* monitoring

in blood. The major advantage of this new proposed technique over previous methods, therefore, is that the estimation of the unknown end-capillary tracer concentrations is not a requirement for the calculation of true shunt. In conclusion, the above theory shows true shunt to have a unique effect on the non-steady state retention of an inert gas. Thus the method described above not only enables the use of Xe^{133} and Kr^{85} in the measurement of true shunt, but is also applicable with any inert tracer gas not already present in the lungs and must now be developed for practical use as a rapid and accurate means of detecting true pulmonary arteriovenous blood shunts.

FUTURE WORK

PART I: Recovery of the distribution of ventilation to specific ventilation in the human lung

In Chapter 6, no conclusions were made as to the possible origin of the two ventilatory peaks observed from the parametrization fits to all twelve subjects. Such distinct bimodality, even amongst young normals, was a very important observation. However, no conclusions as to the origins of the two peaks can be made without further experimental work, and it is suggested that the washout and washin of other inert gases are now studied. If the observed peaks are due to series inequalities then it is likely that the recovered distributions will change with the diffusivity of the particular tracer gas. Thus, it may be possible to identify and understand the true meaning of the two modes of ventilation.

Certain refinements to the actual recovery of the distributions can also be proposed as future work. Although the parametrization of fractional ventilation to specific ventilation has proved very successful in recovering distributions, nevertheless, the results could possibly be improved by continuing theoretical and experimental trials.

It may be possible to find more suitable parametrizations, and extensive work is necessary in this area, particularly in determining the precise extent to which a parametric function may distort the recovered distributions.

The criterion by which a recovered distribution is said to approximate the original has been defined as the value of least squares, L . However, when L is evaluated, equal priority is given to each data point, irrespective of whether a point is known to be badly determined. A more reliable test and one which enables one to account for errors on individual data points is the chi-square test, χ^2 ,

$$\text{where } \chi^2 = \sum_{i=1}^n \left(\frac{C_{\text{th}} - C_{\text{exp}}}{\text{err}_i} \right)^2$$

This test can only be used, however, when the error on each data point is known and therefore was not used in the nitrogen washout analyses described previously. Nevertheless, errors on individual data points can be determined in the detection of radiotracers ($\text{err}_i = \sqrt{n_i}$, where n_i is the number of counts). Here, the error is proportionally *larger* for small n_i and hence such badly determined points have less influence on the value of χ^2 than points where err_i is small. Another theoretical improvement would be the evaluation of the inefficiency parameter E within the parametrization fit as well as the compartmental fit.

Experimentally, the test could be improved by evaluating mixed expired nitrogen content (43) rather than end-expired concentrations. The effect of differing tidal volumes on the recovered distributions would also be a very important and instructive topic of investigation.

PART II: Detecting and quantifying pulmonary
arteriovenous blood shunts

Although the measurement of true pulmonary blood shunts by non-steady state inert gas retention is theoretically feasible, the clinical usefulness of the theory can only be extensively tested experimentally. The evaluation of artificial shunts in dogs (52) must first be verified and an experimental set-up designed for convenient clinical use. Future theoretical work, however, will undoubtedly concentrate on recovering not only true pulmonary blood shunts, but also information concerning the apparent shunt, that is, distributions of pulmonary ventilation and perfusion.

Wagner et al (29) chose to use steady state inert gas retention as a criterion for the recovery of \dot{V}_A/\dot{Q} distributions, but these same distributions could also be recovered using non-steady state inert gas exchange. The rate of increase of tracer concentration in the non-steady state is dependent on

the regional ventilation and perfusion inequalities (50). Hence, it is theoretically possible to recover the distributions of \dot{V}_A and \dot{Q} if these distributions can be expressed mathematically in terms of tracer concentrations in a suitable lung model.

In Part I, a method was described by which a nitrogen clearance curve could be used to recover distributions of fractional ventilation to specific ventilation. Although it has been suggested by previous authors (26,27) that the principle mechanism affecting gas exchange is the relationship between ventilation and lung volume, it is nevertheless important to recover blood flow distributions since these are undoubtedly disturbed in a number of diseases. Wagner et al (29) attempted to use steady state retention of inert tracer gases to recover blood flow distributions, whilst Lenfant and Okubo suggested the use of the washin of oxygen during nitrogen washout. Owing to the criticisms lodged against the work of both these authors, in addition to the experimental difficulties posed by blood flow studies, attention has been focused recently on the recovery of $V(i)/V_T$ and $S(i)$ distributions from inert gas washout tests.

Equation (17), however, suggests a means of measuring *non-steady state* retention, which not only offers a method of determining true shunt blood flow, but can also be used to

recover continuous distributions of \dot{V}_A and \dot{Q} . Rearranging equation (6), the following expression results:-

$$R(\tau) = \sum_{j=1}^{j=n} \frac{\dot{Q}_j}{Q_T} \left[\frac{\lambda}{\lambda + \dot{V}_{Aj}/Q_j} + \left[R_j(\tau - T) - \frac{\lambda}{\lambda + \dot{V}_{Aj}/Q_j} \right] \cdot \exp \left[\frac{-\dot{Q}_j}{\dot{V}_{Aj}} + 1 \right] \frac{t}{\dot{V}_{Lj} / \dot{V}_{Aj}} \right] \quad (18)$$

The above equation expresses non-steady state inert gas retention as a function of the distributions of blood flow, ventilation-perfusion ratio and specific ventilation. If the distribution of fractional ventilation to specific ventilation is initially found from the nitrogen washout analysis and subsequently used as data in equation (18), distributions of \dot{V}_A and \dot{Q} may be recovered.

The problem of detecting and quantifying true pulmonary arteriovenous blood shunts and \dot{V}_A/\dot{Q} inequalities will pose numerous experimental problems. Some of these difficulties are immediately overcome by the new proposed methods of theoretical analysis, but the analysis itself requires

considerable testing to understand and overcome new problems which must necessarily arise from experimental adaption.

APPENDIX 1: LIST OF SYMBOLS

<u>Symbol</u>		<u>Meaning</u>
$h(t)$		Laplace Transform
$Be^{-t/T}$	symbols from equation (1) (Lenfant and Okubo ref.27)	time course of dissolved O_2 content
Q_T		total pulmonary blood flow
T		clearance time constant
$q(T)$		blood flow distribution function
A		alveolar
a		arterial
C		concentration
C_O		concentration of N_2 throughout the lung prior to O_2 breathing
C_I		Injected concentration of tracer
C_m		mixed expired nitrogen concentration of the mth breath
C_{mth}		theoretically calculated mixed expired nitrogen concentration of the mth breath
C_{mexp}		experimentally measured mixed expired nitrogen concentration of the mth breath
E		inefficiency parameter: represents for example, contribution of N_2 from blood and anatomical dead space
E^1		excretion: defined as the ratio of mixed expired tracer gas concentrations to mixed venous concentrations
h_1		half width of left hand peak
h_2		half width of right hand peak

L	value of least squares
N_{compt}	number of lung compartments assumed by model
N_{data}	number of breaths in the experimental N_2 washout curve
N_{para}	number of parameters to be determined from parametrization function
N_{unknown}	total number of unknowns to be determined
P_{AG}	alveolar partial pressured of tracer gas G
P_{aG}	arterial partial pressure of tracer gas G
P_{CG}	end-capillary partial pressure of tracer gas G
P_{VG}	venous partial pressure of tracer gas G
\dot{Q}	blood flow (m^2/sec)
\dot{Q}_P	blood flow part ventilated alveoli (m^2/sec)
\dot{Q}_S	shunt blood flow (m^2/sec)
\dot{Q}_T	total pulmonary blood flow
R	retention: defined as the ratio of mixed arterial partial pressure of tracer to mixed venous partial pressure
R^1	$(\Sigma S_2 / \Sigma S_1) / (\Sigma V_2 / \Sigma V_1)$
S	specific ventilation ($V(i) / V_L(i)$)

ΣS_2	sum of specific ventilations to compartments with significant ventilation under right hand peak
ΣS_1	sum of specific ventilations to compartments with significant ventilations under left hand peak
$S(i)_{\max}$	value of specific ventilation to the compartment with maximum fractional ventilation
t	time (secs)
V	ventilation (m^3/sec)
V	ventilation (tidal volume) (m^3)
$V(i)_{\max}$	maximum fractional ventilation to a compartment
V_L	lung volume (m^3)
$\Sigma V_1/V_T$	sum of fractional ventilations under L.H. peak
$\Sigma V_2/V_T$	sum of fractional ventilations under R.H. peak
V_T	total ventilation (tidal volume) (m^3)
V_{BG}	amount of tracer gas G transferred from blood to lungs per unit time
V_{L1}	sum of compartmental volumes under left hand peak
V_{L2}	sum of compartmental volumes under right hand peak
subscripts i and j	denote i th or j th compartment

λ Ostwald partition coefficient
- denotes 'mixed'
e.g. P_{VG} = *mixed* venous partial
pressure of tracer gas G
 χ^2 chi-square

APPENDIX 2

COMPUTER MINIMIZATION ROUTINE, "MINUIT"

The IBM routine, 'minuit', is designed to minimize an arbitrary function in n parameters, the function being supplied by the user (which in this case is the least squares function, L). Three mathematical procedures for obtaining a minimum solution can be used, either singly, or in sequence. These supplied subroutines are now outlined as follows.

A2.i SEEK

This routine chooses the best set of parameters (that is, those values which give the lowest value of L) found within the specified error for the initial estimates of the parameters. If this is the first call to *SEEK*, the starting values specified by the user are taken as the initial parameter values and the step lengths specified are used for the errors. For each parameter, n , with current value $Y(n)$ and error $\sigma(n)$, a new random value is generated from a normal distribution centred about $Y(n)$ with standard deviation $\sigma(n)$.

The new set of values found in this way is used to evaluate the function (L) at this point in parameter space. If the value of the function is less than the previous one, this new set is used as the optimum set so far evaluated, and the errors on the new set of parameters is estimated. If the new set does not improve on the function value, the old set is retained. This procedure is repeated as many times as specified by the user (in this case 1000 iterations).

Seek provides an effective means of finding the general area of parameter space in which a solution may be found.

A2.ii SIMPLEX

This routine provides the quickest way of moving to a local minimum. Simplex works on the smallest geometrical figure which can be constructed in n dimensions with $n + 1$ points, (where n is the number of unknown parameters). Such a figure is called a *simplex*.

That is, if $n = 1$, simplex produces a straight line figure

$n = 2,$ " " " triangle

$n = 2,$ " " " tetrahedron

and so on.

Simplex requires the function to be specified at $n + 1$ points in parameter space. One point is evaluated at the set of

values for the parameters specified by the user (or at the best set found in SEEK) and the other n points needed are initially evaluated at n random points in parameter space (generated in the same way as in SEEK). Using the values of the function (in this case, L) at each point in parameter space, the position of the '*centre of mass*' of the figure is calculated. The point on the geometrical figure with the largest function value is then reflected through the centre of mass to produce a new simplex.

With successive iterations the "simplex" will move towards a local minima. It will elongate down *valleys* and contour round *peaks*. When the simplex nears the bottom of a minimum it will shrink to a point about the minimum.

The simplex process is generated as many times as specified by the user or until user defined convergence criteria are met (These criteria are specified in the fractional change of the function and in the fractional change in each parameter).

Once simplex has found the approximate position of a local minimum it does not converge very rapidly and its main advantage lies in the speed with which it locates the approximate position of such a minimum and its ability to move round a maximum which would *stop a gradient method*. Once the rough position of the minimum is known MIGRAD should

be used to converge quickly to the exact minimum value.

A2.iii MIGRAD

This is a gradient method and employs as its basis the Newton-Raphson technique.

When we are at a minimum of a function $f(Y(n))$ ($Y(n)$ parameters).

$$\frac{\delta f}{\delta Y_n} = 0$$

and $\frac{\delta^2 f}{\delta Y_n^2} > 0$ for all n

and so on

Hence to find a minimum we have only to determine the root of $\frac{\delta f}{\delta Y_n}$ subject to the constraint $\frac{\delta^2 f}{\delta Y_n^2} > 0$.

Using simplex ensures we are near a minimum, so the constraint $\frac{\delta^2 f}{\delta Y_n^2} > 0$ etc. is not, in general, an essential constraint. For a function of a single parameter Y , then if Y_0 is an estimate of the position of the minimum, a better value will be,

$$Y_1 = Y_0 - \frac{\delta f}{\delta Y} (Y_0) / \frac{\delta^2 f}{\delta Y^2} (Y_0)$$

There are similar, though much more complex, relationships for solving for more than one parameter.

The above procedure is repeated as many times as specified by the user, or until user defined convergence criteria are met.

A2.iv User supplied functions

The following routines are examples of the user supplied *main* functions used to produce,

- (i) direct compartmental fits and,
- (ii) parametrization fits.

Return statements after statement numbers 20, 50 and 60 correspond to subroutines SEEK, SIMPLEX and MIGRAD respectively.

i). DIRECT COMPARTMENTAL FITTING

```

SUBROUTINE FONCFAR(G,F,V,IFLAG)
DOUBLE PRECISION V,FIS,F,VVG,PAG,CJ,CT,ERR,SUMV,G
DIMENSION V(100),VVG(100),PAG(100),CJ(100),CT(100),ERR(100)
DIMENSION C(15)
GOTO (10,20,30,40,50,60),IFLAG

```

```

C C C C C
* * * * *
10 CONTINUE
FIS=0.4878
READ(5,12)NDATA,NCOMPT
12 FORMAT(2I3)
WRITE(6,5)
5 FORMAT(1H,'INIT V(J)',2X,'INIT VVG(J)')
DO 8 J=1,NCOMPT
8 READ(5,16)VVG(J)
16 FORMAT(F8.0)
DO 6 J=1,NDATA
ERR(J)=1.0
7 READ(5,7)PAG(J)
7 FORMAT(F8.0)
6 IF(J.GT.1)CJ(J)=PAG(J)/PAG(1)
DO 102 J=1,NCOMPT
102 WRITE(6,11)V(J),VVG(J)
11 FORMAT(1H,'2E12.4)
DO 9 J=2,NDATA
CT(J)=0.0
DO 14 I=1,NCOMPT
14 CT(J)=CT(J)+(V(I)+(((1.0+FIS+VVG(I))/(1.0+VVG(I))))*(J-1)))
9 CONTINUE
RETURN
* * * * *
C C C C C
* * * * *
20 CONTINUE
RETURN
* * * * *
C C C C C
* * * * *
40 CONTINUE
F=0.0
FIS=Y(8)
DO 41 I=2,NDATA
CT(I)=0.0
DO 42 J=1,NCOMPT
42 CT(I)=CT(I)+(V(J)+(((1.0+FIS+VVG(J))/(1.0+VVG(J))))*(I-1)))
41 F=F+(CT(I)-CJ(I))+((CT(I)-CJ(I))/(ERR(I)+ERR(I)))
SUMV=0.0
DO 43 J=1,NCOMPT
43 SUMV=SUMV+V(J)
IF(V(J).LT.0.0)F=F+1D+12*V(J)*V(J)
F=F+(SUMV-1.0)*(SUMV-1.0)
RETURN
* * * * *
C C C C C
* * * * *
30 CONTINUE
SUMV=0.0
DO 36 J=1,NCOMPT
WRITE(6,35)V(J)
35 FORMAT(1H,'FRACT. VENT.=',D12.4)
1)
36 SUMV=SUMV+V(J)
WRITE(6,37)SUMV
37 FORMAT(1H,'TOTAL FRACT. VENT.=',D12.4)
RETURN
* * * * *
C C C C C
* * * * *
50 CONTINUE
RETURN
* * * * *
C C C C C
* * * * *
60 CONTINUE
RETURN
* * * * *
C
END

```

ii) PARAMETRIZATION FITTING

```

SUBROUTINE FCN(NPAR, G, F, X, IFLAG)
  DOUBLE PRECISION V, Y, F, VVO, FAG, CJ, CT, ERR, SUMV
  DIMENSION Y(100), VVO(100), FAG(100), CJ(100), CT(100), ERR(100)
  1, X(15)
  DIMENSION G(15)
  GOTO (10, 20, 30, 40, 50, 60), IFLAG

```

```

C
C
C *****
*
10 CONTINUE
  READ(5, 12) NDATA, NPAR, NCOMPT
12 FORMAT(3I3)
  FDS=0.484
  DO 6 J=1, NCOMPT
    IF(J-1) 8, 8, 9
  8 VVO(J)=0.01
  GOTO 6
  9 RNM1=NCOMPT-2
  YY=3.8/RNM1
  NC=YY
  RNC=NC
  REM=YY-RNC
  VVO(J)=10.0**((REM*(J-1)))
  VVO(J)=VVO(J)*0.01
  6 CONTINUE
  DO 2 J=1, NDATA
    ERR(J)=1.0
    READ(5, 3) PAG(J)
  3 FORMAT(F8.0)
  2 IF(J.GT.1) CJ(J)=PAG(J)/PAG(1)
  CJ(1)=PAG(1)
  RETURN
  *****
C
C
C *****
20 CONTINUE
  RETURN
  *****
C
C
C *****
40 CONTINUE
  F=0.0
  DO 46 J=1, NCOMPT
    R=DLOG(VVO(J))
  46 Y(J)=X(1)*DEXP(-X(2)*(R-X(3))**2)+X(4)*DEXP(-X(5)*(R-X(6))**2)
  DO 41 I=2, NDATA
    CT(I)=0.0
  DO 42 J=1, NCOMPT
  42 CT(I)=CT(I)+(Y(J)*(((1.0+FDS+VVO(J))/(1.0+VVO(J))))**(I-1)))
  41 F=F+(CT(I)-CJ(I))*(CT(I)-CJ(I))/(ERR(I)*ERR(I))
  SUMV=0.0
  DO 43 J=1, NCOMPT
  43 SUMV=SUMV+V(J)
  IF(V(J).LT.0.0) F=F+10+12*V(J)*V(J)
  F=F+(SUMV-1.0)*(SUMV-1.0)
  RETURN
  *****
C
C
C *****
30 CONTINUE
  SUMV=0.0
  DO 36 J=1, NCOMPT
    WRITE(6, 35) Y(J)
  35 FORMAT(1H , ' FRACT. VENT. =', D12.4)
  36 SUMV=SUMV+V(J)
  WRITE(6, 37) SUMV
  37 FORMAT(1H , ' TOTAL FRACT. VENT. =', D12.4)
  RETURN
  *****
C
C
C *****
50 CONTINUE
  RETURN
  *****
C
C
C *****
60 CONTINUE
  RETURN
  *****
C
  END

```

REFERENCES

1. Geppert J. and N. Zuntz, Ueber die Regulation der Athmung. Arch. Ges. Physiol. 42: 189-245, 1888
(as quoted by Lenfant and Okubo, ref. 27)
2. Krogh, A. On the mechanism of the gas exchange in the lungs. Skan. Arch. Phys. 23: 248-279, 1910
3. Haldane, J. S. and J. G. Priestly, Respiration. Oxford: Clarendon, 1935
4. Ball, W.C., P. B. Stewart, L. G. S. Newsham and D. V. Bates, Regional pulmonary function studied with Xenon¹³³. J. Clin. Invest. 41: 519-531, 1962
5. Harf, A., T. Pratt and J. M. B. Hughes, Regional distribution of V_A/Q in man at rest and with exercise measured with Kr-81m. J.Appl.Physiol. 44: 115-123, 1978
6. Lilienthal, J. L., JR., Riley, R. L., Proemmel, D.D. and R. E. Franke, An experimental analysis in man of the oxygen pressure gradient from alveolar air to arterial blood during rest and exercise at sea level and at altitude. Amer.J.Physiol. 147: 199, 1946
7. Martin, C. J., F. Cline, Jr and H. Marshall
Lobar alveolar gas concentrations: Effect of body position. J.Clin.Invest. 32: 617-621, 1953
8. Mattson, S. B. and E. Carlens. Lobar ventilation and oxygen uptake in man. J.Thoracic Surgery. 30: 676-682, 1955

9. Neufield, G. R., J. J. Williams and P. L. Klineberg
Inert gas a-A differences: a direct reflection of \dot{V}/\dot{Q} distributions. J.Appl.Physiol. 44: 277-283, 1978
10. Anthonisen, N. R., M. B. Dolovich and D. V. Bates,
Steady state measurement of regional ventilation to
perfusion ratios in normal man. J.Clin.Invest.
45: 1349-1356, 1966
11. Bentivoglio, L. G., F. Beerel, P. B. Steward,
A. C. Bryan, W. C. Ball and D. V. Bates,
Studies of regional ventilation and perfusion in
pulmonary emphysema using Xe^{133} .
Amer.Rev.Resp. Diseases 88: 315, 1963
12. Gurtner, H. P., W. A. Briscoe and A. Cournand
Studies of the V_A/Q relationship in the lungs of subjects
with chronic pulmonary emphysema, following a single
intravenous injection of radioactive Krypton (Kr^{85})
I. Presentation and validation of a theoretical model.
J. Clin. Invest. 39: 1080-1089, 1960
13. Rochester, D. F., R. A. Brown, Jr, W. A. Wichern, Jr.
and H. W. Fritts, Jr.
Comparison of alveolar and arterial concentrations of
 Kr^{85} and Xe^{133} infused intravenously in man
J.Appl.Physiol. 22: 423-430, 1967
14. Rahn, H. A concept of mean alveolar air and the
ventilation-blood flow relationships during pulmonary
gas exchange. Amer.J.Phys. 158: 21, 1949
15. Riley, R. L. and A.Cournand. "Ideal" alveolar air and
the analysis of ventilation-perfusion relationships in
the lungs. J.Appl.Physiol. 1, 825, 1949

16. Riley, R. L. and A. Cournand
Analysis of factors affecting partial pressures of oxygen and carbon dioxide in gas and blood of lungs: Theory. J.Appl.Physiol. 4: 77, 1951
17. Briscoe, W. A. and A. Cournand
Uneven ventilation of normal and diseased lungs studied by an open-circuit method
J.Appl.Physiol. 14: 284, 1959
18. Briscoe, W. A.
A method for dealing with data concerning uneven ventilation of the lung and its effects on blood gas transfer. J.App.Physiol. 14: 291, 1959
19. Briscoe, W. A.
Comparison between alveolo-arterial gradient predicted from mixing studies and the observed gradient
J.Appl.Physiol. 14: 299, 1959
20. Lundin, G.
Alveolar ventilation (in normal subjects) analysed breath by breath as nitrogen elimination during oxygen breathing.
Scand. J.Clin. & Lab. Invest. Suppl. no. 20, 7: 39, 1955
21. Fahri, L. E. and H. Rahn
A theoretical analysis of the alveolar-arterial O_2 difference with special reference to the distribution effect. J.Appl.Physiol. 7: 699-703, 1955
22. Gomez, D. M.
A physico-mathematical analysis of the distribution of the tidal volume throughout the human lung.
Fed. Proc. 21: 439, 1962

23. Gomez, D. M.
A mathematical treatment of the distribution of tidal volume throughout the lung.
Nat. Acad. of Sciences, Proceedings 49: 312-319, 1963
24. Gomez, D. M.
A physico-mathematical concept of continuous distribution of specific blood flow through the organs.
Nat. Acad. of Sciences Proceedings, 51: 750-757, 1964
25. Gomez, D. M., W. A. Briscoe and G. Cummins
Continuous distribution of specific tidal volume throughout the lung.
J.Appl.Physiol. 19(4): 683-692, 1964
26. Okubo, T. and C. Lenfant
Distribution of lung volume and ventilation determined by N₂ washout
J.Appl.Physiol. 24: 658-667, 1968
27. Lenfant, C. and T. Okubo
Distribution function of pulmonary blood flow and ventilation-perfusion ratio in man
J.Appl.Physiol. 24(5): 668-677, 1968
28. Peslin, R., S. Dawson and J. Mead
Analysis of multicomponent exponential curves by the Post-Widder's equation
J.Appl.Physiol. 30: 462-472, 1971
29. Wagner, P. D., H. A. Saltzman and J. B. West
Measurement of continuous distributions of ventilation; perfusion ratios: theory
J.Appl.Physiol. 36: 588-599, 1974

30. Fahri, L. E.
Elimination of inert gases by the lung
Resp. Physiol. 3: 1-11, 1967
31. Jaliwala, S. A., R. E. Mate and F. J. Klocke
An efficient optimization technique for recovering
ventilation perfusion distributions from inert gas data
J.Clin.Invest. 53: 188-192, 1975
32. Olszowka, A. J.
Can \dot{V}_A/\dot{Q} distributions in the lung be recovered from
inert gas retention data?
Respr. Physiol. 25: 191-198, 1975
33. Evans, J. W. and P. D. Wagner
Limits on \dot{V}_A/\dot{Q} distribution from analysis of
experimental inert gas elimination
J.Appl.Physiol. 42: 889-898, 1977
34. Lewis, S. M., J. W. Evans and A. A. Jalowayski,
Continuous distributions of specific ventilation
recovered from inert gas washout
J.Appl.Physiol. 44(3) 416-423, 1978
35. Stephenson, G.
Mathematical methods for Science Students
Longman Group Ltd., London
36. Evans, J. W.
The gas washout determination under a symmetry
assumption
Bull.Math.Biophys. 32: 59-63, 1970

37. Scrimshire, D. A.
Theoretical analysis of independent \dot{V}_A and \dot{Q}
inequalities upon pulmonary gas exchange
Resp. Physiol. 29: 163-179, 1977
38. WAGNER, P. D., and J. W. Evans
Conditions of equivalence of gas exchange in series
and parallel models of the lung
Resp. Physiol. 31: 117-138, 1977
39. Alex Crowther Cardiac Laboratory St. Thomas' Hospital
The role of the Nitrogen washout test in routine
exercise physiology.
Centronic Medical Gas Analyser (Application Bulletin 013-4)
40. Jones, H. B.
Respiration System: Nitrogen Elimination
In: Medical Physics (2nd Ed) edited O. Glasser. Year
Book, Vol II 855-871, 1950
41. Cummin, G. and J. G. Jones
The construction and repeatability of N_2 clearance
curves
Resp. Physiol. 1: 238-248, 1966
42. Cumming, G., K. Horsfield, J. G. Jones and D.C.F. Muir
The influence of gaseous diffusion on the alveolar
plateau at different lung volumes
Resp. Physiol. 2: 386-398, 1967
- 42a. Bowcock, J., P. A. Cotterill and N. Queen
Paper to be published in "Il Nuovo Cimento", 1979
Preprint: Mathematical Physics Dept.,
University of Birmingham, England.

43. Jones, J. G.
Ventilatory function in man: Distribution and Mixing
of Inspired Gas
MD Thesis Birmingham, England: University of Birmingham
1967
44. Riley, R. L., Lilienthal, J. L., Jr., Proemmel, D.D.
and R. E. Franke
On the determination of physiologically effective
pressures of oxygen and carbon dioxide in alveolar air
Amer.J.Physiol. 147: 191, 1946
45. Jose, A. D. and Milner, W. R.
The demonstration of pulmonary arteriovenous shunts
in normal human subjects, and their increase in
certain disease states
J. Clin. Invest. 38: 1915, 1959
46. McIlroy, M. B.
Pulmonary Shunts. In: Handbook of Physiology,
Respiration Volume II
Washington D.C., American Physiological Society, 1965
47. Wilson, R. H., Ebert, R. V., Borden, C. W., Pearson, R. T.,
Johnson, R. S., Falk, A. and Dempsey, M. E.
The determination of blood flow through the non-
ventilated portions of the normal and diseased lung
Amer.Rev.Tuber. 68: 177, 1953
48. Dantzker, D. R., P. D. Wagner and J. B. West
Instability of lung units with units with low \dot{V}_A/\dot{Q}
ratios during O₂ breathing
J.Appl.Physiol. 38: 886-896, 1975

49. Thornburn, C. C.
Isotapes and Radiation in Biology
Butterworth & Co. 1972
50. Spry, L. A.
Theoretical investigation into methods of detecting
pulmonary arteriovenous blood shunts
MPhil Thesis, University of Aston in Birmingham,
England 1977
51. Fritts, H. W., Jr., A. Hardewig, D. F. Rochester,
J. Durand and A. Cournand
Estimation of pulmonary arteriovenous shunt flow
using intravenous injections of T-1824 dye and
Kr⁸⁵
J.Clin.Invest. 39: 1841-1850, 1960
52. Copley, D. P., R. A. Klocke and F. J. Klocke
Quantitation of right-to-left shunting by double
indicator and oxygen techniques
J.Appl.Physiol. Special Communications 4: No. 3
409-415, 1976
53. Lassen, N. A., K. Mellemgard and J. Georg,
Tritium used for estimation of right-to-left shunts
J.Appl.Physiol. 16: 321-325, 1961
54. Mellemgard, K., N. A. Lassen and J. Georg,
Right-to-left shunt in normal man determined by the
use of tritium and Krypton 85
J.Appl.Physiol. 17: 778-782, 1962
55. Murray, J. F., F. F. Davidson and J. B. Glazier
Modified technique for measuring pulmonary shunts
using Xenon and indocyanine green
J.Appl.Physiol. 32: 695-700, 1972

56. Scrimshire, D. A.
Theoretical analysis of gas exchange in a lung model
PhD Thesis, 1973, University of Aston in Birmingham,
England
57. West, J. B.
Ventilation-perfusion inequality and overall gas
exchange in computer models of the lung
Resp. Physiol. 7: 88-110, 1969